RUSSIAN FOUNDATION FOR BASIC RESEARCH

RFBR

JOINT INSTITUTE FOR NUCLEAR RESEARCH

IUPAB

CONNECTING THE WORLD OF BIOPHYSICS

International Workshop

Computational and Theoretical Modeling of Biomolecular Interactions

Dubna, Russia – 2013

Институт компьютерных исследований

Moscow ♦ Izhevsk
Institute of Computer Science
2013

International Workshop
Computational and Theoretical Modeling of Biomolecular Interactions
Dubna, Russia – 2013

Organizers

- International Union of Pure and Applied Biophysics (IUPAB)
- The Joint Institute for Nuclear Research (JINR)
- Scientific Council on Biophysics of the Russian Academy of Sciences (RAS)
- Lomonosov Moscow State University
- Division of Physico-Chemical Biology of RAS

The Workshop is supported by the International Union for Pure and Applied Biophysics (IUPAB Sponsorship Agreement № 090/48) and Russian Foundation for Basic Research (RFBR grant № 13-04-06047 Г)

Conference topics

- Macromolecules and supramolecular biological assemblies
- Protein structure and folding
- Protein-protein interactions. New principles and methods
- Breakthroughs in molecular simulations
- Mathematical modeling in radiation and environmental biophysics

Scientific committee

A.B. Rubin
E.A. Krasavin
A.V. Finkelstein
E.E. Fesenko
V.D. Lakhno
G.R. Ivanitsky
R.G. Efremov
V.V. Korenkov
Kh.T. Kholmurodov
G.Yu. Riznichenko
K.V. Shaitan
V. Barsegov
N.G. Esipova
V.G. Tumanyan
I.G. Strankfeld
V.M. Komarov

Computational and Theoretical Modeling of Biomolecular Interactions. Moscow-Izhevsk: Institute of Computer Science, 2013. 92 pages.

ISBN 978-5-4344-0126-5

© by authors, 2013

Conference venue

Plenary lectures and poster sessions are held in the International Conference Hall of the Joint Institute for Nuclear Research, Dubna, Russia (2 Stroitelei Str.) five minutes' walk from "Dubna" hotel (8 Vekslera Str.). Map of nearby streets is shown below.

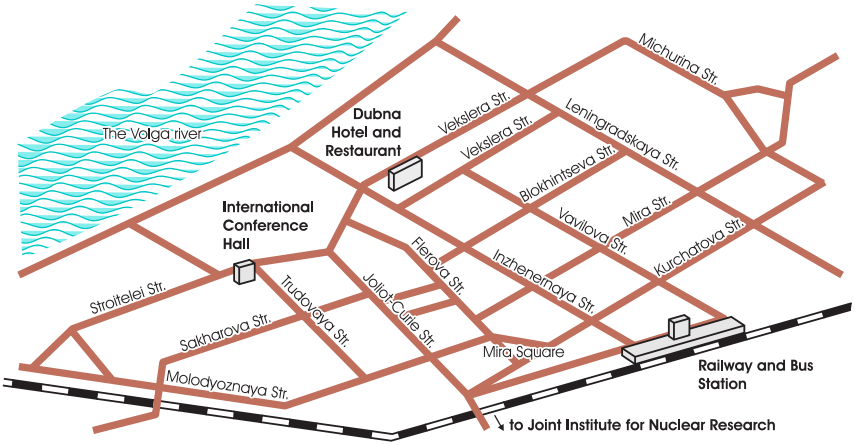

Abstracts

Role of electrostatic interactions in the encounter complex formation of plastocyanin and cytochrome f, barnase and barstar proteins

Abaturova A.M., Khruschev S.S., Kovalenko I.B., Riznichenko G.Yu.

Lomonosov Moscow State University, Faculty of Biology, Department of Biophysics, Russia, 119991, Moscow, 1-12 Leninskie Gory, E-mail: abaturova@list.ru

We used simulation software of multi-particle Brownian dynamics [1] named ProKSim [2] to investigate formation of an encounter complex of small and middle-sized proteins: plastocyanin (pc) and cytochrome f (cytf), barstar (bs) and barnase (bn). The proteins plastocyanin and cytochrome f are reaction partners in a photosynthetic electron transport chain. Barnase is a bacterial extracellular ribonuclease and barstar is its intracellular inhibitor.

In ProKSim the proteins are considered as rigid bodies. The proteins are subjected to electrostatic and random Brownian force. For simulation we used the coordinates of protein complexes from the Protein Data Bank. For barnase and barstar complex PDB ID is 1BGS, for plastocyanin and cytochrome f PDB ID is 2PCF, model 9. Ionic strength was 100 mM or infinity (simulation without electrostatic interactions), and the temperature was 300 K. Time step was 100 ps. Amino acid charges were calculated using the Henderson–Hasselbalch equation at pH 7.0.

We present an analysis of trajectories from Brownian dynamics simulations. ProKSim registers "successful" events of encounter complex formation. In "successful" complexes the distance between protein partners is less than 5 Å (at infinite ionic strength) or the energy of electrostatic attraction is greater than kT (at ionic strength of 100 mM). In the process of simulation the center of mass of the first protein was mapped into a three-dimensional grid with 1 Å spacing around the second (reference) protein, and the algorithm sums the number of successful events at each cell of the grid. After the simulation we have the total number of the successful events at each cell of the grid which we call occupancy values. To get a high statistics for the occupancy 200,000 successful events (encounter complexes during simulation) were registered for each protein pair. Cytf and bn were used as reference proteins.

Fig. 1 and Fig. 2 show the results of the simulations for 100 mM and infinite ionic strength. Molecules of cytochrome f and barnase where aligned separately during analysis of the results of the simulation. Cells where centers of mass of bs or pc appeared more than 20 times are shown. At infinite ionic strength (without electrostatic interactions) probabilities to find the center of mass for pc and bs do not depend on the cells around their protein partners. At 100 mM ionic strength there is one energetically favorable position of pc

molecule relative to cyt f (shown as blue sphere on Fig. 1A). This position corresponds to the place where pc is found in 2PCF complex.

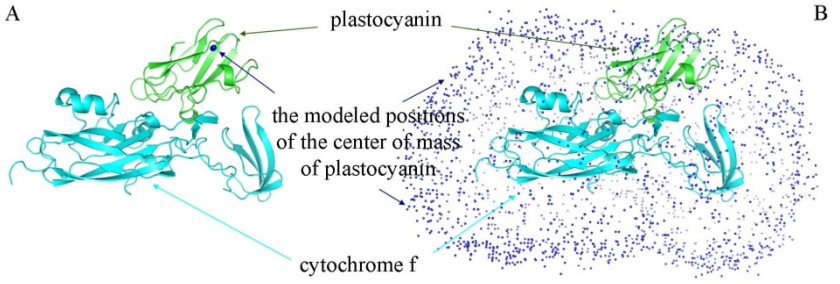

Figure 1. Structure of cytochrome f-plastocyanin complex (PDB id 2PCF, model 9) in a cartoon representation (cyan and green ribbons for cytochrome f and plastocyanin, respectively) and calculated positions of plastocyanin center of mass in respect to cytochrome f (blue dots). Blue dots indicate grid cells with occupancy higher than 20. (A) Ionic strength is 100 mM (B) Ionic strength is infinite (simulation is performed without electrostatic interactions). The picture was generated with PyMOL [3].

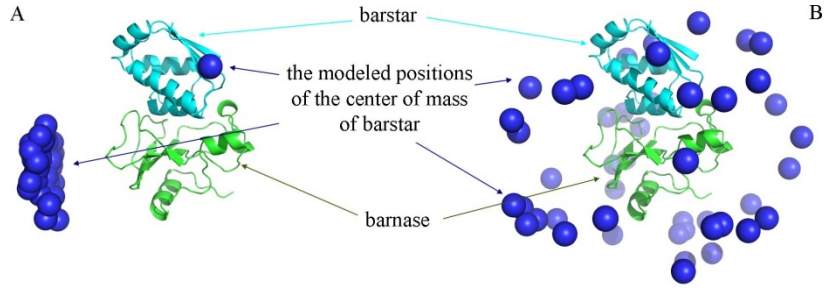

Figure 2. Structure of barnase-barstar complex (PDB id 1BGS, chains A and E) in a cartoon representation (cyan and green ribbons for barstar and barnase, respectively) and calculated positions of barstar center of mass in respect to barnase (blue spheres). Blue spheres indicate grid cells with occupancy higher than 20. (A) Ionic strength is 100 mM (B) Ionic strength is infinite (simulation is performed without electrostatic interactions). The picture was generated with PyMOL [3].

Fig. 2 shows two energetically favorable positions of bs center of mass in respect to bn at 100 mM ionic strength. Both positions correspond to the locations where bs is found in 1BGS complex. However, one of the positions corresponds to physiological protein complex (displayed in the figure) and the

other corresponds to the location of bs in the crystal complex with respect to crystal symmetry. The latter position is near Lys66 on bn, far away from the bs binding site. Quite similar results were obtained in [4]. Thus we can conclude that electrostatic interactions are essential for formation of distinct encounter complexes.

The work was supported by Russian Foundation for Basic Research RFBR Project 12-07-33036-мол_а_вед and 12-04-31839-мол_а. The reported study was supported by the Supercomputing Center of Lomonosov Moscow State University [5].

1 Kovalenko I.B., Abaturova A.M., Gromov P.A., Ustinin D.M., Grachev E.A., Riznichenko G.Yu., Rubin A.B. *Direct simulation of plastocyanin and cytochrome f interactions in solution* // Phys. Biol. **2006**, 3:121–129

2 Khrushchev S.S., Abaturova A.M., Diakonova A.N., Ustinin D.M., Zlenko D.V., Fedorov V.A., Kovalenko I.B., Riznichenko G.Yu., Rubin A.B. *Multi-particle Brownian Dynamics software ProKSim for protein-protein interactions modeling* // Computer Research and Modeling (Russian). **2013**. Vol. 5, no. 1, P. 47–64.

3 *The PyMOL Molecular Graphics System, Version 1.5.0.3*. Schrödinger, LLC.

4 Spaar A., Dammer C., Gabdoulline R.R., Wade R.C., Helms V. *Diffusional encounter of barnase and barstar* // Biophys. J. **2006**. Vol. 90, P. 1913–1924.

5 Voevodin Vl.V., Zhumatiy S.A., Sobolev S.I., Antonov A.S., Bryzgalov P.A., Nikitenko D.A., Stefanov K.S., Voevodin Vad.V. *Practice of "Lomonosov" Supercomputer* // Open Systems J. (Russian). **2012**. № 7. [http://www.osp.ru/os/2012/07/13017641/]

Mathematical modeling of postsynaptic processes in the CA3 region of the hippocampus

Aksenova S.V.[1], *Belov O.V.*[1], *Sokol O.E.*[1,2]

[1] Laboratory of Radiation Biology, Joint Institute for Nuclear Research, Dubna, Russia
E-mail: kgyr@mail.ru
[2] Faculty of Physics, M.V. Lomonosov Moscow State University, Russia

Recent studies revealed a number of facts indicating the effect of ionizing radiation on the behavior and memory functions in laboratory animals. In particular, it was found that irradiation with heavy charged particles at relatively low doses causes significant impairments of behavior and memory. The physical characteristics of the particles that cause these effects are similar to those of the galactic cosmic rays.

To date, few molecular mechanisms have been identified which may be responsible for these effects. An important role is played by the processes of

synaptic transmission, which, apparently, are also undergoing changes after radiation exposure.

In the present study, a comparative evaluation of the functional activity of neurons in the brain for different membrane potentials of Ca^{2+} was performed. For this purpose, we used the model describing the functioning of the CA3 pyramidal neurons of the hippocampus, which plays a key role in the processes of learning and memory [1]. The mathematical description of the mechanisms of synaptic transmission takes into account transport of K^+, Ca^{2+}, and Na^+ ions. As a method of describing synaptic transmission, a Hodgkin-Huxley model based [2] approach is selected.

The proposed model is a quantitative description of a series of biochemical processes that occur in the membrane and within the dendritic spine of pyramidal neurons during the induction of long-term potency and prolonged depression, taking into account the dependence of these processes on the value of the calcium potential. The long-term task is to use such models for the assessment of the functional changes caused by heavy charged particles.

1 Murzina G.B., Silkis I.G. *A model for the posttetanic efficiency of a neuron dendritic spine* // Institute of Higher Nervous Activity and Physiology, Russian Acad. Sci. **1997**. V. 42. P. 702-710.

2 Hodgkin A., Huxley A. *A quantitative description of membrane current and its application to conduction and excitation in nerve* // J. Physiol. **1952**. V. 117. P. 500-544.

Effects of hydrodynamic interactions on biological matter

Alekseenko A.[1], *Kononova O.*[2,1], *Kholodov Ya.*[1], *Barsegov V.*[2,1]

[1] Moscow Institute of Physics and Technology, Dolgoprudny, Moscow Region, Russia
[2] University of Massachusetts Lowell, Lowell, MA, USA

The structure and functioning of biomolecules are greatly affected by surrounding solvent. In computer-based modeling of biological systems, a proper care has to be taken to correctly describe the solvation effects, which determine electrostatic and entropic properties of the system in question. Except for explicit solvent schemes employed, e.g., in all-atom Molecular Dynamics simulations in explicit water, the description of solvent hydrodynamics is typically limited to stochastic kicks modeled by zero-averaged and delta function correlated random forces. Although the collective behavior of water molecules can potentially dramatically alter the dynamics of the system, this behavior is neglected in Langevin simulation schemes, which in conjunction with coarse-grained models of biomolecules are widely used to access large-amplitude molecular motions in biological systems. Here, we

report the results for the GPU-accelerated implementation of Tensor Ersatz Approximation [1] (TEA), an algorithm for describing pairwise hydrodynamic interactions fully incorporated into the Self Organized Polymer model of a polypeptide chain [2] (SOP-GPU package). The implementation of a fast yet accurate perturbative TEA-based approach was first tested against the results of exact hydrodynamic treatment of the solvent degrees of freedom, and then used to model the influence of solvent drag forces on force-induced unfolding of the trimer $(WW)_3$ formed by the all-β-sheet WW domains [3] (see Figure).

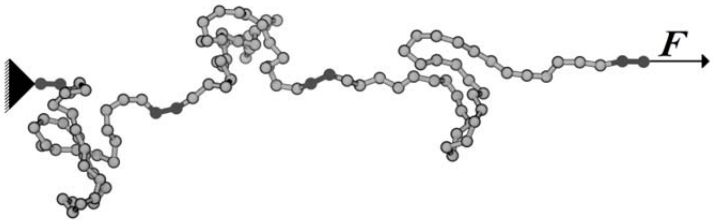

Figure. The schematic representation of the force-clamp experiment in silico. The N-terminal of the trimer $(WW)_3$ is constrained and the constant pulling force (F, indicated by the arrow) is applied to the C-terminal to induce the unfolding in 33-residue long WW domains forming the trimer (light gray), connected by 2 residue long GLY-linkers (dark gray).

Force	With hydrodynamics			Without hydrodynamics		
	Average total unfolding time, ms	Pearson correlation coefficient	Spearman rank correlation coefficient	Average total unfolding time, ms	Pearson correlation coefficient	Spearman rank correlation coefficient
100 pN	*4648±2238*	*-0.08*	*-0.09*	*1463±962*	*0.04*	*0.03*
120 pN	*537±233*	*-0.14*	*-0.22*	*97±44*	*-0.08*	*-0.17*
140 pN	*213±43*	*-0.47*	*-0.52*	*36±8*	*-0.36*	*-0.31*
160 pN	*147±16*	*-0.65*	*-0.56*	*38±5*	*-0.60*	*-0.21*

Table. Statistical measures quantifying the unfolding transitions in the trimer (WW)3 and dynamic correlations between the unfolding times for the first WW domain and second WW domain as a function of the applied constant force in the 100–160 pN range. Presented are the average time for unfolding of all three monomers, the Pearson correlation coefficient, and the Spearman rank correlation coefficient (sample size = 1,000 trajectories of forced unfolding).

Interestingly, we found that the inclusion of solvent hydrodynamics leads to the several-fold speedup in the average unfolding times for all three WW domains and the emergence of dynamic correlations in unfolding times, which are not observed in the simulations with hydrodynamics switched off (see Table).

1 Geyer T., Winter U. *An O(N^2) approximation for hydrodynamic interactions in Brownian dynamics simulations* // J. Chem. Phys. **2009**. 130, 114905–114913.
2 Zhmurov A., Dima R. I., Kholodov Ya., Barsegov V. *Sop-GPU: accelerating biomolecular simulations in the centisecond timescale using graphics processors* // Proteins. **2010**. 78, 2984–2999.
3 Zhmurov A., Dima R. I., Barsegov V. *Order statistics theory of unfolding of multimeric proteins* // Biophysical J. **2010**.99, 1959–1968.

Influence of cholesterol on activation of the β_2-adrenergic receptor: Molecular dynamics simulations

Alekseev E.S., Bogdan T.V.

Lomonosov Moscow State University, Faculty of Chemistry, E-mail: esalexeev@gmail.com

According to modern concepts membrane receptors may exist in different conformational states, which contribute to the specific mechanism of the signal transduction [1]. It is assumed that receptor activation may occur even in the absence of agonist [2]. Stabilization of the specific conformation is achieved by various external influences [3]. Several conformation states with different ligands (such as agonist, nanobody or G-protein) were studied for β_2-adrenoceptor. Current experimental results [4, 5] point to a significant modification of the receptor's properties in the presence of cholesterol. However, conformational changes in the receptor that occur upon binding of cholesterol, were not studied.

The goal of this study was to determine specific features of the receptor activation in the presence of cholesterol and to investigate the functional role of the cholesterol binding site through mutation.

Molecular dynamic simulations of native (PDB ID 2RH1) and mutated receptor in hydrated lipid bilayer in the presence and absence of cholesterol were performed. Hydrogen bond between helices **II** and **IV** in the cholesterol binding site was removed in the mutated receptor. Molecular dynamics trajectories were obtained using GROMACS software on "Lomonosov" supercomputer. NPT-ensemble simulations were performed with periodic boundary conditions at $T = 323.0$ K, $p_x = p_y = 2$ atm and $p_z = 1$ atm using CHARMM36 force field (TIP3P model for water molecules). Conformation of the cholesterol binding site in different systems was analyzed. Moreover,

conformational changes in the agonist binding site and in the ionic lock state formed by Arg131 helix **III** and Glu268 helix **VI** residues were studied.

It was found that the hydrogen bond between Ser74 and Trp158 residues persists in the presence of cholesterol. In the absence of cholesterol, the receptor stays half the time in a conformational state with a broken hydrogen bond. The break of the H-bond is accompanied by rotation of the indole ring in Trp158 from 100º to 60º. The native receptor arrives to a state where the ionic lock between Arg131 and Glu268 is formed, both in the presence and absence of cholesterol; but in the absence of cholesterol the transition is faster. In the mutated receptor in the absence of cholesterol the conformation of Trp158 changes. In the mutated receptor ionic lock was not formed, and in the presence of cholesterol conformational changes occur in the agonist binding site, that mediate receptor transition to the active form.

These results allow to suggest that cholesterol stabilizes conformation of the cholesterol binding site both in native and mutated receptor. In the absence of cholesterol the equilibrium ratio between the active and inactive receptor forms is changed towards the inactive form. The interhelical hydrogen bond in the cholesterol binding site stabilizes its conformation which is necessary for the efficient receptor-cholesterol interaction. The mutation in the cholesterol binding site facilitates transition of the receptor into the active form.

Thus we have shown the importance of the receptor-cholesterol interaction for the receptor activation and the signal transduction by β_2-adrenergic and related receptors.

1 Yao X.J., Velez Ruiz G., Whorton M.R., Rasmussen S.G., DeVree B.T., Deupi X., Sunahara R.K., Kobilka B.K. *The effect of ligand efficacy on the formation and stability of a GPCR-G protein complex* // Proc. Natl. Acad. Sci. USA. **2009**. V.106. P.9501-9506.

2 Milligan G. *Constitutive activity and inverse agonists of G protein-coupled receptors: a current perspective* // Mol. Pharmacol. **2003**. V.64. P.1271-1276.

3 Canals M., Lane J. R., Wen A., Scammells P. J., Sexton P. M., Christopoulos A. *A Monod-Wyman-Changeux mechanism can explain G protein-coupled receptor (GPCR) allosteric modulation* // J. Biol. Chem. **2012**. V.287. P.650-659.

4 Hanson M.A., Cherezov V., Griffith M.T., Roth C.B., Jaakola V.-P., Chien E.Y.T., Velasquez J., Kuhn P., Stevens R.C. *A specific cholesterol binding site is established by the 2.8 Å structure of the human β_2-adrenergic receptor* // Structure. **2008**. V.16P.897-905.

5 Zocher M., Zhang C., Rasmussen S.G.F., Kobilka B.K., Müller D.J. *Cholesterol increases kinetic, energetic, and mechanical stability of the human β_2-adrenergic receptor* // Proc. Natl. Acad. Sci. USA. **2012**.V.109. P.3463-3472.

Order statistics inference for describing topological coupling and mechanical symmetry breaking in multidomain proteins

Barsegov V.

University of Massachusetts Lowell, Lowell, MA, USA

Cooperativity is a hallmark of proteins, many of which show a modular architecture comprised of discrete structural domains. Detecting and describing dynamic couplings between structural regions is difficult in view of the many-body nature of protein-protein interactions. By utilizing the GPU[1]-based computational acceleration, we carried out simulations of the protein forced unfolding for the dimer WW-WW of the all-beta-sheet WW domains used as a model multidomain protein. We found that while the physically non-interacting identical protein domains (WW) show very similar (symmetric) mechanical properties at low tension, reflected, e.g., in the equality of their distributions of unfolding times, these properties become distinctly different when tension is increased. Moreover, the uncorrelated unfolding transitions at a low pulling force become increasingly more correlated (dependent) at higher forces. Hence, the applied force not only breaks "the mechanical symmetry"' but also couples the non-interacting protein domains forming a multidomain protein. We call this effect "the topological coupling". These results demonstrate the need to develop a reliable statistical approach for interpretation of force spectroscopy data. We developed a new theory, inspired by Order statistics, to characterize protein-protein interactions in multidomain proteins. The method utilizes the squared-Gaussian model, but it can also be used in conjunction with other parametric models for the distribution of unfolding times. The formalism can now be taken to the single-molecule experimental lab to probe mechanical cooperativity and domain communication in multidomain and oligomeric proteins.

[1] Graphics Processing Unit

Interaction of environmental electrostatic structure with ionized DNA sequence: Mixed quantum-classical study

Boyda D.L.[1], *Shirmovsky S.Eh.*[2]

[1] Laboratory of living matter physics,
[2] Theoretical and experimental physics cathedra,
Far Eastern Federal University, 8 Sukhanov St., Vladivostok, 690950, Russia

In the work, the nature of DNA conductivity was investigated. We are trying to answer whether and in what manner solvent factors and DNA dynamics affect the nature of the hole migration through DNA molecule [1, 2]. Two DNA–charge models were studied.

The first one is a quantum-classical nonlinear double-stranded model. In the model the full DNA-charge Hamiltonian H is determined as a sum of two terms

$$H = H_{Cl} + < \psi | H_Q | \psi >, \quad (1)$$

where the first term describes DNA as a classical object. DNA macromolecule is considered a system of oscillators formed by two strands. The strands are joined to compose DNA. H_{Cl} is determined as follows

$$H_{Cl} = \sum_{n=1}^{N} \left(\frac{M\dot{y}_{1,n}^2}{2} + \frac{M\dot{y}_{2,n}^2}{2} + \frac{k_v(y_{1,n}-y_{1,n-1})^2}{2} + \frac{k_v(y_{2,n}-y_{2,n-1})^2}{2} + \frac{k_h(y_{1,n}-y_{2,n}+l)^2}{2} \right), \quad (2)$$

where the first and second terms correspond to kinetic energy of the bases located on two different DNA strands with the coordinates of y_1 and y_2. The bases are coupled together with hydrogen bonds, which are modeled by the last term. The third and fourth terms form stacking interactions through each DNA strand. Dot indicates time derivative. The model parameters are: M is the effective base mass, k_h and k_v are force constants; l is horizontal distance between the bases in equilibrium. The summation in the expression is performed over the number of base pairs in the sequence under consideration. The second term in expression (1) is determined by a charged particle quantum dynamics, where H_Q, a tight-binding Hamiltonian operator, is determined by the properties of the charge located on the n, m bases.

$$H_Q = \sum_{n=1}^{N} \varepsilon_n |n><n| + \sum_{n \neq m}^{N} v_{n,m} |n><m|. \quad (3)$$

Here $\varepsilon_n = \alpha_n^0 + \alpha_n'(y_{1,n} - y_{2,n} + l)$ are ionization potentials where the first term α_n^0 is static and corresponds to the ionization potentials of a separate base while the second one is a dynamic value. The interaction between the charged particle and DNA in the model is determined by the second component, where α_n' is a fitting parameter of the model and $(y_{1,n} - y_{2,n} + l)$

means stretch of n^{th} DNA base pair. The coupling matrix elements $v_{n,m}$ determine the rate of charge transport between the donor n and acceptor m bases. $v_{n,m}$ are static values.

In the second model DNA is considered as a sequence of the sites with vertical coordinate y_n and horizontal coordinate x_n. In this case H_{Cl} is determined as follows

$$H_{Cl} = \sum_{n=1}^{N} \left(\frac{M\dot{y}_n^2}{2} + \frac{M\dot{x}_n^2}{2} + \frac{k_v(y_{n+1}-y_n)^2}{2} + \frac{k_h x_n^2}{2} \right). \quad (4)$$

The first and second terms correspond to kinetic energy of the bases, third term determines stacking interaction and the last term describes hydrogen bonds. In this model the quantum operator H_Q is determined by the relationship

$$H_Q = \sum_{n=1}^{N} (\varepsilon_n + \frac{k_c e Q}{\varepsilon y_n}) \, |n><n| + \sum_{n \neq m}^{N} \nu_{n,m} \, |n><m|, \quad (5)$$

where the first term determines energy of the charge on n^{th} base. In this case the ionization potentials are $\varepsilon_n = \alpha_n^0 + \alpha_n' x_n$, where α_n^0 is static while the $\alpha_n' x_n$ is a dynamic value and depends on horizontal coordinates x_n. The second part of the charge energy is determined by electrostatic interaction with charged particle. In this case: Q – charge of the particle, e - elementary charge, k_c is Coulomb's constant, ε - dielectric constant of the medium. The second term is determined by the coupling matrix elements which are dynamic values: $\nu_{n,m} = \nu_{n,m}^0 + \nu'_{n,m}(L - y_n - y_m)$. Here $\nu_{n,m}^0$ is a static coupling matrix element, and $\nu'_{n,m}$ are fitting parameters of the model (L is vertical distance between the bases in equilibrium).

Figures show the probable hole location on the bases of the sequence G(+)AAAGGG. Calculation was performed using the first (Figure 1) and the second (Figure 2) models. At initial time moment charge was at the guanine G(+) base. It is seen that behavior of the hole is governed by dynamics of DNA and environmental factors.

1 Kubar T., Woiczikowski P. B., Cuniberti G., Elstner M. *Efficient calculation of charge-ransfer matrix elements for hole transfer in DNA* // J. Phys. Chem. B **2008**. V. 112. P. 7937-7947.

2 Voityuk A. A. *Electronic couplings and on-site energies for hole transfer in DNA: Systematic quantum mechanical/molecular dynamic study* // J. Chem. Phys. **2008**. V.128 P.115101-115106.

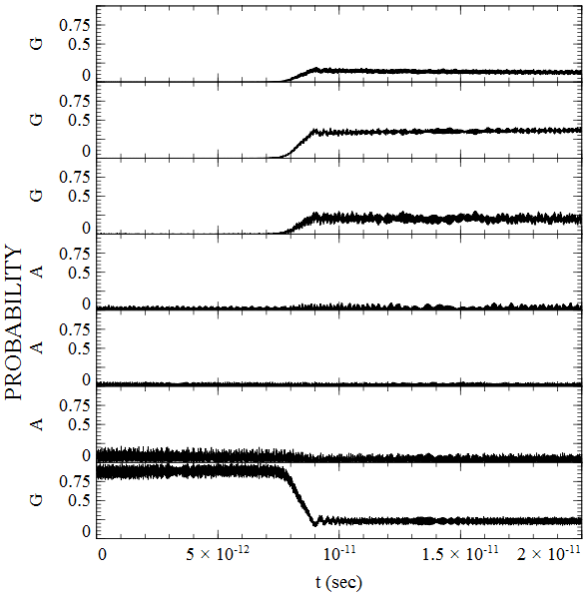

Figure 1

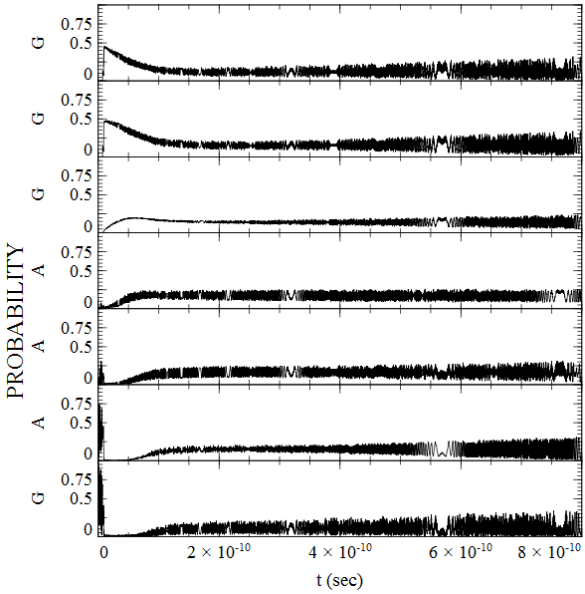

Figure 2

Direct multiparticle simulation of ferredoxin interactions with FNR and hydrogenase. Dependence upon ionic strength and pH

Diakonova A.N., Khrushchev S.S., Kovalenko I.B., Riznichenko G.Yu.

Lomonosov Moscow State University, Biological Faculty, Department of Biophysics, Moscow, Russia. E-mail: alex.diakonova@gmail.com

Ferredoxin (Fd) protein transfers electrons from photosystem I (PSI) to ferredoxin:$NADP^+$-reductase (FNR) in photosynthetic electron transport chain. In some photosynthetic organisms including cyanobacteria and green unicellular algae under anaerobic conditions Fd transfers electrons not only to FNR but also to hydrogenase – an enzyme that catalyzes reduction of atomic hydrogen to H_2. Therefore in photosynthetic electron transport chain FNR and hydrogenase compete for ferredoxin [1]. Molecular hydrogen can be utilized as biological fuel, and development of methods of its production using microorganisms is an important new area of bioenergetics. One of the questions posed by this challenge is which characteristics of thylacoid stroma media allow to switch electron flow from linear path PSI-Fd-FNR-$NADP^+$ to path PSI-Fd-hydrogenase-H_2.

The study for conducted using direct multiparticle simulation approach [2]. In this method protein molecules are considered as individual objects that experience Brownian motion and electrostatic interaction with surrounding media and each other. The method allows to simultaneously simulate motion and complex formation of hundreds of protein molecules of each type in solution.

Using the model we studied effects of pH and ionic strength (I) upon complex formation between ferredoxin and FNR and ferredoxin and hydrogenase. It is known that pH of chloroplast stroma changes from about 6 in the dark to 8-8.5 in the light. We showed that electrostatic potentials of the proteins calculated using Poisson-Boltzmann equation vary dramatically with pH and ionic strength. Moreover these changes affect rate of complex formation. Dependence of second-order rate constant upon ionic strength is presented in Figure 1.

Dependence upon ionic strength for Fd-FNR protein pair is non-monotonic (Fig. 1, red line). At ionic strengths larger than 100 mM rate constant rapidly decreases which can be attributed to electrostatic shielding of the charges on proteins' surfaces that allow proteins to approach each other and form a complex. At low ionic strengths from 0 to 100 mM, rate constant increases with I. At this range of I electrostatic interactions between ferredoxin and FNR are so strong that the proteins form ineffective complexes, i.e.

complexes in which proteins are oriented not the way they are supposed to for effective electron transport to occur. This effect is not observed for Fd-hydrogenase complex, and the rate constant for these two proteins monotonically decreases with ionic strength.

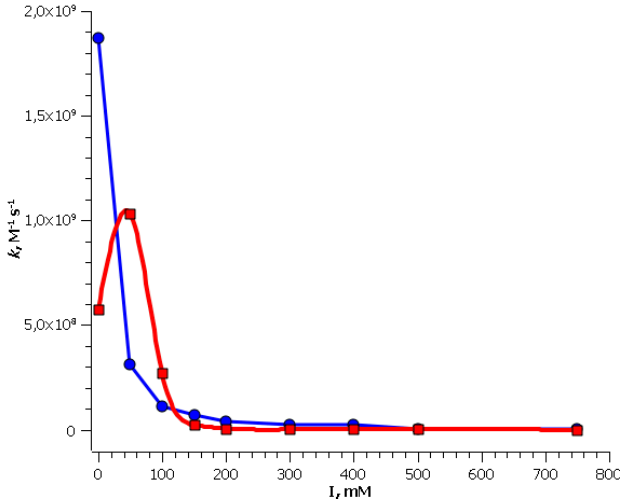

Figure 1. Dependence of the rates of Fd-FNR (red line) and Fd-hydrogenase (blue line) complex formation upon ionic strength.

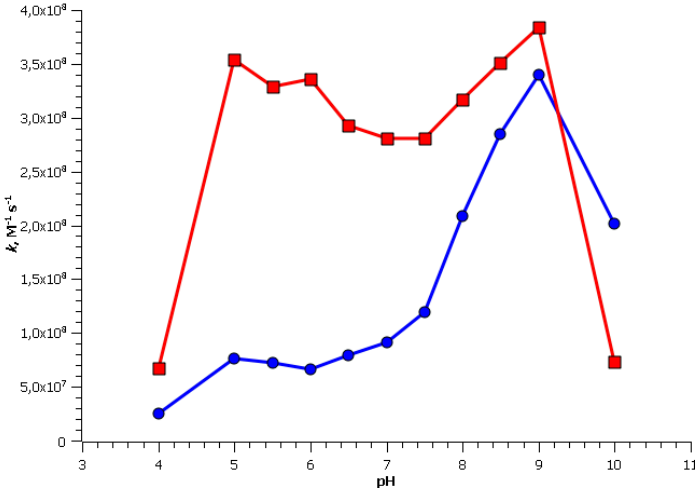

Figure 2. Dependence of the rates of Fd-FNR (red line) and Fd-hydrogenase (blue line) complex formation upon pH.

Dependence of rate constant upon pH for two protein pairs is presented in Figure 2. Minimal values of rate constant for both Fd-FNR and Fd-hydrogenase complex formation correspond to pH 4 and 10; at these pH values native protein conformation is damaged. In the pH range 5-7.5 rate constant for Fd and hydrogenase interaction is almost constant. Then it starts to rapidly increase with pH and achieves maximum at pH 9. Rate constant of complex formation for ferredoxin and FNR doesn't change in the pH range from 5 to 7.5 and has a small maximum at pH ~ 9.

Using the model we showed that rate constant of Fd-FNR complex formation is constant in a wide range of physiologically significant pH values. This type of dependence upon pH is common among proteins. Therefore it can be argued that regulation of FNR activity doesn't involve pH changes in stroma. On the other hand in the model rate constant of Fd-hydrogenase interaction dramatically depends upon pH: in the range 7-9 it increases threefold. It may seem that because hydrogenase reduces protons it must be more active when pH is acidic. Apparently regulation of hydrogenase's affinity to both her reaction partners (H^+ and Fd) is carried out by changes in its electrostatic properties. In the dark the protein is inactive and in the light it is activated and starts to interact both with Fd and H^+.

The work was supported by Russian Foundation for Basic Research RFBR Project 12-07-33036-мол_а_вед and 12-04-31839-мол_а. The reported study was performed using the Supercomputing Center of Lomonosov Moscow State University [3].

1 Yacobi I., Pochekailov S., Toporik H., Ghirardi M.L., King P.W., Zhang S. *Photosynthetic electron partitioning between [Fe-Fe]-hydrogenase and ferredoxin:NADP$^+$-oxidoreductase (FNR) enzymes in vitro* // PNAS, **2011**. V. 108. Pp. 9396-9401.

2 Kovalenko I.B., Abaturova A.M., Diakonova A.N., Knyazeva O.S., Ustinin D.M., Khruschev S.S., Riznichenko G.Yu., Rubin A.B. *Computer simulation of protein-protein association in photosynthesis* // Mathematical Modeling of Natural Phenomena, **2011**. V. 6. Pp. 39-54.

3 Voevodin Vl.V., Zhumatiy S.A., Sobolev S.I., Antonov A.S., Bryzgalov P.A., Nikitenko D.A., Stefanov K.S., Voevodin Vad.V. *Practice of "Lomonosov" Supercomputer //* Open Systems J. (Russian). **2012**. № 7. [http://www.osp.ru/os/2012/07/13017641/]

How to determine the size of the nucleus of protofibrils from the concentration dependence of the lag-time of aggregation? Experimental application: Insulin and Lys-Pro insulin

Dovidchenko N.V., Suvorina M.Yu., Selivanova O.M., Eliseeva I.A., Surin A.K., Schmatchenko V.V., Finkelstein A.V., Galzitskaya O.V.

E-mail: ogalzit@vega.protres.ru

The question about the size of nuclei of protofibrils formed by different proteins and peptides is yet open. According to the nucleation mechanism, the formation of protofibrils begins with the thermodynamically unfavorable steps resulting in the formation of a critical nucleus consisting of *n* monomers. A kinetic model of the process of formation of amyloid fibrils is suggested in our work allowing us to calculate the size of the nucleus using kinetic data. In addition to the stage of nucleation, the proposed model includes both linear growth of protofibrils (proceeding only at the cost of attaching monomers to the ends) and exponential growth of protofibrils at the cost of branching and fragmentation. Theoretically, only exponential growth is compatible with the existence of a lag-period in the fibril formation kinetics.

Insulin is a commonly used protein for studies of amyloidogenesis. There are several insulin analogues with different pharmacokinetic characteristics, in particular onset and duration of action. As the duration of action may be connected with the duration of the lag-phase, the challenge is to consider the process of amyloid formation for different analogs of insulin. One of them is LysPro insulin. The behavior of LysPro insulin in the process of amyloid formation has not yet been studied in detail. To quantitatively investigate the differences between the two substances in the aggregation reaction and to estimate the difference in the lag-time, we used thioflavin T fluorescence assay, electron microscopy, X-ray diffraction methods, and theoretical modeling.

Kinetic experimental data for both insulin and LysPro insulin samples demonstrated increase of the lag-time for LysPro insulin at low concentrations of monomers, particularly at 2 and 4 mg/ml, which corresponds to the pharmaceutical concentration. The obtained analytical solution and computer modeling allow us to determine the size of the nucleus from the experimentally obtained concentration dependences of the relationship between the lag-time and the time of growth of amyloid fibrils. In case of both insulin and LysPro insulin, this relationship is independent of the protein concentration. According to the developed theory, this means that the size of the nucleus corresponds to one monomer in both insulin and LysPro insulin.

This study was supported by the Russian Foundation for Basic Research and by the Russian Academy of Sciences programs "Molecular and Cell Biology" and "Fundamental Sciences to Medicine".

Computer simulation of intermolecular complex formation of photosynthetic electron transport proteins plastocyanin and cytochrome f

Fedorov V.A., Kovalenko I.B., Khrushchev S.S.

Lomonosov Moscow State University, Faculty of Biology, Department of Biophysics

Protein-protein interactions are the basis of most biological processes. Various methods including certain simulation techniques are used to study these processes at different levels of organization from atomic to organismic. Reconstruction of intermolecular protein-protein complex formation requires combined application of these methods. We combine techniques of Brownian and molecular dynamics (Figure 1) and apply them to studying of protein-protein complex formation of plastocyanin and cytochrome f, proteins involved in the photosynthetic electron transport chain of chloroplasts of higher plants. Atoms that make up the molecules oscillate in the timescale of the order of femtoseconds whereas complex formation of electron-transport proteins takes up to hundreds of microseconds. We use the method of Brownian dynamics to simulate formation of encounter protein complexes in a rigid body approximation [1]. Full atom molecular dynamics which takes into account flexibility of the protein-protein interface is then used to simulate the transformation of encounter complexes into final complexes.

Method of Brownian dynamics allows to simulate processes of diffusion of proteins, their approaching each other, and subsequent formation of encounter complexes. These processes happen on the scale of hundreds of microseconds and are simulated with time step of 100 picoseconds. In this model protein molecules are considered rigid bodies, which perform translational and rotational motion under the influence of electrostatic and random forces. This approach allows us to simulate the interaction of several hundreds of proteins simultaneously, which makes it possible to describe this process as it occurs in cells. In its turn, molecular dynamics is used to simulate the process of further protein converging and formation of the final complex with account of conformational flexibility of molecules.

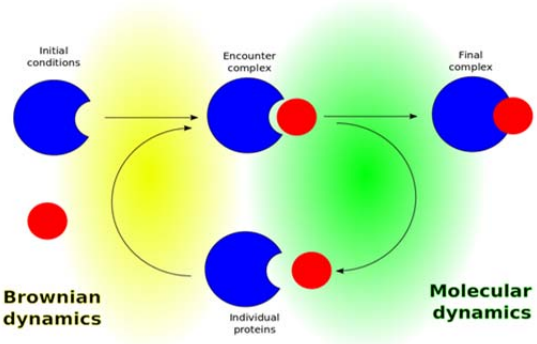

Figure 1. Schematic representation of the method combining Brownian and molecular dynamics for calculation of protein-protein complex formation kinetics.

Transformation of encounter complexes obtained by Brownian dynamics into final occurs within 1-5 nanoseconds. Simulation of this process requires taking into account mobility of each atom in the molecule. Method of molecular dynamics with explicit solvent allows us to study these processes in detail. In our work, we used the software package GROMACS [2]. For system of plastocyanin-cytochrome f in water (220,000 atoms) we used two approaches to increase performance of calculations: first, we used all-bond PLINKS constraints and mass rescaling [3] to increase the time step of the model up to 4 fs; second, we used software which allows parallel computing on hybrid architecture. We reached performance up to 80-100 ns model time per day using 32 cluster nodes (Figure 2).

For plastocyanin and cytochrome f we obtained 100 molecular dynamics trajectories of 20 ns. Copper atom of plastocyanin and iron atom of cytochrome f are the redox centers of the proteins between which electron transfer occurs. Distance between them may be used as the main criterion of complex formation in the model. For some of these trajectories the distance was increasing, indicating withdrawal of these proteins from each other. For other trajectories this distance is decreasing, which potentially indicates formation of the final complex. In these trajectories encounter complexes in several ns transform into structures with the distance between the cofactors of about 14 Å and this distance does not change significantly in the process of further transformation, and different mutual configurations of the proteins are possible. So, in this case all such structures may be considered as final complexes with the same distances between the cofactors and slightly different structures.

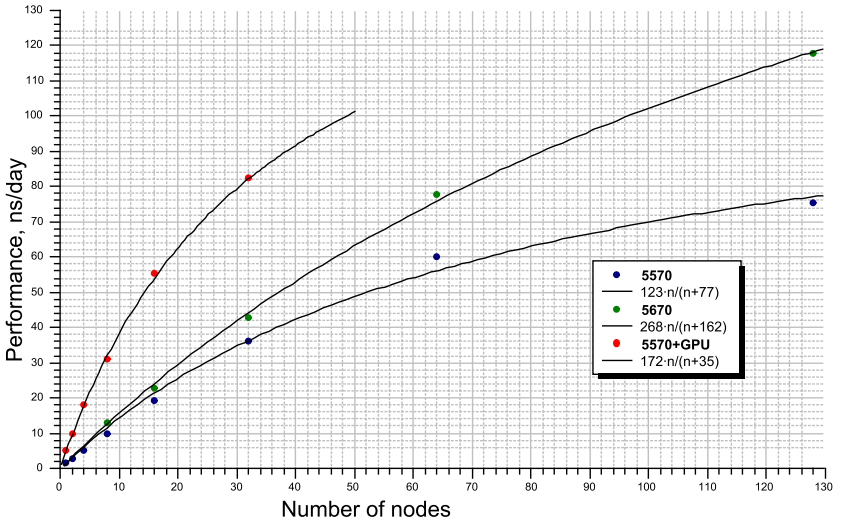

Figure 2. Benchmark of calculation of protein-protein plastocyanin-cytochrome f interaction using GROMACS full atomic molecular dynamic simulation. Each node contains two Intel Xeon (4-core 5570 or 6-core 5670) CPUs and two Nvidia Tesla X2070 GPUs. The curves are hyperbolic approximation of the benchmark points.

This work is supported by RFBR grants #11-04-01268-a, 12-07-33036-мол_а_вед and 12-04-31839-мол_а and by the Supercomputing Center of Lomonosov Moscow State University [4].

1 Kovalenko I.B., Abaturova A.M., Gromov P.A., Ustinin D.M., Grachev E.A., Riznichenko G.Y., Rubin A.B. *Direct simulation of plastocyanin and cytochrome f interactions in solution* // Phys. Biol. **2006**. Vol. 3. P. 121–129.

2 Hess B., Kutzner C., Van Der Spoel D., Lindahl E. *GROMACS 4: Algorithms for Highly Efficient, Load-Balanced, and Scalable Molecular Simulation* // Journal of Chemical Theory and Computation. American Chemical Society, **2008**. Vol. 4, № 3. P. 435–447.

3 Feenstra K.A., Hess B., Berendsen H.J.C. *Improving efficiency of large time-scale molecular dynamics simulations of hydrogen-rich systems* // Journal of Computational Chemistry. **1999**. Vol. 20, № 8. P. 786–798.

4 Voevodin V.V., Zhumatiy S.A., Sobolev S.I., Antonov A.S., Bryzgalov P.A., Nikitenko D.A., Stefanov K.S., Voevodin V.V. *Practice of "Lomonosov" Supercomputer* // Open Systems J. (Russian). **2012**. № 7.

"Golden triangle" for protein folding rates

Finkelstein A.[1,2], *Garbuzynskiy S.*[1]

[1] Institute of Protein Research, Russian Academy of Sciences,
142290 Pushchino, Moscow Region, Russia
[2] Pushchino Branch of the Moscow State Lomonosov University,
142290 Pushchino, Moscow Region, Russia

The ability of protein chains to spontaneously form their spatial structures is a long-standing puzzle in molecular biology. Experimentally measured rates of spontaneous folding of single-domain globular proteins range from microseconds to hours: the difference (11 orders of magnitude!) is akin to the difference between the life span of a mosquito and the age of the Universe. We show that physical theory with biological constraints outlines a "golden triangle" limiting the possible range of folding rates for single-domain globular proteins of various size and stability, and that the experimentally measured folding rates fall within this narrow triangle built without any adjustable parameters, filling it almost completely. In addition, the "golden triangle" predicts the maximal allowed size of the "foldable" protein domains, and the size of domains found in known protein structures is in a good agreement with this limit.

This work was supported by the Howard Hughes Medical Institute, the MCB RAS Program, RFBR, "Dynasty Foundation" and the Russian Young Scientists' grants.

Creation of potassium voltage-gated channel Kv1.2 model for molecular dynamic simulations

Gorkovets T.K., *Shaytan A.K.*

Faculty of Biology, Lomonosov Moscow State University

Voltage-gated ion channels are ubiquitous transmembrane proteins involved in electrical signaling in excitable cells. Potassium selective channels constitute the most diverse family among all ion channels.

Potassium voltage-gated channels are homotetrameres. Each subunit consists of six transmembrane helices, named S1 to S6 and connected by intra- and extra-cellular loops. S5 and S6 helices form the pore domain with the aqueous pore in the middle. Selectivity filter which picks out potassium ions over others lies on the extracellular side of the pore. Selectivity filter includes conservative amino acid sequence – threonine, valine, glycine, tyrosine, and glycine. Four subunits join to form a gate on the intracellular side.

S1-S4 helices form the voltage sensor domain. These helices have a lot of charged amino acids. Thus, the S4 helix contains six positively charged residues - five arginines and one lysine. These amino acids are not placed one after another, they are separated by hydrophobic residues, so they are stacked one above the other in alpha helices. The S1 helix contains three glutamates and one aspartate.

Dormantly the channel Kv1.2 is closed. It opens during depolarization. Increase of membrane potential results in conformational changes in the voltage sensor domain and the S4 helices move toward the outer side of the membrane. The opening of the channel is not instantaneous process. Between open and closed states there is intermediate state when the voltage sensor domains are activated but the pore is closed.

The pore domain is in closed state if connection between voltage sensor and pore domains is broken. This disorder leads to failures in cell work.

The malfunction of ion channels lead to serious diseases of the nervous, cardiovascular and muscular systems (epilepsy, long QT syndrome, episodic ataxia).

Molecular dynamics is a very useful method which allows to understand process of closing and opening on atomistic level. In our work we create a molecular dynamic model of open potassium voltage-gated channel Kv1.2 in lipid bilayer.

Now we have a stable system which consists of an open channel Kv1.2 embedded in POPC bilayer, water molecules and Cl^- and K^+ ions. System is prepared to further simulations with use of steered MD for channel closure.

Molecular dynamics studies of the DNA photolyase enzyme and visual pigment rhodopsin: Specifics of the chromophore conformations

Kholmurodov K.[1,2]

[1] Laboratory of Radiation Biology, Joint Institute for Nuclear Research, 141980, Dubna, Russia
[2] Dubna University, 141980, Dubna, Moscow Region, Russia
E-mail: mirzo@jinr.ru

Photolyases are monomeric proteins of 450-550 amino acids with two noncovalently bound chromophore cofactors (Fig. 1). One of the cofactors is always flavin adenine dinucleotide (FAD), and the second is either methenyltetrahydrofolate (MTHF) or 8-hydroxy-7,8-didemethyl-5-deazariboavin (8-HDF). The latter, MTHF or 8-HDF, acts as a photoantenna and transfers excitation energy to the catalytic $FADH^-$ cofactor through non-radiative Forster resonance energy transfer (FRET) – via dipole–dipole

coupling between folate and flavin. It is worth noting that the unique FAD-binding domain with its high degree of sequence identity in the environment forms a family of highly homologous photolyase/cryptochrome proteins. From bacteria to mammals, these two types of proteins carry out distinct functions: photolyase harnesses blue light energy to break bonds and repair UV photoproducts in DNA; and cryptochrome is a sensor of environmental light-regulating circadian entrainment in animals and plants. In the present work, the FAD conformational and dynamic behaviors were studied in the whole DNA photolyase enzyme structure. Unlike earlier works, our study simulates the complex structure of the DNA photolyase protein containing $FADH^-$, MTHF, and DNA molecules and embedded in different water solvent baths. Using molecular dynamics (MD) simulation, we aimed to compare conformational changes of the FAD cofactor with the constituent fragments of the molecular system under consideration. The molecular surfaces of the MHF, DNA, and FAD indicate that the MTHF and DNA molecules undergo negligible configuration changes; MTHF and DNA remain in a frozen state at a low temperature. At the same time, the FAD configuration changes periodically throughout the simulation period, from the "closed" U-shaped to the "open" I-shaped one. Such FAD configuration behavior looks like "butterfly motion". The transition from the U-shaped configuration, the FAD's original one revealed by X-ray structure analysis, to the I-shaped configuration results in the FAD molecule not being allowed to stay inside the enzyme pocket. Obviously, the DNA photolyase enzyme cannot properly place FAD's I-shaped configuration and keep FAD at the binding site [1].

The FAD chromophore binding inside the DNA photolyase pocket has many similarities with 11-*cis* retinal chromophore binding in opsin proteins (Fig. 2). Opsins are expressed in the rods and cones in the back (outer) part of the retina; photolyase/cryptochrome proteins are expressed in the front (inner) part of the retina. Opsins initiate phototransduction by *cis*-*trans* isomerization of retinal by light; the transition from 11-*cis* to all-*trans* dislodges 11-*cis* retinal from the protein. Thus, all-*trans* retinal behaves like I-shaped FAD and cannot be allowed to stay any longer inside the chromophore pocket [2]. On the other hand, the FAD chromophore, as its form changes from the "closed" U-shaped to the "open" I-shaped, should also leave the protein. Thus, two photosensory systems in mammals – the 3D visual system and the circadian photosensory system – are related by their chromophores. We should note that for the opsin+retinal photoreceptors, the signal phototransduction mechanism is already known; for the cryptochromes (circadian photoreceptors with the folate (MTHF) and flavin (FAD) chromophores), the phototransduction mechanism is still unknown.

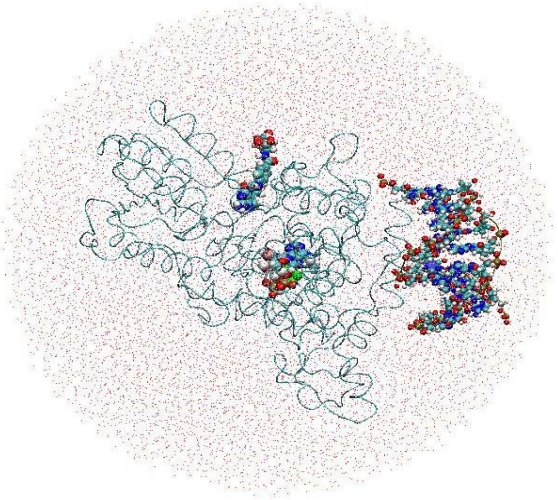

(A)

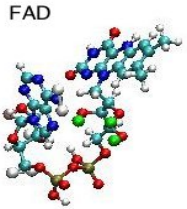

(B)

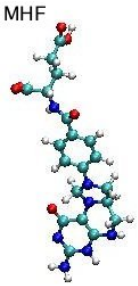

(C)

Figure 1. (A) A model of a DNA photolyase protein with two cofactors and the DNA chain is shown. The $FADH^{-}$ (B; FAD) and MTHF (C; MHF) cofactors and DNA (right) are shown as spherical balls.

1 Kholmurodov K., Dushanov E., Yasuoka K. *Molecular Dynamics Simulations of a DNA Photolyase Protein : High-Mobility and Conformational Changes of the FAD Molecule at Low Temperatures* // Advances in Bioscience and Biotechnology, Vol.3 No.3, June **2012**, PP.169-180, DOI: 10.4236/abb.2012.33025.

2 Kholmurodov K.T. *Computer Molecular Dynamics Studies on Protein Structures (Visual Pigment Rhodopsin and Cyclin-Dependent Kinases)* / AIP Conf. Proc. 912, 495 (**2007**); Outlined by the American Institutes of Physics, AIP Journal and Proceedings Articles Related to G-Protein-Coupled Receptors http://journals.aip.org/NobelChemistry2012.html

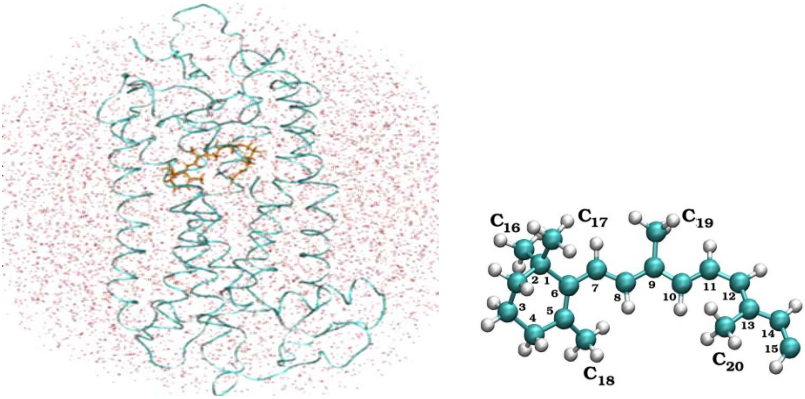

(A) (B)

Figure 2. A model of a visual pigment rhodopsin (A) with 11-*cis*-retinal in the rhodopsin chromophore center (B).

Density-based clustering as a tool for analysis of molecular simulation data and its application to barnase-barstar co-diffusion case study

Khruschev S.S., Kovalenko I.B., Riznichenko G.Yu.

Lomonosov Moscow State University, School of Biology, Biophysics Department
E-mail: styx@biophys.msu.ru

Protein-protein interactions are of central importance for virtually every process in living matter. Modeling the dynamics of protein association is crucial for understanding their functionality. We don't have any silver-bullet technique for such modeling. Computational complexity of *ab initio* methods allows to apply them for systems of up to a few hundreds of atoms, thus forcing to use a set of empirical methods for protein modeling. Molecular dynamics (MD) is a valuable method for studying conformational changes in proteins. Modern MD software such as GROMACS [1] utilizing hybrid (CPU+GPU[2]) computing acceleration allows full-atomic simulation of up to 80–100 nanoseconds model time per day for two proteins in explicit solvent box [2]. MD may be combined with Brownian dynamics (BD) techniques (multiparticle BD [3] in particular) to allow complete reconstruction of protein-protein interaction over large temporal and spatial scales. Nowadays we don't

[2] Central Processor Unit + Graphics Processing Unit

have one conventional procedure to analyze data produced by such techniques. Obtaining protein-protein and protein-solvent interaction energies is rather straightforward, but taking entropy into account may be quite tricky.

Cluster analysis is widely used to determine metastable conformations of simulated systems, but most algorithms lack mathematical rigor and thus produce unpredictable results in non-standard conditions. Most algorithms rely on direct access to object data that may be unacceptable in the case of MD data due to very high dimensionality of such data and requirement to use very special comparison functions for these data. Thus in general only clustering algorithms considering data points as graph vertices are quite robust. Density-based clustering [4] is a generic family of hierarchical algorithms that relies upon distances between two datapoints. Such distances may be calculated in various ways; atomic root-mean-square displacement (RMSD [5]) may be taken as a good measure for geometrical dissimilarity. Unlike convenient distances such as Euclidean or Mahalanobis, RMSD computational cost is rather high, so existing density-based clustering algorithms [6, 7] should be adopted to use pre-calculated distance matrix. To smooth random fluctuations in structure distribution *core distance* (*CD*) for each structure is calculated as RMSD distance to *minPts*-th most similar structure. Building cluster hierarchy is a two-stage process. The first stage implies ordering structures according to their *reachability distance* (*RD*) from already processed set of structures. This set may be initiated by a single structure chosen as a structure with minimal *CD* (an arbitrary datapoint in original algorithm). A single unprocessed structure having minimal RMSD to any of already processed structures is processed at each iteration; its *RD* is taken as above mentioned RMSD value if it is greater than structure's *CD* or as its *CD* value otherwise. Dataset ordered by such procedure is a direct representation of a classical hierarchical clustering diagram, so the second stage is to extract reasonable-sized clusters from it [8]. It is assumed that clusters are "valleys" separated by local maxima of *RD*; clusters with less than *minPts* structures are not taken into account. So, intuitively clusters are defined as "dense" groups of structures separated by more "loose" areas.

We implemented OPTICS/DeLiClu-like [6, 7] hierarchical density-based clustering algorithms modified according to mentioned above peculiarities as a patch to GROMACS `g_cluster` utility. To use this algorithm one should pass `-method density` parameter and specify *minPts* value in `-M` parameter (which should be generally set to approximately 1% of total number of structures). Input and output files are standard for other clustering methods; if pre-calculated distance matrix is used it should be saved and loaded in binary rather than XPM format as quantization used in this format may lead to clustering artifacts (corresponding `-dmb` parameter is introduced for `g_cluster`, matrix can be calculated by `g_rms` utility; `-dmb` parameter for

`g_cluster` is introduced to load such matrix). To visualize cluster tree on the reachability distance plot `-rd` parameter should be used to save it as an XVG file.

Density-based clustering was used to study energetically favorable states observed in multiparticle BD simulation of co-diffusion of barnase and barstar proteins [9]. 22,707 structures of encounter complexes with electrostatic attraction energy higher than $k \cdot T \approx 2.5$ kJ·mol^{-1} were sampled. Cluster analysis with *minPts* = 300 was performed and 13 clusters were obtained. *Reachability distance* plot and corresponding structures visualized by PyMOL are shown on the figure below. It is shown that most probable energetically favorable diffusional encounter structures (a) considerably differ from physiologically significant complex (d) and resemble one of crystal symmetry position (b) [10]. This result is in accordance with [11] and confirms that mutual orientation of barnase and barnase in inhibitory complex is achieved due to hydrophobic effects and conformational changes ignored in BD simulation. Minor configuration group (c) is quite similar to physiological inhibitory complex (d). Another minor configuration group (e) does not have any physiological or X-ray structure counterpart; however it is much more "loose" than above mentioned structures.

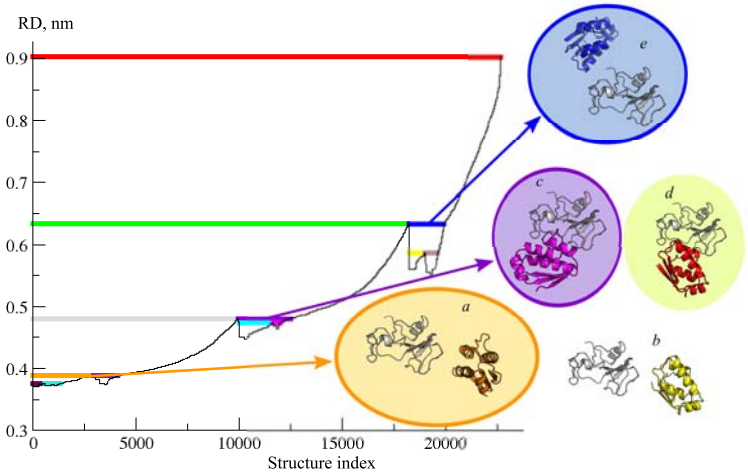

Figure. Reachability distance plot for 22,707 energetically favorable encounter complexes of barnase and barstar obtained by multiparticle Brownian dynamics simulation. "Central" structures (i.e. structures having minimal average RMSD to all other structures in cluster) of several clusters are shown (a, c, e) beside corresponding X-ray structures (PDB ID: 1BGS).

This work is supported by RFBR grants №11-04-01268-a, 12-07-33036-мол_а_вед and 12-04-31839-мол_а and by the Supercomputing Center of Lomonosov Moscow State University [12].

1 Hess B., Kutzner C., Van Der Spoel D., Lindahl E. *GROMACS 4: Algorithms for Highly Efficient, Load-Balanced, and Scalable Molecular Simulation* // Journal of Chemical Theory and Computation. American Chemical Society, **2008**. Vol. 4, № 3. P. 435–447.

2 Fedorov V.A., Khruschev S.S., Kovalenko I.B. *Computer simulation of intermolecular complex formation of photosynthetic electron transport proteins plastocyanin and cytochrome f* / Computational and theoretical modeling of biomolecular interactions. Moscow-Izhevsk: Institute of Computer Science, **2013**.

3 Riznichenko G.Y., Kovalenko I.B., Abaturova A.M., Diakonova A.N., Knyazeva O.S., Ustinin D.M., Khruschev S.S., Rubin A.B. *Multiparticle computer simulation of protein interactions in the photosynthetic membrane* // Biophysics. **2011**. Vol. 56, № 5. P. 757–767.

4 Kriegel H.-P., Kröger P., Sander J., Zimek A. *Density-based clustering* // Wiley Interdisciplinary Reviews: Data Mining and Knowledge Discovery. **2011**. Vol. 1, № 3. P. 231–240.

5 Kabsch W. *A solution for the best rotation to relate two sets of vectors* // Acta Crystallographica Section A. International Union of Crystallography, **1976**. Vol. 32, № 5. P. 922–923.

6 Ankerst M., Breunig M.M., Kriegel H.-P., Sander J. *OPTICS: Ordering Points To Identify the Clustering Structure* // Proceedings of ACM SIGMOD, Philadelphia, PA. **1999**. P. 49–60.

7 Elke A., Böhm C., Kröger P. *DeLiClu: Boosting Robustness, Completeness, Usability, and Efficiency of Hierarchical Clustering by a Closest Pair Ranking* // Proceedings of the 10th Pacific-Asian Conference on Advances in Knowledge Discovery and Data Mining. **2006**. P. 119–128.

8 Sander J., Qin X., Lu Z., Niu N., Kovarsky A. *Automatic Extraction of Clusters from Hierarchical Clustering Representations* // Proceedings of the 7th Pacific-Asia Conference on Knowledge Discovery and DataMining (PAKDD), Seoul, Korea. Springer-Verlag, **2003**. P. 75–87.

9 Khrushchev S.S., Abaturova A.M., Diakonova A.N., Ustinin D.M., Zlenko D. V., Fedorov V.A., Kovalenko I.B., Riznichenko G.Y., Rubin A.B. *Multi-particle Brownian Dynamics software ProKSim for protein-protein interactions modeling* // Computer Research and Modeling (Russian). **2013**. Vol. 5, № 1. P. 47–64.

10 Guillet V., Lapthorn A., Hartley R.W., Mauguen Y. *Recognition between a bacterial ribonuclease, barnase, and its natural inhibitor, barstar* // Structure. **1993**. Vol. 1, № 3. P. 165–176.

11 Spaar A., Dammer C., Gabdoulline R.R., Wade R.C., Helms V. *Diffusional Encounter of Barnase and Barstar* // Biophys. J., **2006**. Vol. 90, № 6. P. 1913–1924.

12 Voevodin V.V., Zhumatiy S.A., Sobolev S.I., Antonov A.S., Bryzgalov P.A., Nikitenko D.A., Stefanov K.S., Voevodin V.V. *Practice of "Lomonosov" Supercomputer* // Open Systems J. (Russian). **2012**. № 7. [http://www.osp.ru/os/2012/07/13017641]

Simulation of the mammalian retina's electrical response

Kolesnikova E.A., Belov O.V.

Joint Institute for Nuclear Research, Dubna, Russia

The main aim of the study is development of a computational method that would allow use of data from experimental animal studies to estimate key biophysical parameters of the retina and their changes under environmental factors of the physical and chemical nature. Electroretinography (ERG) is a common method of assessing the retina's functional activity. The curve obtained in electroretinographic research characterizes the integral response of different types of cells in the retina to a light flash. Mathematical models are used for the quantitative analysis of the measured data. Among them, Hood-Birch and Ashmore-Falk models are widely used. However, a simple combination of these models does not allow a detailed description of a number of ERG patterns with a set of multiple distinct maximums and minimums. An example of such curve is the mouse ERG. Using Hood-Birch and Ashmore-Falk models in their original forms, it is not possible to perform a detailed mathematical analysis of the curve and estimate the change in the basic parameters of the processes occurring in the retina.

We propose a new approach based on the chosen models. It allows determination of numerical values of the parameters that characterize the maximum response of the photoreceptors and their sensitivity, taking into account the ERG pattern complicacy. Separate parts of the ERG pattern were described with the expansion of the model parameters to the components, which allows a more detailed quantitative analysis of the curves and appliance of the approach to the electrical responses of specific forms. We used the proposed computational method to perform a comparative analysis of an ERG pattern obtained in experiments on the effect of the chemical agent methylnitrosourea (MNU) on the functional activity of the mouse retina. It is known that MNU is a potent mutagen. It can cause serious disorder in the retina’s functioning and, in certain concentrations, lead to its degeneration. The mathematical analysis of the experimental curves allows estimating quantitatively the change in the maximum response and sensitivity of the photoreceptors in response to the effect of MNU in different concentrations.

We plan to apply the proposed computational method to the analysis of the experimental data on the effects of ionizing radiations of different quality on the functional activity of the mammalian retina. In addition, the proposed approach can be used to build a mathematical model relating the retina's integral response measured in an ERG study with electrochemical processes in the retina.

The work was partially supported by JINR grant No. 13-092-02.

1 Hood D.C., Birch D.G. *Computational models of rod-driven retinal activity* // IEEE Engineering in Medicine and Biology, Volume 14, Issue 1, **1995**. Pp. 59-66.
2 Ashmore J.F., Falk G. *Responses of rod bipolar cells in the dark-adapted retina of the dogfish, Scyliorhinus Canicula* // Journal of Physiology, Volume 300, Issue 1, **1980**. Pp. 115-150.
3 Ostrovsky M.A., Tronov V.A., Vinogradova Yu.V. *Changes in the functional activity of the mouse retina after the effect of genotoxic* // JINR News, Issue 4, **2011**. Pp. 22-24.

Stability of a pore in phospholipid bilayer in different phase states in the presence of SDS molecules: MD simulations and free energy perturbation analysis

Kolganov A.S.[1], *Nesterenko A.M.*[1,2]

[1] Lomonosov Moscow State University, Faculty of Biology, Department of Biophysics
[2] A.N. Belozersky Institute of Physico-Chemical Biology MSU

Poration of plasmatic membrane plays a crucial role in the life of a cell. This process is responsible for the passive transport of hydrophilic molecules and for membrane lysis in the presence of different agents. Pore formation is often studied on bilayer lipid membranes in natural and computational experiments. A pore can be induced by mechanic, electric or osmotic stress and its formation occurs with characteristic time of about tens of nanoseconds. Direct observations are very hard on such small timescale so computational experiments become a handy tool for studying molecular mechanisms of the pore formation process.

The goal of this study was to simulate a bilayer poration in different phases states and in the presence of simplest detergent, SDS, and to estimate a stability of porated bilayers. The general measure of stability of an equilibrium molecular system is a free energy. In order to calculate free energy difference, gradual transition between initial and final states (porated and intact) was simulated. Model systems were simulated with molecular dynamics by GROMACS in Berger force-field implemented for OPLS-AA force field [1]. An integration step of 0.2 fs was used for calculations. A model scene includes lipid bilayer in OXY-plane surrounded by the solution (explicit TIP3P water) with 150 mM concentration of NaCl. The porated bilayer stability was achieved by introducing semi-cylindric LJ potential between central *z*-axis and carbon atoms of lipid alcane chains (Fig. A). Initial system contains a pore of radius 1.5 nm. Parameter λ was included into LJ potential as:

$$U = (1-\lambda)\varepsilon\left[\left(\frac{\sigma}{r}\right)^{12} - \left(\frac{\sigma}{r}\right)^{6}\right]$$

Thus pore size can be varied with λ parameter ($\lambda = 0$ corresponds to the biggest pore while $\lambda = 1$ means that there's no pore). 6 different model systems were studied: 3 bilayers in gel state constituted by DPPS and SDS in ratios 1:0, 9:1 and 7:3, and 3 bilayers in liquid-crystalline state constituted by DOPE and SDS in the same ratios. Each model was equilibrated for different λ values varying from 1 to 0. Thus gradual pore vanishing was simulated and a "reaction returning force" (the force that returns bilayer to the unporated state) was calculated from MD as analytical derivative $\frac{\partial U}{\partial \lambda}$. This derivative was further used to calculate free energy difference between intact and porated states that is valid in the case of quasi-equilibrium process.

Theoretical descriptions of pores distinguish hydrophilic and hydrophobic pores. Only hydrophilic pores were formed in simulations i.e. polar head groups were exposed into a transmembrane water channel after the equilibration. A general view of the "reaction returning force" is presented in the figure B. It can be concluded that pore formation has three different phases: a phase of elastic growth, a phase of inelastic growth and a phase of irreversible growth. In the phase of elastic growth reaction force is proportional to the pore radius, in the inelastic phase force becomes much smaller. In the plot of "returning force" there is a maximum in inelastic phase. In the last phase force becomes negative and the pore grows spontaneously.

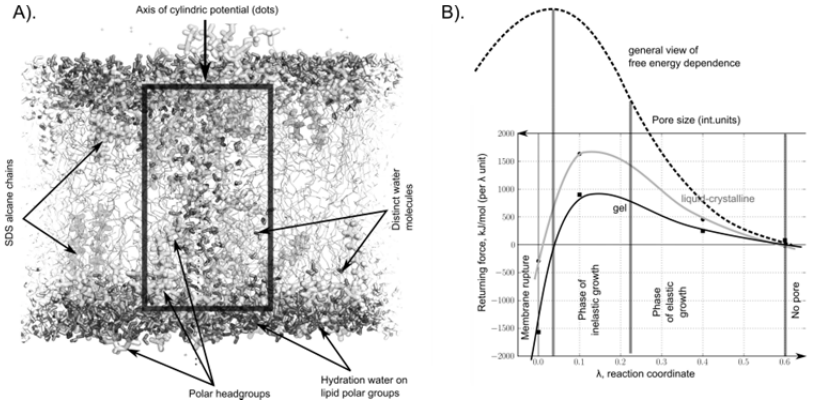

Figure.

A. View of the model scene of DOPS:SDS bilayer system with pore in equilibrium state ($\lambda = 0.3$). Only one hydration shell is depicted. **B.** The dependence of a "reaction returning force" on λ value for the bilayer in gel and liquid-crystalline phase state. Common view of free energy dependence is also plotted. Three phases of pore growth are separated with vertical lines.

The behavior of free energy depending on the pore radius qualitatively reproduces the classic model proposed by Lister [2]. For the system constituted by DOPS:SDS (7:3) free energy of formation of the pore with radius 1.5 nm equals 425 kJ/mol that agrees with value obtained in computational study using technique called "Potential of Mean Constraint Force" [3]. A kinetic barrier of the pore formation proposed by other studies [3] was not observed for chosen reaction pathway in our computational experiments. It's possible to draw a conclusion that present implementation of FEP technique is applicable for estimation of the pore formation free energy. This energy decreases both when SDS is added to the bilayer and when bilayer changes its phase state to gel state. These conditions also lead to decrease of the pore critical radius (radius of irreversible growth start).

The work is supported by the RFBR (project no. 11-03-01109-a). MD calculations were performed using supercomputers of MSU Research Computing Center [4].

1 Nesterenko A.M., Ermakov Yu.A. Biochemistry (Moscow) Supplement Series A: Membrane and Cell Biology, **2013**, 6(4), 320–328. doi:10.1134/S1990747812050145

2 Lister J.D. Physics Letters, **1975**, 53(3), 193–194. doi:10.1016/0375-9601(75)90402-8

3 Wohlert J., den Otter W.K., Edholm O., Briels W.J. The Journal of chemical physics, **2006**, 124(15), 154905. doi:10.1063/1.2171965

4 Voevodin V.V., Zhumatiy S.A., Sobolev S.I., Antonov A.S., Bryzgalov P.A., Nikitenko D.A., Stefanov K.S., Voevodin V.V. Open Systems J. (Russian). **2012**. № 7. [http://www.osp.ru/os/2012/07/13017641]

Structural transitions and energy landscape for Cowpea Chlorotic Mottle Virus capsid mechanics from nanoindentation *in vitro* and *in silico*

Kononova O.[1], Snijder J.[2], Brasch M.[3], Cornelissen J.[3], Dima R.I.[4], Marx K.A.[1], Wuite G.J.L.[2], Roos W.H.[1,#], Barsegov V.[1,]*

[1] Department of Chemistry, University of Massachusetts, Lowell, MA 01854, USA
[2] Natuur- en Sterrenkunde and LaserLab, Vrije Universiteit, 1081 HV Amsterdam, The Netherlands
3 Biomoleculaire Nanotechnology, Universiteit Twente, 7500 AE Enschede, The Netherlands
4 Department of Chemistry, University of Cincinnati, Cincinnati, OH 45221, USA
[*] E-mail: Valeri_Barsegov@uml.edu, tel: 978-934-3661, fax: 978-94-3013
[#] E-mail: wroos@few.vu.nl, tel: +31 20 59 83974, fax: +31 20 59 87991

Physical properties of viral capsids are important factors in capsid self-assembly, virus survival in the extracellular environment, and cell infectivity. By comparing AFM experiments [1] with computational modeling, using GPU based molecular dynamics simulations [2] on sub-second timescales of the indentation nanomechanics of Cowpea Chlorotic Mottle Virus (CCMV) capsid, we show that the capsid's physical properties are in agreement with obtained by the two methods. Furthermore, the modeling demonstrates that the capsid's physical properties are dynamic and local characteristics, which depend on the magnitude and geometry of mechanical input. Surprisingly, under large deformations the CCMV capsid transitions to the collapsed state without substantial structural alterations. The enthalpy change (11.5–12.8 MJ/mol) and entropy change (5.1 – 5.8 MJ/mol) in this state are due to large-amplitude out-of-plane excitations (capsid bending) and coherent in-plane rearrangements of protein chains (capsid stiffening), respectively. Dynamic coupling of these modes defines the extent of reversibility of deformation. This emerging picture illuminates how the capsids' unique physico-chemical properties help determine their corresponding viruses' biological function.

1 Roos W.H., Bruinsma R., Wuite G.J.L. *Physical virology* // Nat. Phys. **2010**. 6, 733-743.
2 Zhmurov A., Dima R.I., KholodovY., Barsegov V. *SOP-GPU: accelerating biomolecular simulations in the centisecond timescale using graphic processors* // Proteins. **2010**. 78, 2984-2999.

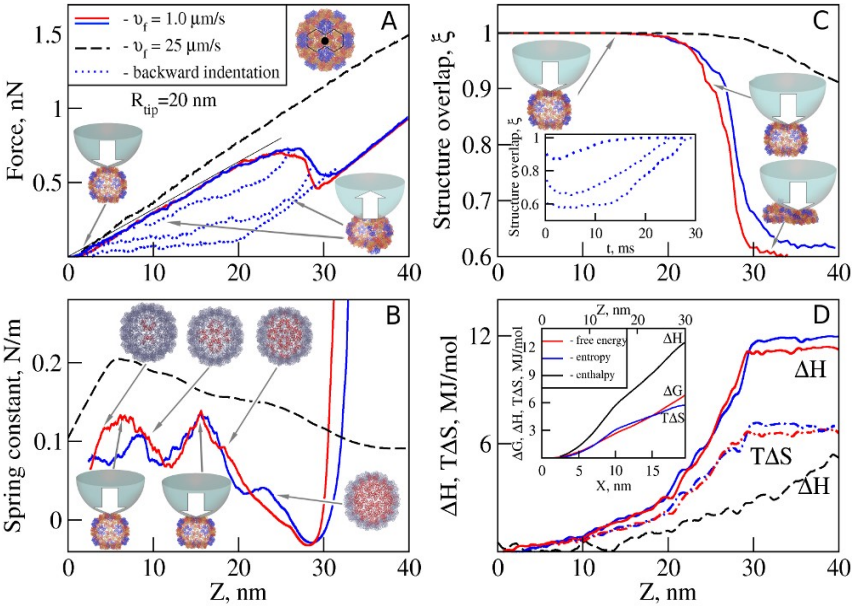

Figure 1. Forced indentation *in silico* of CCMV capsid along the two-fold symmetry axis. The cantilever tip (*Rtip* = 20 nm) indents the capsid in the direction perpendicular to the capsid surface (*vf* = 1.0 μm/s). Results for the forward deformation and backward retraction are represented by the solid and dotted curves, respectively; results obtained for *vf* = 25 μm/s are shown for comparison (dashed black curve). (A): The FZ curves (a linear fit to the initial portion of the curve is shown as a gray line). (B): Capsid spring constant, *kcap* versus *Z*. (C): Structure overlap function *ξ* versus *Z* (the *inset* shows the time-dependence of *ξ* for the backward retraction, which quantifies the progress of capsid restructuring). (D): The enthalpy change *ΔH* and entropy change *TΔS* from the FZ curves generated for *vf* = 1.0 μm/s (the curve of *ΔH* generated for *vf* = 25 μm/s is presented for comparison). The *inset* shows equilibrium energy change *ΔG* along the reaction coordinate *Z* (piezo displacement, top *x*-axis) and *X* (extent of indentation, bottom *x*-axis) from Umbrella Sampling calculations. Also shown are the CCMV capsid structures (top view and profile) for different extents of indentation. The top view displays the tip-capsid surface contact area shown in red color.

The study of lipopolysaccharides and metallophtalocyanines binding mechanism

Kovalenko I.B.[1,2], *Galochkina T.V.*[1,2], *Strakhovskaya M.G.*[1], *Kovalenko S.Yu.*[2], *Zlenko D.V.*[1], *Mamonov P.A.*[1], *Nesterenko A.*[1], *Khruschev S.S.*[1], *Averyanov A.V.*[2]

[1] Lomonosov Moscow State University
[2] Federal Research and Clinical Center of the Federal Medical Biological Agency of Russia

Despite of the significant progress achieved in the field of infectious diseases treatment, sepsis is one of the important problems of modern medicine. In sepsis caused by the gram-negative infection endotoxins entering the bloodstream from the destroyed bacteria cells play a key role in the development of system inflammatory response, sepsis and septic shock. By its chemical structure endotoxins are considered to be lipopolysaccharides (LPS), and they are the main component of the outer membrane which is part of the cell wall of gram-negative bacteria. The hydrophilic part of the LPS molecule carries a negative charge. The total negative charge of LPS is connected to high content of negatively charged groups in the central part of these molecules – phosphoric acid residues in the lipid A D-glucosamine and/or core heptoses, carboxyl groups of 3-desoxy-D-manno-octulosonic acid residues and core acidic sugars (galactose, glucuronic acid). The high density of negative charges on LPS from cell walls of the gram-negative bacteria causes effective electrostatic attraction of cations and polycations. As the authors have discovered, polycationic metallophtalocyanines effectively bind LPS molecules of the bacteria cells by the electrostatic mechanism which is indicated by a dramatic drop in fluorescence signal.

The authors have synthesized a number of cationic phtalocyanines [1]. The synthesized heterogeneous sorbents are characterized by their physico-chemical and spectral properties allowing further testing of their affinity for LPS. Synthesized sorbents differ by a number of parameters: a charge of a metallophtalocyanine molecule (4+, 6+, 8+ for the different number of the cationic lateral substituents), the nature of the metal central atom in metallophtalocyanine molecule (zinc, aluminium or silicon), the length of spacer which binds the molecules of the phtalocyanines to the medium, and quantity of the bound phtalocyanines and the size of the medium pores.

We study the complex formation process between the LPS molecules from the cell walls of microorganisms and phtalocyanines by methods of molecular and Brownian dynamics. We develop an algorithm for determining the binding affinity of phtalocyanines to LPS with different surface charges. Spatial configurations of LPS complexes and phtalocyanines agents are

studied. This will allow choosing the optimal structures of LPS-binding agents for LPS from the different types of bacteria.

Computer simulation of molecular complex formation process considering diffusion, electrostatic and hydrophobic interaction, conformational mobility of molecules is a problem which requires a lot of computational resources. The calculations are performed using supercomputer complex of Moscow State University.

1 Kuznetsova N. A., Yuzhakova O. A., Strakhovskaya M. G., Shumarina A. O., Kozlov A. S., Krasnovsky A. A., Kaliya O. L. *New heterogeneous photosensitizers with phthalocyanine molecules covalently linked to aminopropyl silica gel* // Journal of Porphyrins and Phthalocyanines, **2011**, 15(07n08), 718–726. doi:10.1142/S1088424611003690

Computer simulation of interaction of electron transport proteins in photosynthetic membranes of cyanobacteria

Kovalenko I.B., Knyazeva O.S., Riznichenko G.Yu., Rubin A.B.

Lomonosov Moscow State University, Leninskie Gory, Moscow, 119992, Russia
E-mail: ikovalenko78@gmail.com

This work is devoted to computer simulation of complex formation of protein plastocyanin (Pc) with transmembrane pigment-protein complex photosystem I (PSI) and subunit f of cytochrome bf complex (Cyt f) in cyanobacterium *Phormidium Laminosum*. Pc is a small copper containing protein. Pc molecules transfer electrons in chloroplast thylakoid lumen from Cyt f to photooxidized P700 in PSI.

To a good approximation, the initial preliminary protein-protein complexes form by rigid-body association [1] in which diffusion and long-range electrostatic interactions play the key role. Efficiency of electrostatic interactions depends on charge distribution on the proteins and ionic strength and can be estimated by methods of computer modeling such as Brownian dynamics.

We present computer models of complex formation of *Phormidium laminosum* Pc with PSI and Cyt f in solution based on our theoretical Brownian dynamics method for computer simulation of encounter complex formation described in detail in [3]. The algorithm explicitly considers diffusion and electrostatic interactions of protein molecules, taking into account the final complex formation and electron transfer implicitly. In the algorithm each protein molecule is represented as a 3D rigid body, its individual geometric surface is designed using the structure from the Protein Data Bank (PDB,

www.pdb.org). We used Pc and Cyt f structures from *Phormidium laminosum* (PDB IDs are 2Q5B and 1CI3, respectively) and PSI structure from *Thermosynechococcus elongatus* (PDB ID is 1JB0).

For calculation of the rate constants of Pc-PSI and Pc-Cyt f bimolecular reactions we simulated protein-protein complex formation in solution. In the process of simulation a hundred of protein molecules of each type diffuse and interact in the cubic reaction volume with 160 nm sides. For simulation of translational and rotational Brownian diffusion of molecules we used the Langevin equation as described in [3].

To simulate electrostatic interactions of the proteins the electrostatic potential grid around each type of the protein was calculated by solving numerically the linearized Poisson-Boltzmann equation as described in (Knyazeva et al., 2010). In this calculation proteins were presented as low dielectric areas ($\varepsilon = 2$) with spatially fixed partial charges, the solution was presented as a high dielectric area ($\varepsilon = 80$) with mobile charges (ions), implicitly described through ionic strength. pH 7.5 of the solution is taken into account in the Poisson-Boltzmann calculation.

In the simulation two proteins are supposed to form a complex if the distances between the redox centers of the protein molecules become less than a certain parameters of the model named the docking distances. For Pc-PSI reaction we used 28 Å as a docking distance between Mg atom in P700 of PSI and Cu atom in Pc. As docking distances we chose 22 Å between Fe atom in Cyt f haem and Cu atom in Pc, and also 14 Å between CD1 atom of Phe3 residue in Cyt f and nitrogen atom of His82 of Pc.

After any two protein molecules form a complex they are not further considered in the simulation. By calculating directly the number of the complexes formed at each time step, we obtain the time curve of the complex formation process. We use this calculated curve to estimate the second order association rate constant of the reaction by fitting the calculated curves by the mass action law and compare them with the experimental data.

The results of the computer simulation show that in cyanobacteria for wild-type (wt) Pc the rate constant of complex formation only slightly depends on ionic strength for both reactions, Pc-PSI and Pc-Cyt f. This means that electrostatic interactions do not play any significant role in protein binding, at least for wt proteins, and the reaction occurs mainly due to diffusion. In our recent papers [3, 4] we calculated the ionic strength dependence of complex formation of the similar proteins from higher plants (spinach Pc and turnip Cyt f, PDB ID is 2PCF; PSI with light harvesting complex I, PDB ID is 2O01). In contrast to cyanobacterial proteins, in higher plants electrostatic interactions play a very important role accelerating Pc-cyt f and Pc-PSI reactions by more than an order of magnitude (Figure 1).

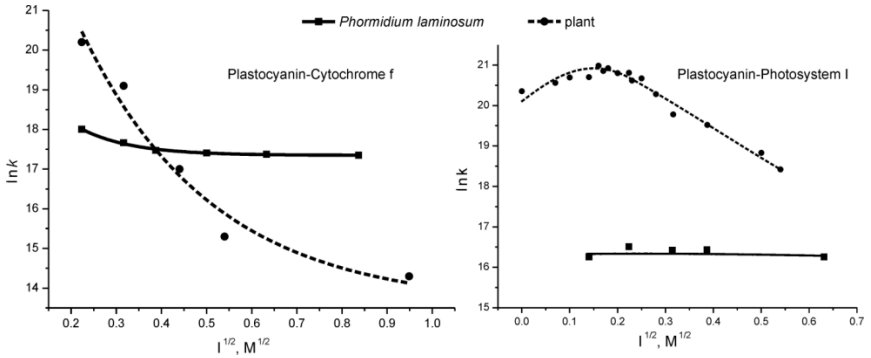

Figure 1. Logarithm of the rate constant of complex formation between plastocyanin and cytochrome f (left) and plastocyanin and photosystem 1 (right) obtained in computer simulations as a function of square root of ionic strength for cyanobacteria (solid line) and higher plants (dashed line, [3, 4].

Charge-changing mutations alter the distribution of electric charge on the protein surface thus making the reaction dependent on electrostatic interactions. Using the computer model we studied the dependence of *Phormidium laminosum* protein-protein complex formation rate on ionic strength and type of Pc mutation. We compare the results of the calculation with the experimental ionic strength dependence for *Phormidium laminosum* Pc-Cyt f reaction [5] and Pc-PSI reaction [6]. There is an agreement between the experiment and the calculation: D44A mutant is faster than the wt, while K53A and R93A are slower and R93E is the slowest both in experiment and computer simulation.

The calculated rate of Pc-PSI complex formation in cyanobacteria is 50 times lower than in higher plants at 100 mM ionic strength ($5 \cdot 10^8$ $M^{-1}s^{-1}$ in higher plants [4] and 10^7 $M^{-1}s^{-1}$ in cyanobacteria). The cause of this difference in the reaction rate values and the character of the ionic strength dependence may be related to the electrostatic properties of the photosystems. In cyanobacteria the electrostatic repulsion between Pc and PSI dominates whereas in higher plants electrostatic interactions favor the attraction of negatively charged Pc to positively charged docking site on PSI. Indeed, in higher plants, Pc binds to the luminal parts of subunits PsaA, PsaB and PsaF of PSI, and N-terminus of PsaF is longer compared to cyanobacteria and carries positively charged amino acid residues which promote effective binding of Pc to PSI.

This work was supported by the Russian Foundation for Basic Research (project nos. 11-04-01268, 12-07-33036 and 12-04-31839).

1 Janin J., Hames B. D., Glover D. M. *Kinetics and Thermodynamics of Protein-Protein Interactions* / In C. Kleanthous (Ed.), Protein-Protein Recognition (pp. 1–32). Oxford: Oxford University Press, **2000**.
2 Knyazeva O. S., Kovalenko I. B., Abaturova A. M., Riznichenko G. Y., Grachev E. A., Rubin A. B. *Multiparticle computer simulation of plastocyanin diffusion and interaction with cytochrome f in the electrostatic field of the thylakoid membrane* // Biophysics, **2010**, 55(2), 221–227.
3 Kovalenko I. B., Abaturova A. M., Gromov P. A., Ustinin D. M., Grachev E. A., Riznichenko G. Y., Rubin A. B. *Direct simulation of plastocyanin and cytochrome f interactions in solution* // Phys. Biol., **2006**, 3, 121–129.
4 Kovalenko I. B., Abaturova A. M., Riznichenko G. Y., Rubin A. B. *Computer simulation of interaction of photosystem 1 with plastocyanin and ferredoxin* // BioSystems, **2011**, 103, 180–187.
5 Schlarb-Ridley B. G., Bendall D. S., Howe C. J. *The role of electrostatics in the interaction between cytochrome f and plastocyanin of the cyanobacterium Phormidium laminosum* // Biochemistry, **2002**, 21, 3279–3285.
6 Schlarb-Ridley B. G., Navarro J., Spencer M., Bendall D. S., Hervás M., Howe C. J., De la Rosa M. *Role of electrostatics in the interaction between plastocyanin and photosystem I of the cyanobacterium Phormidium laminosum* // European Journal of Biochemistry, **2002**, 269(23), 5893–5902. doi:10.1046/j.1432-1033.2002.03314.x

Specificity of DNA and Zn-finger domain binding. MD simulation and MM-PBSA thermodynamic analysis

Kukushkin D.V.[1], *Nesterenko A.M.*[1,2], *Zlenko D.V.*[1]

[1] Lomonosov Moscow State University, Faculty of Biology, Department of Biophysics
[2] A.N. Belozersky Institute of Physico-Chemical Biology, MSU

Specific interactions of the macromolecules play a crucial role in different biological processes. One of the most important interactions is binding of DNA-recognizing proteins to specific DNA sequences. The present work is devoted to study of mechanisms of specific Zn-finger protein domains binding to a DNA molecule with a certain sequence. Zn-finger domain is a common part of transcription factors. This domain consists of approximately 30 amino acid residues, its tertiary structure is supported by coordination bonds between amino acid residues and zinc cation. Proteins containing a single Zn-finger domain recognize several DNA sequences however proteins containing several Zn-domains are more specific. The DNA-Zn-finger interaction is a subject of many theoretical and experimental studies. Nevertheless physical basis of such specificity remains unclear. In this work several different contributions into free energy of interaction between DNA and Zn-finger protein Zif268 were estimated separately with the help of computational chemistry methods.

Molecular dynamics simulations were performed using GROMACS software package [1]. AMBER2003 force field [2] was used for calculations. Initial structure of DNA-protein complex was based on X-ray crystallographic data (1ZAA [3]). A model containing the same protein and a DNA molecule with random sequence was used for comparison. The random DNA molecule was created using X3DNA utility. An integration step of 0.5 fs was used for calculations and an equillibration time was at least 75 ns. TIP3P explicit water molecule model was used for solute simulation. Ionic strength of NaCl was 150 mM. Magnesium cations were used as counterions for DNA molecule and chlorine anions – as counterions for the protein molecule. Coordination interactions for Zn ion were simulated with bonded potentials (valent bond and valent angle), parameters were fitted according to atom positions in the crystal structure. Force constants for Zn-amino acids bonded interactions were obtained from Peter's study [4].

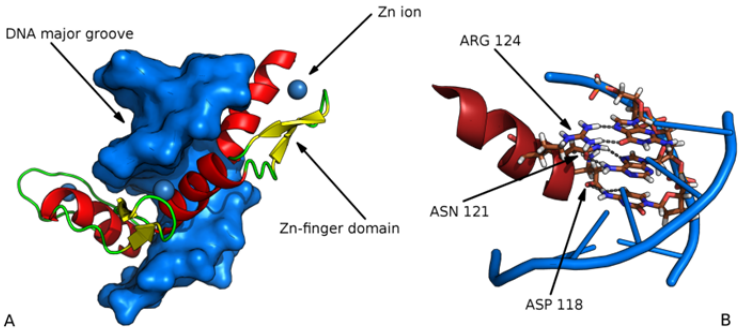

Figure. General view of Zif268 – DNA complex (A) and site of specific interaction (B).

Free energy of DNA-protein complex, pure DNA and pure protein were estimated using MM-PBSA technique [5]. This technique considers the energy to be a sum of:

$$G_{mol} = (H_{mol} - TS_{mol}) + \Delta G_{PB} + \Delta G_{SA}$$

where H_{mol} is the enthalpy of macromolecule, S_{mol} is the entropy of macromolecule, ΔG_{SA} is the free energy of macromolecule solvation, ΔG_{PB} is the energy of the double electrical layer (DEL) on the surface of the macromolecule. H_{mol} equals to the potential energy in case of NPT ensemble averaging. So it can be evaluated from an MD simulation directly. The entropy of a macromolecule (S_{mol}) could only be estimated as entropy of a solid body from normal mode analysis of MD model. Empirical coefficients for a set of chemical groups with different properties were obtained from analysis of large experimental data on solvation energies of small organic molecules [6].

Solvation free energy of macromolecule was estimated according to the total solvent accessible surface area of each chemical group. We've additionally calibrated the values of coefficients in simulations of distinct amino acids and nucleotides in aqueous solution. The energy of DEL was estimated as a difference between energy of the molecule dissolved in pure implicit water and of the molecule dissolved in 150 mM NaCl solution. Post-simulation analysis was performed using GROMACS utilities, APBS program and our own software developed using MDAnalysis and OpenBabel libraries.

Free energy was computed for every simulated system: pure protein, pure DNA with recognizable sequence, pure DNA with random sequence, protein-DNA specific complex and protein-DNA unspecific complex. Free energy of complex formation was calculated as a difference between protein-DNA complex energy and the sum of energies of protein and DNA simulated separately. All the systems were simulated in aqueous solutions. Difference in DEL energy through complex formation was estimated as 0.1 MJ/mol. Solid body calculation of $T\Delta S$ gave a value about 0.2-0.4 MJ/mol but standard error appeared to be much bigger than the estimated value and so this term was not considered. The major contribution into reaction free energy comes from enthalpy of macromolecule (approx. -7 MJ/mol) and solvation energy (approx. +1 MJ/mol). Such a big absolute value of reaction enthalpy occurs because of overestimation of an ion adsorption enthalpy on the surface of DNA-protein contact. This occurs because of an incorrect force field parametrization. Finally total MM-PBSA energy for DNA-protein interaction could not be calculated properly and only the difference in energy contribution could be analyzed.

Enthalpy of specific complex was -8.9 ± 2.5 MJ/mol whereas enthalpy of the unspecific one was -6.4 ± 2.5 MJ/mol. Energy decomposition showed that the effect was mostly underlined by intermolecular electrostatic interactions. The energy of solvation was 1.1 ± 0.1 and 1.0 ± 0.1 MJ/mol for specific and unspecific complexes respectively. Residues that give major contribution to solvation energy are phosphates of DNA backbone and arginine/lysine residues of Zif268. Some of them were described in literature but there are several residues whose role was not shown previously. In the figure of DNA-protein complex important amino acids are shown and labeled separately. According to calculation results we concluded that (i) specificity of DNA-protein interaction mainly comes from pure electrostatics. The proposition that electrostatic interactions play a key role in Zif268-DNA binding specificity allows us to determine key residues responsible for such specificity. And (ii) MM-PBSA and AMBER03 force field cannot be used as an accurate technique for analysis of protein-DNA interaction.

The work is supported by the RFBR (project no. 12-04-33111). MD calculations were performed using LOMONOSOV supercomputer complex in MSU Research Computing Center [7].

1 Pronk S., Páll S., Schulz R., Larsson P., Bjelkmar P., Apostolov R., Shirts M.R., Smith J.C., Kasson P.M., van der Spoel1 D., Hess B., Lindahl E. *GROMACS 4.5: a high-throughput and highly parallel open source molecular simulation toolkit.* // Bioinformatics. **2013**. 29 (7): 845-854.

2 Cornell W.D., Cieplak P., Bayly C.I., Gould I.R., Merz K.M., Ferguson D.M., Spellmeyer D.C., Fox T., Caldwell J.W., Kollman P.A. *A Second Generation Force Field for the Simulation of Proteins, Nucleic Acids, and Organic Molecules* // J. Am. Chem. Soc. **1995**. 117: 5179–5197.

3 Pavletich, N.P., Pabo, C.O. *Zinc finger-DNA recognition: crystal structure of a Zif268-DNA complex at 2.1 A* // Science. **1991**. 252: 809-817.

4 Peters M.B., Yang Y., Wang B., Füsti-Molnár L., Weaver M.N., Merz K.M. *Structural Survey of Zinc Containing Proteins and the Development of the Zinc AMBER Force Field (ZAFF)* // J Chem Theory Comput. **2010**. 6(9): 2935–2947.

5 Kollman P.A., Massova I., Reyes C., Kuhn B., Huo S., Chong L., Lee M., Lee T., Duan Y., Wang W., Donini O., Cieplak P., Srinivasan J., Case D.A., Cheatham T.E. *Calculating Structures and Free Energies of Complex Molecules: Combining Molecular Mechanics and Continuum Models.* // Acc. Chem. Res. **2000**. 33: 889-897.

6 Privalov P.L., Makhatadze G.I. *Contribution of Hydration to Protein Folding Thermodynamics. II. The Entropy and Gibbs Energy of Hydration* // J. Mol. Biol. **1993**. 232: 660–679.

7 Voevodin V.V., Zhumatiy S.A., Sobolev S.I., Antonov A.S., Bryzgalov P.A., Nikitenko D.A., Stefanov K.S., Voevodin V.V. *Practice of "Lomonosov" Supercomputer* // Open Systems J. (Russian). **2012**. № 7. [http://www.osp.ru/os/2012/07/13017641]

Estimating the role of single residues in the transmembrane helix-helix association using free energy decomposition approach

Kuznetsov A.S.[1,2], *Volynsky P.E.*[1], *Efremov R.G.*[1]

[1] Laboratory of Biomolecular Modeling, Shemyakin-Ovchinnikov Institute of Bioorganic Chemistry, Russian Academy of Sciences, Moscow, Russia.
[2] Moscow Institute of Physics and Technology, Dolgoprudny, Moscow Region, Russia.

Membrane receptors represent a wide class of proteins that have transmembrane (TM) alpha-helical segments. Association of TM helices leads to formation of their spatial structure for multiple-span membrane proteins and plays an important functional role in case of single-span ones, for example,

receptor tyrosine kinases. Dimerization or oligomerization of receptors is thought to be very important for signal transduction and TM helix-helix interactions play a crucial role in that process. Amino acid sequence is considered to be the main factor that affects dimerization [1], but the environment (membrane) can also play an important role [2]. Mutations in TM domains can be associated with diseases [3, 4]. There are two main properties that define a TM dimer formation: three-dimensional (3D) structure and free energy of association [2, 3]. 3D structure can be determined by experimental structural biology methods, but quantitative estimation of association energy requires sophisticated methodological approaches [4]. Dimerization energy of TM helices can be assessed using computational techniques. Simulation methods provide information about the system on atomic level so the role of each residue in helix-helix association can be estimated. Thus, such computations can reveal the driving factors of the dimerization process. These results can be used for prediction and ranging of association ability of arbitrary sequences in membrane environment. This data is indispensable for rational *de novo* construction of new molecules affecting association of TM helices of membrane receptor systems.

Algorithms of estimation of free energy profiles are described elsewhere [3, 5]. There are two main approaches: weighted histogram analysis method (WHAM) and estimation of free energy by direct integration of mean force acting between molecules. These methods can be used for calculation of contributions from different types of interactions into the total free energy. This was done by many groups, but in present work we are trying to estimate the residual contributions to get additional insight into dimerization process. Glycophorin A (GpA) TM dimer is known as one of the most studied by experimental and theoretical methods [2, 3]. Effect of some mutations on the dimerization process is known, but the role of interfacial residue Thr87 remains unclear. So, TM segments of wild-type (WT) GpA and its T87V mutant were selected as a model system for introducing our technique. Molecular dynamics simulations and explicit membrane model were used to obtain the effective energy of association. To estimate the influence of membrane composition, two model lipid bilayers were used: palmitoyl-oleoylphosphatidylcholine (POPC) and dimyristoylphosphatidylcholine (DMPC). Corresponding free energy profiles were calculated by integration of mean forces as a function of the distance between monomers. The total free energy of association was decomposed into protein-protein, protein-lipids and protein-water terms. Next, the contribution of an individual residue into the aforementioned binding energy was delineated.

The results reveal that the T87V mutant has less pronounced minimum on the PMF profile than WT dimer. It is noteworthy that the values of association energies are approximately equal in POPC, but in DMPC free energy of

dimerization for WT dimer is two-fold greater. Contribution of Val87 residue itself into the association energy of the mutant was slightly more unfavorable than from Thr87 in WT. This single mutation causes positive unfavorable shift in energy contributions of the nearest non-interfacial residues and negative (favorable) shift for other interfacial residues that compensate each other. The largest contribution into the free energy profiles is given by lipid-protein interactions. Based on this observation, we suggest that interaction with lipid environment can play a crucial role in association of TM helices. Further work is required to establish proper balance of various factors governing helix-helix interactions in lipid bilayers. In future, this method will be used as a prediction tool for estimating effects of mutations in TM domains of receptor tyrosine kinases on their biological activity.

1 Lemmon M.A., Flanagan J.M., Treutlein H.R., Zhang J., Engelman D.M. *Sequence specificity in the dimerization of transmembrane α-helices* // Biochemistry, **1992**, 31(51), 12719-12725.
2 Polyansky A.A., Volynsky P.E., Efremov R.G. *Multistate organization of transmembrane helical protein dimers governed by the host membrane* // Journal of American Chemical Society. **2012**, 134(35), 14390-14400.
3 Taylor M.S., Fung H.K., Rajgaria R., Filizola M., Weinstein H., Floudas C.A. *Mutations affecting the oligomerization interface of G-protein-coupled receptors revealed by a novel de novo protein design framework* // Biophysical Journal, **2008**, 94(7), 2470–2481.
4 Duong M.T., Jaszewski T.M., Fleming K.J., MacKenzie K.R. *Changes in apparent free energy of helix-helix dimerization in a biological membrane due to point mutations* // Journal of Molecular Biology. **2007**, 371(2), 422–434.
5 Polyansky A.A., Volynsky P.E., Efremov R.G. *Structural, dynamic, and functional aspects of helix association in membranes: a computational view* // Advances in protein chemistry and structural biology. **2011**, 83, 129-161.

Dynamic model of DNA double-strand break repair by non-homologous end joining

Lyashko M.S.[1,2], *Belov O.V.*[1,2], *Avvakumova I.L.*[2]

[1] Laboratory of Radiation Biology, Joint Institute for Nuclear Research, Dubna, Russia
[2] Dubna International University of Nature, Society, and Man, Dubna, Russia

Studying DNA repair in cells after irradiation by high-energy and high-Z particles is one of the topical problems of radiation biophysics. Modern experimental data make it possible to identify the main biophysical mechanisms of DNA double-strand break (DSB) repair. This is the most harmful type of DNA lesions, which can lead to various negative effects, such

as the induction of chromosomal aberrations, genomic instability, cell death, etc. Application of mathematical modeling for studying DNA repair processes in living cells assists in the systematization of experimental data and is significant for the development of a common DNA repair concept.

The subject of this study is a major DNA DSB repair mechanism in mammalian cells: non-homologues end joining (NHEJ). The special feature of NHEJ is that it can be realized without any homology in the cell, so it can take place in any phase of the cell cycle. The purpose of this study is to develop a new mathematical model of the NHEJ repair pathway in the mammalian cell after radiation exposures of different quality.

The NHEJ mechanism is represented as a mathematical model with kinetics schemes describing the concentration balance of the participating protein complexes, taking into account the rate constants of the direct and reverse reactions. The kinetic parameters were estimated by fitting the model to experimental data, which quantitatively describes kinetics at different stages of DNA repair. The proposed model correctly describes the kinetics of the NHEJ mechanism in a cell culture of normal human skin fibroblasts after irradiation by accelerated iron, silicon, and oxygen ions with energies of 0.3 and 1 GeV/nucleon, which corresponds to the energy spectrum of the galactic cosmic rays. Compared with other mathematical models, this approach includes detalization corresponding to the current level of the knowledge of NHEJ molecular mechanisms. Also, the proposed model, along with the kinetics of the key proteins, takes into account the metastable DNA states occurring at different stages of the repair process.

The results of this work can be of interest in many fields of fundamental radiobiology, as well as in molecular and cellular biology. The model adequately describes the kinetics of DSB repair after exposure to heavy ions with physical characteristics corresponding to the spectrum of galactic cosmic rays. The proposed computational approach can be used for solving problems in space radiobiology associated with estimation of the radiation risk during long-term manned missions outside the Earth's magnetosphere.

1 Reynolds P., Anderson J.A., Harper J.V., Hill M.A., Botchway S.W., Parker A.W., O'Neill P. *The dynamics of Ku70/80 and DNA-PKcs at DSBs induced by ionizing radiation is dependent on the complexity of damage* // Nucleic Acids Research, **2012**, 1–11, doi:10.1093/nar/gks879.

2 Cucinotta F.A., Pluth J.M., Anderson J.A., Harper J.V., O'Neill P. *Biochemical Kinetics Model of DSB Repair and Induction of γH2AX Foci by Non-homologous End Joining* // Radiat. Res. **2008**, 169, 214–222 .

3 Asaithamby A., Uematsu N., Chatterjee A., Story M.D., Burma S., Chen D.J. *Repair of HZE-Particle-Induced DNA Double-Strand Breaks in Normal Human Fibroblasts* // Radiation Research, **2008**, 169(4):437-446. doi:10.1667/RR1165.1.

Revealing proton transfer pathways within photosynthetic reaction center of *Rb. sphaeroides*

Mamonov P.A.

Lomonosov Moscow State University, Moscow, Russia
Biological faculty, dept. of biophysics

A process of proton transfer from the bulk to the secondary quinone is a crucial step in light energy conversion into the form of transmembrane electrochemical potential, performed by photosynthetic reaction centers. Various studies aim to reveal such proton transfer pathways within reaction centers' structures. Most studies that deal with the problem use static structures, obtained from X-ray crystallography. However in many cases agility of protein side chains permits alternate proton transfer pathways. The situation becomes even more complicated if one takes into account water molecules, which constitute considerable part of such proton transfer pathways.

Molecular modeling is a primary tool for investigation of an intrinsic life of molecular systems and permits one to deal with the described problem. However certain complications arise. The major complication is due to the fact, that correlated protein side-chains rearrangements and water molecules diffusion can take the amount of time exceeding timescale available for direct modeling using all-atomic molecular mechanical models. In order to facilitate the process of alternate hydrogen paths formation advanced molecular modeling techniques should be used.

Current study deals with the problem of revealing hydrogen bonded clusters of protein side-chains in the vicinity of secondary quinone molecule within photosynthetic reaction center of purple bacteria *Rb. sphaeroides*. The strategy for searching hydrogen bonded networks within reaction center is based on the molecular dynamics approach, supplemented by connectivity analysis. In order to facilitate hydrogen bonds formation the metadynamics approach is used [1].

A molecular mechanical model of reaction center was constructed using crystallographic structure 1AIG and all-atomic force field OPLS/AA. Molecular dynamics simulation of the reaction center model in vacuum was performed in the NVT ensemble, utilizing Nose-Hoover thermostat. In order to preserve the model structure motion of the main chain atoms was constrained. In order to facilitate hydrogen bonds formation during molecular dynamics, the metadynamics approach was used. A single collective variable was chosen to be an average coordination number of protonable atoms within sidechains of the reaction center and water molecules. The simulation was performed using extended Lagrangian scheme. Calculations were performed using CP2K molecular modeling package [2], at the SKIF "Lomonosov" supercomputer

(Research Computing Center of Moscow State University) [3]. A molecular dynamics trajectory of length 500 ps was used for further analysis.

The analysis of hydrogen bonding was performed throughout the molecular dynamics trajectory. The analysis of hydrogen bonding revealed two networks of hydrogen bonded amino acids, extending between secondary quinone binding pocket and reaction center surface (see Figure). Revealed clusters of amino acids include most of the components of hydrogen transfer pathways confirmed/predicted earlier [4]. This includes group of amino acids in the vicinity of secondary quinone (SerL223, AspL213), which were shown by point mutations to crucially affect proton transfer, a group of amino acids on the reaction center surface (AspH124, HisH126, HisH128), which were shown to decrease proton transfer rate upon binding of transitional metals ions, as well as AspL210 in the middle of the pathway, which was also shown to affect proton transfer considerably upon mutation. One notable failure of presented analysis is the lack of GluL212 in the list, which was shown to be a crucial part of proton transfer pathway. Presented analysis revealed it to be a part of a separate small hydrogen bonded cluster. However this failure is probably due to insufficient number of water molecules in its neighborhood. Several other amino acids proposed as possible proton entry points were revealed (AspM17, TyrM3, GluH224, ArgM13). Presented analysis also revealed TyrM3 to be a part of separate cluster of amino acids, which has no direct connection to the main cluster, which includes residues crucial for proton transportation. TyrM3 was speculated to be an alternate entry point for protons, however presented analysis does not support this point of view. Finally the analysis has also revealed a number of other residues, constituting parts of various proposed proton transfer pathways in the interior of the reaction center.

In order to characterize dynamic properties of the revealed hydrogen bonded network additional analysis was performed. Namely, a probability of disconnecting from hydrogen bond network was calculated for each residue constituting the cluster. Highest probabilities were found to be associated with water molecules as well as some residues at the edges of the reaction center, however the latter result is probably due to the lack of bulk water in the model. The analysis also showed relatively high disconnection probability for AspL210, constituting the middle of the proton transfer pathway between the reaction center surface and the secondary quinone. This result indicates that this part of the pathway may be one of the rate limiting steps of proton transfer.

Current study demonstrated effectiveness of the proposed molecular modeling technique to reveal clusters of hydrogen bonded protein residues. It has successfully revealed well established as well as expected components of proton transfer pathways within photosynthetic reaction center of *Rb. sphaeroides*. Proposed technique may be useful for preliminary analysis of proton transfer pathways within complex biomolecular systems.

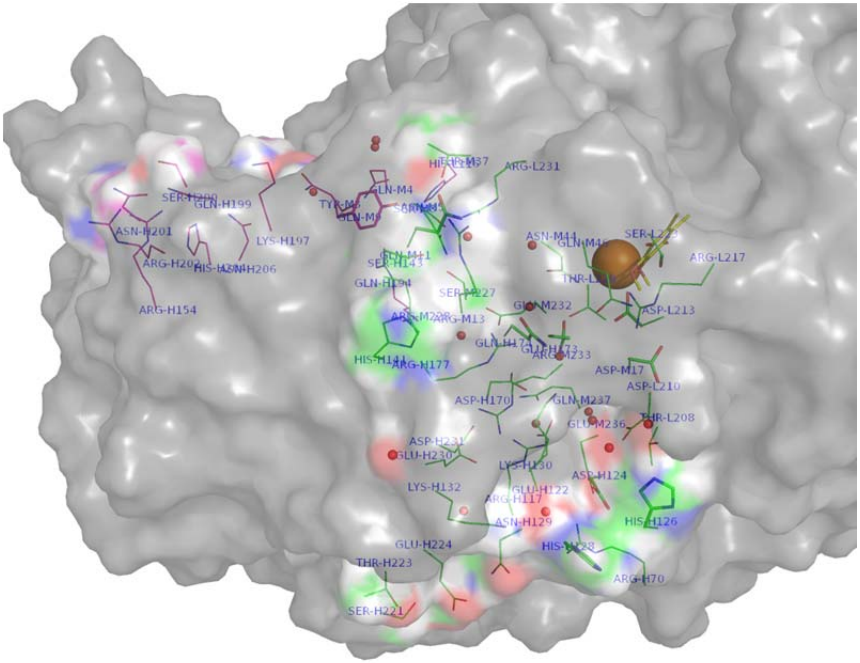

Figure. General view of revealed hydrogen bonded clusters of amino acid residues within photosynthetic reaction center of purple bacteria *Rb. sphaeroides*.

This study was supported by Russian Foundation for Basic Research (project no. 13-04-00403).

1 Laio A., Gervasio F.L. Rep. Prog. Phys. **2008**, 71, 126601
2 http://cp2k.berlios.de/
3 Voevodin V.V., Zhumatiy S.A., Sobolev S.I., Antonov A.S., Bryzgalov P.A., Nikitenko D.A., Stefanov K.S., Voevodin V.V. Open Systems J. (Russian). **2012**. № 7. [http://www.osp.ru/os/2012/07/13017641]
4 Krammer E.-M., Till M.S., Sebban P.,Ullmann G.M. JMB, **2009**, 388, 3, 631-643

Large scale modeling of membrane protein self-assembly

Marrink S.-J.

University of Groningen, Netherlands

Biomembranes are composed of hundreds of different lipids and contain a large number of membrane proteins essential for the proper functioning of the cell. To understand the lateral organization of biomembranes, we use large scale coarse-grained computer simulations that allow us to probe the lipid mediated sorting and clustering of embedded proteins at near-atomic detail. In this lecture, I will provide a brief introduction to the coarse-grained Martini force field [1], and illustrate its power with two recent applications. The first deals with identifying the role of cardiolipins in the formation and stability of supercomplex formation of respiratory chain complexes [2]. The second application models the sorting and clustering of membrane proteins in multi-domain membranes [3, 4].

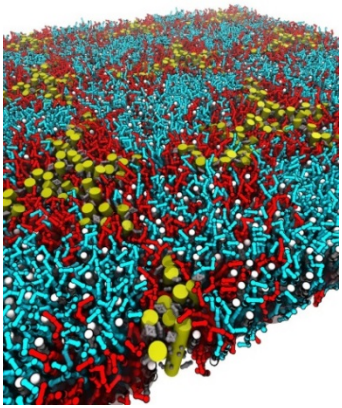

Figure. Transmembrane peptides (yellow) inducing phase separation between liquid-ordered (blue) and liquid-disordered (red) domains in bilayers composed of saturated and unsaturated lipids and cholesterol. See [4] for details.

1 Marrink S.J., Risselada H.J., Yefimov S., Tieleman D.P., de Vries A.H. *The MARTINI forcefield: coarse grained model for biomolecular simulations*. JPC-B, 111:7812-7824, **2007**.

2 Arnarez C., Mazat J.P., Elezgaray J., Marrink S.J., Periole X. *Evidence for cardiolipin binding sites on the membrane-exposed surface of the cytochrome bc1*. JACS, 135:3112–3120, **2013**.

3 Schafer L.V., de Jong D.H., Holt A., Rzepiela A.J., de Vries A.H., Poolman B., Killian J.A., Marrink S.J. *Lipid packing drives the segregation of transmembrane helices into disordered lipid domains in model biomembranes*. PNAS, 108:1343-1348, **2011**.

4 Domanski J., Marrink S.J., Schafer L.V. *Transmembrane helices can induce domain formation in crowded model biomembranes.* BBA Biomembr., 1818:984-994, **2012**

Molecular dynamic simulation of C4-azo-C9-TAB association in the presence and absence of DNA molecule

Nesterenko A.M.[1,2], *Ramazanov R.R.*[3]

[1] A.N. Belozersky Institute of Physico-Chemical Biology MSU,
[2] Lomonosov Moscow State University, Faculty of Biology, Department of Biophysics
[3] Saint-Petersburg State University, Faculty of Physics, Department of Molecular Biophysics

Various mono- and polycationic compounds are used as DNA compaction agents for construction of genetic vectors. Cationic surfactants are widely presented among these substances. They are able to induce DNA compaction when cation to nucleotide ratio is about 20:1 [1]. C4-azo-C9-TAB becomes increasingly popular compaction agent among cationic surfactants because of its unique optical properties. Azobenzene derivatives having two phenyl groups connected with azo-group (-N=N-) are studied very intensively at the present time. UV-light can induce *cis*-*trans* conversion in azobenzene whereas visible light induces the reverse one. As it was shown, one can switch CMC of azo-TAB in solution by irradiation with light of different wavelengths. Preliminary studies demonstrated that DNA compaction process with the help of azo-TAB may be regulated by light [2], however molecular mechanisms of both DNA compaction and TAB-DNA interaction remain unclear.

The goal of the present study is an atomistic description of interaction of azo-TAB with each other and a DNA molecule. The simulations of azo-TAB self-association process in pure ionic solution and same process in the presence of a DNA molecule were performed. All systems were simulated using molecular dynamics approach with GROMACS package, utilizing modified PARMBSC0 force field [3]. Original force field was patched to provide a correct description of *cis*- and *trans*-azo-TAB, in accordance to *ab initio* calculations. Quantum chemistry calculations were performed in 6-31p* basis with RHF-DFT technique (B3LYP5 functional). Quantum chemical calculations were performed using FireFly package [4]. Force field parameters for *cis*- and *trans*-isomers were determined separately because *cis*-azoTAB has a stressed conformation due to steric constraints of benzene groups. Note that *trans*-*cis* isomerisation is accompanied by redistribution of the electron density that leads to a change in partial charges of atoms near the azo-bond. Partial charges were calculated from *ab initio* electrostatic potential with help of AMBER RESP algorithm [5]. High-performance calculations were performed at the SKIF MSU supercomputer [6].

In several randomized MD simulations of initially homogeneous solutions of azo-compound micelles with diameter of 3-4 nm were formed within approx. 40 ns. *Cis*-isomers form almost spherical micelles with randomly oriented hydrophobic “tails” inside and methylammonium groups on the

surface. *Trans*-isomers form slightly elliptic micelles where most of the molecules are parallel to a common plane: such fold maximizes an amount of intermolecular stacking interactions.

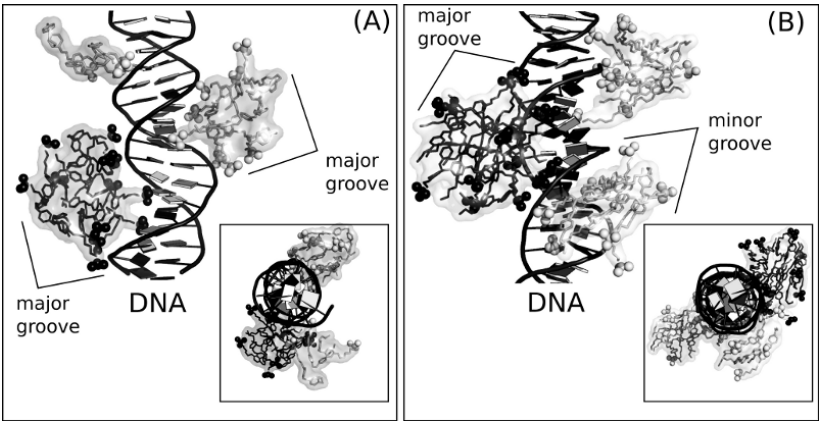

Figure. Pseudomicelles of *cis*-azoTAB (A) *trans*-azoTAB (B) on the DNA surface after 50 ns MD simulation.

The formation of micelle-like structures by *trans*- and *cis*-isomers was simulated in the presence of an infinite DNA molecule (DNA double helix was connected to itself through periodic boundaries). In the course of computational experiments for 50-100 ns azo-TAB molecules formed pseudomicelles on the DNA surface. Generally molecules at first formed self-associates (dimers, trimers etc.), then associates bound to the surface of double helix. Obviously, pseudomicelles interacted with DNA due to ionic bridges formation between azo-TAB methylammonium groups and DNA backbone phosphates. In most cases pseudomicelles were found in the major groove, nevertheless in few cases *trans*-azo-TAB bound to the minor groove and initiated association of surfactants in this region.

In sum, micelles in azo-TAB solution were simulated in pure water and in the presence of DNA helix. Micelles of *trans*- and *cis*-isomers formed during the course of MD differed in both internal structure and shape. Pseudomicelle formation was shown at different concentrations of azo-compound and their size was always about 2 nm. DNA with associates on its surface may be a first stage of DNA compaction by azo-compounds. Further study in this direction may help to develop light-induced DNA compaction/decompaction experimental models.

1 Dias R.S., Innerlohinger J., Glatter O., Miguel M.G., Lindman B. (2005). The journal of physical chemistry B. 109 (20), 10458–63. doi:10.1021/jp0444464
2 Le Ny A.-L. M., Lee C. T. (2006). Journal of the American Chemical Society. 128(19). 6400–8. doi:10.1021/ja0576738
3 Sorin E.J., Pande V.S. (2005). Biophysical journal. 88(4). 2472–93. doi:10.1529/biophysj.104.051938
4 Granovsky A.A. (2011). The Journal of chemical physics. 134(21). 214113. doi:10.1063/1.3596699
5 Bayly C.I., Cieplak P., Cornell W., Kollman P. A. (1993). The Journal of Physical Chemistry. 97(40). 10269–10280. doi:10.1021/j100142a004
6 Voevodin V.V., Zhumatiy S.A., Sobolev S.I., Antonov A.S., Bryzgalov P.A., Nikitenko D.A., Stefanov K.S., Voevodin V.V. Open Systems J. (Russian). **2012**. № 7. [http://www.osp.ru/os/2012/07/13017641]

Multiscale computational modeling of protein folding and dynamics

Papoian G.

University of Maryland

Protein folding and dynamics can be modeled as a diffusional process on a free energy surface. Contributions to this dissipative process can be separated into solvent dependent or wet friction and internal or dry friction, where frictional effects are due to the chain itself.

Despite these recent experimental advances to measure the internal friction contribution, the molecular origins of these effects have remained largely elusive. Using extensive all-atom molecular dynamics simulations we studied the dynamics of the unfolded cold-shock protein (CSP) from *Thermotoga maritima* at different solvent viscosities and at different denaturant concentrations (including the denaturant free case). We systematically analyzed the reconfiguration dynamics of relevant structural features such as dihedral angle rotations, hydrogen bonds (native and non-native) and hydrophobic contacts forming and breaking. Reconfiguration times obtained from MD simulations are consistent with experimental results. These results have important implications for the folding kinetics of proteins especially when considering protein folding in the context of the denaturant-free environment of a living cell. Under these conditions, the internal friction contribution may be dominant in the folding process.

Excitation spectra of thread-like silver clusters

Ramazanov R.R., Kononov A.I.

Saint-Petersburg State University, Faculty of Physics, Department of Molecular Biophysics

Fluorescent noble metal nanoclusters (NCs) containing up to tens of metal atoms have been paid more and more attention as a special class of nanoobjects. Their electronic states may be treated as discrete energy levels leading to essentially different optical, electrical and chemical properties from nanoparticles [1–4]. Different stabilizing agents such as dendrimers [5,6], and peptides [3] are used for the production of NCs. In particular, DNA is most widely used in the synthesis of fluorescent silver nanoclusters (AgNCs) due to potential biocompatibility and high brightness of the obtained AgNCs [7–11]. Very few theoretical studies were concerned with the electronically excited states of Ag-DNA complexes. Comparison of the calculated spectra of clusters of different shape (planar or spherical) and corresponding Ag-DNA complexes with the fluorescence excitation spectra reported in the literature, as well as analysis of the nature and oscillator strengths of the lowest transitions has revealed a poor fit. These facts allow us to conclude that fluorescent clusters must possess another structure stabilized by a polymer. Therefore we distinguish a group of thread-like shaped clusters containing up to 8 atoms with elongated shape, so that each atom is connected with only one or two neighbors. In contrast to planar shapes formation of elongated forms of clusters necessarily involves several binding sites on polymer. In such model, the polymer structure and positioning of binding sites determine the geometry parameters and absorption spectra of thread-like clusters. We have constructed different linear chains containing up to 8 Ag atoms with imposed constraints allowing to get a thread-like optimized clusters, and then we have calculated absorption spectra (Figure 1). In our calculations we have used a DFT [12] approach to perform ground state geometry optimizations and computing of the excitation spectra (time-dependent DFT) as implemented in GAMESS US program [13]. Silver atoms were represented through a LANL2DZ, relativistic effective core potential RECP with 28 inner electrons [14]. The other atoms were represented through a valence double-zeta polarized basis set 631g* [15].

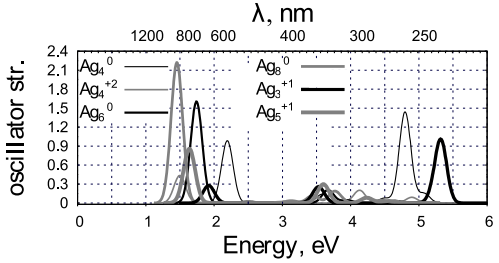

Figure 1. Excitation spectra for thread-like clusters containing up to 8 Ag atoms.

It appears that just by means of variation of the bend in the chain of atoms one can get different low-energy peaks which cover the entire visible region (~1.7-3 eV) of the excitation spectra (Figure 2).

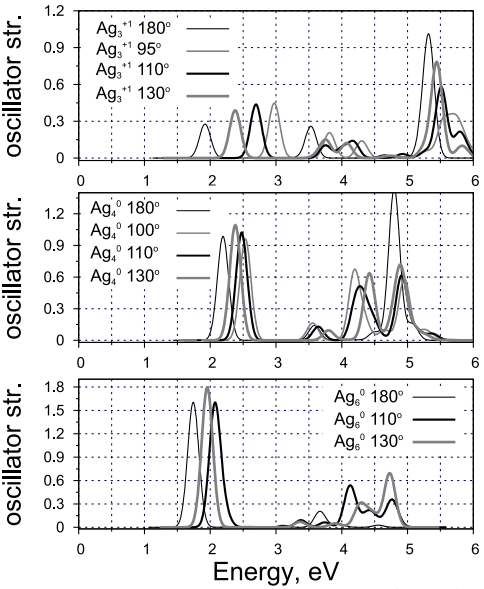

Figure 2. Excitation spectra for thread-like Ag_3^{+1}, Ag_4^0, Ag_6^0 with varying bend angle.

This work is supported by a grant 11.0.56.2010 of St. Petersburg State University. The reported calculations were performed in the Supercomputing Center of Lomonosov Moscow State University [16].

1 Xu, H.; Suslick, K. S. ACS nano **2010**, 4, 3209–14.
2 Wilcoxon, J. P.; Abrams, B. L. Chemical Society reviews **2006**, 35, 1162–94.
3 Yu, J.; Patel, S. A.; Dickson, R. M. Angewandte Chemie (International ed. in English) **2007**, 46, 2028–30.
4 Xu, H.; Suslick, K. S. Advanced materials (Deerfield Beach, Fla.) **2010**, 22, 1078–82.
5 Zhang, J.; Xu, S.; Kumacheva, E. Advanced Materials **2005**, 17, 2336–2340.
6 Zheng, J.; Dickson, R. M. Journal of the American Chemical Society **2002**, 124, 13982–13983.
7 Han, B.; Wang, E. Analytical and bioanalytical chemistry **2012**, 402, 129–38.
8 Richards, C. I.; Choi, S.; Hsiang, J.-C.; Antoku, Y.; Vosch, T.; Bongiorno, A.; Tzeng, Y.-L.; Dickson, R. M. Journal of the American Chemical Society **2008**, 130, 5038–9.
9 Yeh, H.-C.; Sharma, J.; Han, J. J.; Martinez, J. S.; Werner, J. H. Nano letters **2010**, 10, 3106–10.
10 Huang, Z.; Pu, F.; Hu, D.; Wang, C.; Ren, J.; Qu, X. Chemistry (Weinheim an der Bergstrasse, Germany) **2011**, 17, 3774–80.
11 Feng, L.; Huang, Z.; Ren, J.; Qu, X. Nucleic acids research **2012**, 40, e122.
12 Calais, J.-L. International Journal of Quantum Chemistry **1993**, 47, 101–101.
13 Gordon, M.; Schmidt, M. **2005**, 1167 – 1189.
14 Hay, P. J.; Wadt, W. R. The Journal of Chemical Physics **1985**, 82, 270.
15 Haharan, P. C.; Pople, J. A. Theoretica Chimica Acta **1973**, 28, 213.
16 Voevodin V. V., Zhumatiy S. A., Sobolev S. I., Antonov A. S., Bryzgalov P. A., Nikitenko D. A., Stefanov K. S., Voevodin V. V. Open Systems J. – Moscow: Open Systems Publ. **2012**, 7. [http://www.osp.ru/os/2012/07/13017641]

Simulation of the processes in photosynthetic membrane

Riznichenko G., Rubin A.

Biological Faculty of Moscow State University, 119991 Moscow, Leninskie Gory 1, b.12,
e-mail: riznich46@mail.ru

The work presents the results of the work on kinetic and multiparticle computer modelling performed at the Dept. of Biophysics, Biological faculty MSU [11, 12, 13].

The general kinetic model of the primary photosynthetic processes in a thylakoid membrane is based on the system of ordinary differential equations, describing the processes in multi-enzyme complexes of Photosystem I (PSI), Photosystem II (PSII) and Cytochrome b_6f complex (Cyt b_6f), coupled to transmembrane proton and other ions' transport and generation of transmembrane electrochemical potential. This model describes simultaneous kinetic changes of different variables, including concentrations of electron carriers in different redox states, electrical and electrochemical potential values; it adequately simulates a set

of fluorescence induction curves experimentally recorded at different light intensities under continuous illumination and after a short laser flash [3, 4].

The multiparticle computer models describe processes occuring in the simulated membrane "scene", which includes stroma, lumen and intramembrane compartments constructed according to structural data. We simulate interactions of ensembles of molecules in solution and in the heterogeneous interior of a cell. In the models protein molecules move according to the laws of Brownian dynamics, mutually orient themselves in the electrical field and form complexes in the 3D scene. The method allows to visualize the processes of molecule interactions and to evaluate the rate constants for protein complex formation reactions. 3D multiparticle computer models were created for simulation of complex formation kinetics for plastocyanin (Pc) with photosystem 1 and cytochrome bf complex [7, 9], ferredoxin with photosystem 1 and ferredoxin:$NADP^+$-reductase [5], flavodoxin with PSI [1]. Effects of ionic strength are described for wild type and mutant proteins.

The models [8] of formation of complexes Cyt-Pc and Pc-PSI in lumen of thylakoid taking into account the influence of the charge of the membrane are developed [6], which allow simulation of the directional electron transport from Cyt b_6f to PSI by means of mobile Pc molecules. The computer multiparticle models demonstrate non-monotonic dependences of complex formation rates on ionic strength as a result of long-range electrostatic interactions. Simulated kinetics of Cyt f oxidation and PSI reduction after the short flash are in good agreement with the experimental data. The models reveal the role of complicated geometry of the interacting proteins and spatial organization of photosynthetic membrane [6, 7, 8, 9]. Novel simulation software ProKSim (Protein Kinetics Simulator) was used to simulate transient encounter complex formation and to estimate the role of electrostatic interactions in this process [2, 10]

To simulate the dynamics of electrochemical potential and ATP formation the models describing state probabilities of photosynthetic complexes (PSI, PSII, Cyt b_6f, ATP-synthase) were coupled with the multiparticle Brownian dynamics description of mobile carrier interactions and with the description of proton gradient creation by means of reaction-diffusion equations [14]. Thus different stages of primary photosynthetic processes are simulated using different mathematical approaches, which are integrated into a combined model. We implemented this model as software which utilizes parallel computations on high-performance clusters and GPUs for better performance. The dynamics of ATP production similar to experimental was simulated.

Kinetic and multiparticle computer models allow evaluation of the parameters of photosynthetic processes which have not been determined experimentally and reveal the role of physical mechanism and geometry of

reaction volume in regulation of photosynthetic electron transport and coupled processes of energy transformation.

The work was supported by grants of the RFBR (grants #11-04-01019, 11-04-01268) and FCP (grant #8077).

1 Abaturova A.M., Kovalenko I.B., Riznichenko G.Y. et al. *Investigation of complex formation of flavodoxin and Photosystem I by means of direct multiparticle computer simulation* // Computer research and modeling, **2009**,1(1) 85-91 (Rus)
2 Abaturova A.M., Khruschev S.S., Kovalenko I.B., Riznichenko G.Yu. *Role of the electrostatic interactions in the encounter complex formation of plastocyanin and cytochrome f, barnase and barstar proteins* / Computational and theoretical modeling of biomolecular interactions. Moscow-Izhevsk: Institute of Computer Science, **2013**.
3 Belyaeva N. E., Schmitt F.-J., Paschenko V.Z. et al. *PSII model-based simulations of single turnover flash-induced transients of fluorescence yield monitored within the time domain of 100ns-10 s on dark-adapted Chlorella pyrenoidosa cells* // Photosyn. Res., **2008**, 98:105-119.
4 Belyaeva N.E., Schmitt J., Paschenko V.Z. et al. *PS II model based analysis of transient fluorescence yield measured on whole leaves of Arabidopsis thaliana after excitation with light flashes of different energies* // BioSystems, **2011**, 103 (2):188-195
5 Dyakonova A.N., Abaturova A.V., Kovalenko I.B. et al. *Direct computer modeling of ferredocsin-FNR complex formation* / In: Mathematics, Computer, Education, **2008**, vol 15(3). ICS-RCD, Moscow-Izhevsk, p 263 (Rus)
6 Knyazeva O.S., Kovalenko I.B., Abaturova A.M. et al. *Multiparticle computer simulation of plastocyanin diffusion and interaction with cytochrome f in the electrostatic field of the thylakoid membrane* // Biophysics, **2010**, 55: 221-227.
7 Kovalenko I.B., Abaturova A.M., Gromov P.A. et al. *Direct simulation of plastocyanin and cytochrome f interactions in solution* // Phys. Biol. **2006**, 3:121–129
8 Kovalenko I.B., Abaturova A.M., Diakonova et al. *Computer simulation of protein-protein association in photosynthesis* // Math, Model, Nat, Phenom., **2011**, 6(7):39–54
9 Kovalenko I.B., Abaturova A.M., Riznichenko G.Y. et al. *Computer simulation of interaction of photosystem 1 with plastocyanin and ferredoxin* // BioSystems, **2011**, 103:180-187
10 Khrushchev S.S., Abaturova A.M., Diakonova A.N. et al. *Multi-particle Brownian Dynamics software ProKSim for protein-protein interactions modeling* // Computer Research and Modeling, **2013**, 5(1)
11 Riznichenko G.Y., Belyaeva N.E., Kovalenko I.B. et al. *Mathematical and computer modeling of primary photosynthetic processes* // Biophysics, **2009**, 54: 10–22
12 Riznichenko G.Y., Kovalenko I.B., Abaturova A.M. et al. *New direct dynamic models of protein interactions coupled to photosynthetic electron transport reactions* // Biophys. Rev., **2010**, 2: 101–110.

13 Rubin A.B., Riznichenko G.Y. *Modeling of the primary processes in a photosynthetic membrane* / In: Laisk A, Nedbal L, Govindjee (eds) Photosynthesis in silico: Understanding complexity from molecules to ecosystems // Advances in Photosynthesis and Respiration, **2009**, Vol 29, Springer, Dordrecht p 151-176
14 Ustinin D.M., Kovalenko I.B., Riznichenko G.Yu., Rubin A.B. *Combination of different simulation techniques in the complex model of photosynthetic membrane* // Computer Research and Modeling, **2013**, 5(1)65-81

Functional dynamics of proteins based on conformational mobility

Shaitan K.V.[1,2]

[1] M.V. Lomonosov Moscow State University, 119991 Moscow, Russia
[2] N.N. Semenov Institute of Chemical Physics RAS, 119991, Moscow, Russia

Modern trends in research of biomacromolecules and supramolecular structure dynamics are discussed. Emphasis is placed on the work being developed in the last 30 years in the Lomonosov Moscow State University (MSU) and Institute of Chemical Physics RAS. Physical mechanisms of the fluctuations dynamics in the angstrom and sub-angstrom ranges in condensed matter are considered on the basis of Mössbauer spectroscopy data and molecular simulations. The all-atom simulation results for the ion channels functioning produced by supercomputer "Lomonosov" (MSU) are reported. Self-organization dynamics of macromolecular structures are discussed with use of model polymer structures and nanostructures as examples. Topology of multi-dimensional energy levels surfaces for the molecules with conformational mobility and its dynamic properties are considered. In conclusion we discuss functional dynamics of simple molecular machines based on catenane and rotaxane molecular structures. The role of conformational mobility to ensure their functioning is demonstrated.

It is well known that 3D structures of proteins have various but specific functional roles. 3D structure of proteins is non-periodic. The amino acid sequence of a protein predisposes it towards its native conformation. It will fold spontaneously during or after its synthesis.

How the 3D structure of the protein in the native state is related to the amino acid sequence? It is an old and very difficult problem. Historically, one of the first successful works was performed in the area of *de novo* protein design.

Creation of *de novo* proteins (albebetin, albeferon, etc.) was historically one of the first projects in the field of nanobiotechnology, which had gone through all the stages from modeling to construction and synthesis of

functionally interesting nanoobjects. This project was accomplished in the USSR in the mid 80s–beginning of 90s by a group of researches including Pticin, Finkelstein, Kirpichnikov, Dolgih, and their colleagues. By that moment thanks to the works of prof. Pticin's group main geometrical motifs of natural protein folds were understood and sufficient statistical data about the influence of primary sequence on protein fold motifs was gathered. Further we will see that the geometry of chain folds or geometrical factor exists not only for proteins but for a wider range of objects as well.

It must be emphasized that at that time a reliable energy computation for different conformational states of protein globule was practically impossible, and now it is still a tough task. However, there was enough knowledge about geometrical motifs of protein folds for qualitative modeling of an amino acid sequence, which can never be found in biological objects, but that can spontaneously fold into a predicted 3D structure. We should admit that not every amino acid sequence can fold into a compact and strictly determined spatial structure.

But from energy point of view albebetin has some peculiarities in comparison with native states of the natural proteins. Due to excess of negatively charged amino acid residues in the albebetin sequence the globular state of the protein is not as compact as native state. In this case we deal with a molten globular state for albebetin. Molten globule is a transition state towards the native state of natural proteins. Albebetin is a protein which is delayed in this transition state. Note that it is very close to native state.

On the basis of qualitative modeling, amino acid sequences were suggested and that by the means of genetic engineering first artificial proteins or nanoobjects were created. It means the *de novo* proteins - albebetin, albeferon, etc. These artificial proteins have a number of useful properties. They, for example, can be carriers of different pharmacophores. Their combination with fragments of interferon possesses antiviral properties without side effects. Some data is also available on the modification of the activity spectra of other functional peptides chemically bonded to the de novo proteins.

The *de novo* protein project explicitly showed that artificial systems can also fold spontaneously into strictly determined spatial structures. But is this a property that is pertinent only to macromolecules composed of natural "bricks", such as amino acids? Computer simulations and available experience reveal that it is not. Further we will rely on the results of all atom computer molecular modeling based on solution of classical equations of motion. We use a force field that describes all types of atoms including hydrogen atoms. The total potential energy of a molecule is the sum of terms related to valence bonds, valence angles, torsion angles and non-covalent interactions, including the Coulomb interaction.

The system of classical motion equations is numerically solved. The temperature and pressure or volume are kept constant. Modern computational facilities allow studying systems consisting of up to several hundred thousand atoms in a rather detailed way. We would like to point out that not only objects of biological nature but also objects of non-biological and hybrid nature can exhibit properties of self-organization and self-assembly. And the result of this self-organization can be predictable. Rational design of self-assembling structures is the principle problem of biology and nanotechnology.

In our numerical experiments with nano and bio structures two factors governing the scenario of self-assembly can be pointed out. The first one is the geometrical factor connected to the ratio of chemical bond length to the van der Waals sizes of atomic groups. The geometrical factor determines the range of allowed spatial configurations, that may occur during the self-assembly of macromolecule or motifs of chain folds. There are different possibilities of spatial arrangement of a polymer chain depending on geometrical factor. The selection of 3D structure from the pool of possible forms takes place due to representative point dynamics along the potential energy funnel. For a simple polymer chain the landscape of the funnel is less complicated than for a protein. Even for a simple polymer chain different spatial configurations (single and double helices, pins etc.) can be realized dependent on this geometrical factor. Addition of side groups to monomers allows formation of planar helices similar to beta-sheets. This means that spatial organization of non-biological chains can be similar to biological ones.

Using molecular simulations we can observe formation of single and double helices. It is important that a simple polymer chain can generate different fold types typical for secondary structures of biopolymers (proteins, RNA, DNA) depending on the geometrical factor.

Let us further consider the possibilities of application of molecular design to intermolecular self-organization. We can demonstrate this by an example of spider web nano fiber. This is a very interesting fiber. Firstly, it is absolutely biocompatible and can be used in different biomedical applications. Amino acid sequence of spidroin, the protein of the web, has poly-alanine fragments and fragments of alternating glycine and alanine. However it is not possible to create web filament only by the means of spontaneous self-assembly, a special procedure is needed. Secondly, this filament has a unique rupture energy that is close to the theoretical strength of materials. Often the following example is considered: regular spider's web can catch a fly. But if spider's web was constructed from filaments as thick as a pencil it could catch a heavy airplane.

The speed of ejection of spidroin solution combined with rapid dehydration due to the action of special membrane pores is of importance. The detailed structure of the filament is not yet fully understood. But numerical experiments reveal a rather plausible picture of self-organization of the

filament and the methods of its formation in artificial conditions. They also give some hints for the design of amino acid sequence in order to vary the properties of the filament.

Let us consider our understanding of the process. In a hydrodynamic flow taking place in spiders' glands the extension of protein filament occurs. At a speed of 50-100 km/h we can expect the formation of beta-needles. The modeling reveals that beta-needle is a stable conformation under the extension force of the order of 100 pN.

Numerical experiments showed that beta-needles of polyalanine are susceptible to self-organization with formation of superhelical structure of a nano fiber. These beta-needles consist of 12 alanine residues. The susceptibility of beta-needles to form super-helix is very high. Different variations of initial and boundary conditions do not influence the result - formation of a super-helix from beta-needles. This super-helix has additional strength and it would be quite hard to stretch it to a beta-filament conformation. The alternation in the peptide fragment of alanine and glycine leads to formation of different coil structures. These coils are presumably responsible for the elasticity of the fiber.

Let us now consider self-organization of hybrid nano-objects containing a biopolymer and a non-biological structure using a very popular nano-object – a single layer carbon nanotube as an example. It is known that in general carbon nanoparticles are good sorbents. If the geometrical factor is such that a molecule can enter the carbon nanotube then the number of atomic contacts of an adsorbed molecule inside the nanotube is bigger than at the surface and thus the adsorption energy greater. Thus the energy factor favors the accommodation of the molecule inside the nanotube. Cholesterol adsorbed at first at the wall of the nanotube is then captured by the cavity 13 Å wide. Here the combination of energy and geometrical factors works in a trivial way. A more interesting situation occurs when nanotube interacts with a polypeptide (in this case a peptide consisting of 15 alanine residues). Polyalanine adsorbed at the surface of the nanotube under the action of thermal fluctuations approaches the entrance of the nanotube. The number of atomic contacts of polyalanine with the nanotube at this stage is minimal and this state is energetically unfavorable. The activation barrier is approximately 7 kcal/mol.

The interesting stage of self-organization begins. The adsorption energy of polypeptide inside the nanotube is higher than on the surface, but geometrically not every conformation is possible inside the nanotube. Namely in the conformation close to alpha-helical the energy balance is mostly favorable. Thus in this case nanotube plays the role of not only sorbent but also of a kind of shaperone, stabilizing the alpha-helical conformation of polypeptide.

We have considered actual self-assembly of a simple nano-device – a nano syringe. If we find a way to expel the contents of the nano syringe then

such type of device can be used for instance for targeted drug delivery. In this case under the cap of a nanosyringe a number of molecules is placed that can explode.

We have already touched on the problems of functioning of nanobiodevices. In biology these are the processes involving enzymes, membrane receptors, ion channels, transport proteins, molecular motors, which use the energy stored in ATP to move atomic groups or ions. We consider one of these types of objects – ion channels. These objects are of special interest, in particular, for creation of biosensors, for organizing interfaces between nerve tissues and microelectronic devices, etc. Ion channels also allow demonstration of the principles of rational design, based on the analysis of geometrical and energy factors.

Ion channels are formed by helix peptide structures. For example there is an acetylcholine receptor which supports sodium ion channel. After jointing of two molecules of acetylcholine this ion channel transitions into the open state, and sodium cation can move across the membrane. Another example is a potassium channel Kcsa - this channel opens due to influence of transmembrane electric field.

A simple example is an ion channel, formed by peptide antibiotic gramicidin A. There are carbonyl oxygens exposed inside the channel that create partial negative charge. This is an important moment since gramicidin channel conducts positively charged sodium ions. In solution the sodium ion is hydrated by 6 water molecules. The size of this hydrated complex is too big for it to enter the channel, but an ion without its hydration shell geometrically can fit in the channel. But here the energetics of the process is of big importance. The energy needed for dehydration of an ion is larger than 200 kcal/mol. Thus the interior of the channel must be constructed in such a manner that the energy loss due to dehydration would be compensated by some interaction with the channel interior. But this interaction should not be too strong so that the ion would not remain irreversibly in the channel. Therefore from the point of view of energy interactions the interior of the channel is quite well constructed specifically for the sodium ion, and carbonyl oxygens that form the belts of partial negative charge play an important role in the process of ion transfer. The kinetics of ion transfer also reflect the energy profile of the channel. In the regions of the negative charge the slowing of ion movement can be seen. But this slowing is not irreversible. Is it possible to change the selectivity of the channel by modification of its interior charge? The answer is “yes”.

We can consider two channels that are homologous in their structure – the chlorine channel of glycine receptor and sodium channel of nicotine acetylcholine receptor. Both channels play an important role in the functioning of the nervous system. Apart from some minor details the main difference between the channels is in the charge of their interior. In chlorine channel there

are belts of positively charged arginine residues and sodium channel has belts of negative charge formed by glutamine acid residues. But if we take the mutant forms of glycine receptor where part of arginines is replaced by glutamine acids the selectivity of the channel is dramatically changed, and it becomes conductive for sodium ions. The process of ion transfer is also governed by the geometrical and energy factors as in the simplest case of gramicidin channel.

We briefly discussed the role of geometrical and energy factors in design of nanobiostructures by the example of self-assembly of spatial structures and relatively simple functional processes. But if we consider more complex devices such as molecular motors and machines we should take into account some additional factors. One example of molecular machines is a famous enzyme - ATP synthase. This is a fantastic molecular device. All energetics of life are based on this molecular machine. You see that ATP generation from ADP and phosphate is conjugated with rotation of the subunits of this machine. The energy for rotation and reaction comes from transmembrane proton flux due to proton chemical potential gradient. How we can create nonbiological molecular machines? A simple example is a molecular shuttle based on rotaxane, the system where a molecular ring (in this case cyclic crown ether) put on a molecular rod. Reversible attachment of proton to the amine group changes the potential energy surface of the crown, which moves to a new equilibrium position. Detachment of proton moves the crown to the initial position. This is a very simple system. Analogy with a classical machine is also rather vivid. We have a given degree of freedom for the directed movement of the ring around the rod. We should only note that unlike the case of macroscopic machine these movements are diffusion in a potential well, and we now deal with a Brownian shuttle. The driving force for this vehicle originates due to the changes in the potential energy surface. These changes are induced by a chemical reaction, in our case the attachment of a proton. Such potential energy change for a relatively big molecular degree of freedom is called electronic-conformational interaction. Namely, the change of equilibrium state before and after chemical reaction is the principle factor for constructing molecular machines. We have obtained the system of equations which describes the molecular machine functioning.

There is another example of molecular machine. It reveals that the principles of organization of molecular machines are a bit different from the case of macroscopic ones. The machine depicted here is made of catenane, which means ‘two interconnected rings’. The change in the oxidation state of one of these rings (tetrathiofulvalen groups) induces rotation of the rings. After rotation the resistance of the catenane layer changes and some devices can be constructed based on this effect. One of the questions for the design is this: what ring or rings do actually rotate? Here we have two rings. One rigid ring –

cyclophane ring, and the other conformationally flexible with a tetrathiofulvalen group.

In macro machines rotating elements should be rigid so that bends and curves of rotating parts would not hinder rotation and induce additional friction. But here is what molecular modeling reveals. On the probability map for different rotation states of catenane (the color is as on a geographical map, the more red is the color the higher is the probability) we can see that actually the more flexible ring is rotating. The rigid ring in practice does not rotate. This occurs because the rotational movement bears the characteristics of diffusion or Brownian movement. At atomic scale the relative movement of molecular parts gives rise to collision and hooking of atoms. If a molecular system is put into configuration unfavorable for further movement it can escape this configuration due to flexibility of molecular fragments.

Now we can formulate the following key principles for rational design of nanobiostructures. For self-assembly of spatial structures the geometrical factor plays an important role. It determines the possible fold motifs for chains and molecular fragments. In real molecules the possible variations of bond length and van der Waals sizes of molecular fragments are restricted, so we have a finite set of possible fold motifs. The ultimate choice between possible spatial configurations is determined by the energy factor, which can be also investigated by molecular simulations.

In case of functioning of bionanosystems, geometry and energy determine possible approaches for rational design as well. By example of ion channels we have seen that Coulomb interactions can control the selectivity and efficiency of the channel.

In case of molecular machines we have to consider two additional factors. A degree of freedom for mechanical movement should be present. This movement has stochastic or Brownian nature. The degree of freedom itself should be formed by molecular groups with flexible conformations.

And the last point. The machine by its definition is a device that uses external power supply. This influence induces redistribution of electronic density due to a chemical reaction, charge transfer of photo excitation. Consequently, for molecular machine to function it is necessary to make the position of equilibrium state along the quasimechanical degree of freedom dependant on the electron density redistribution in the molecular device.

The work is supported by the Ministry of Education and Science of Russian Federation (GK № 07.514.11.4125) and Russian Foundation for Basic Research.

3D rigid body model of an MT lattice for simulation of microtubule dissassembly

Shuvalov N.[1], *Alekseenko A.*[1], *Kholodov Ya.*[1], *Barsegov V.*[1,2]

[1] Division of Computational Mathematics, Moscow Institute of Physics and Technology, Dolgoprudny, Russia 141700
[2] Department of Chemistry, University of Massachusetts at Lowell, Lowell, USA 01854

Microtubules are components of the cytoskeleton that are essential for cell division. The basic structural subunit of a microtubule are two globular proteins, α- tubulin and β-tubulin. These form a dimer, which polymerize to form microtubule (MT) protofilaments. An MT lattice is formed by thirteen protofilaments associated laterally in an imperfect helix (Figure 1a). MTs are metastable, which triggers sudden transitions between their growth and shortening. In a dynamic process called "catastrophe", slow MT growth is switched to rapid disassembly, in which the protofilaments bend outward and individual tubulin dimers (Figure 1b) dissociate from the lattice [1]. Despite the biological importance of MT assembly-disassembly, the mechanics of these processes is not understood. Long timescales (seconds) and large size (~10^5 residues) make computational exploration of MT dynamics in atomic detail impossible.

We developed a three-dimentional rigid body model of the MT lattice, in which α- tubulin or β-tubulin are represented by rigid spherical beads with three translational and three rotational degrees of freedom (Figure 1c). The potential energy includes the next-neighbor interactions of each monomer with its four neighbors. The longitudinal and lateral interactions are described by the sigmoidal potential energy function $U(r)=a+b/(a+exp[c(r-z)])$, where r is a distance between the interaction sites, and a, b, c and z are the constant coefficients. To account for the outward bending and twisting of the protofilament chains we use the harmonic potentials, namely the bending potential $U(\varphi)=C_{bend}(\varphi-\varphi_0)^2/2$, where C_{bend} is the bending constant, φ_0=0.2 rad is the equilibrium angle, and φ is the angle for outward bending, and the twisting potential $U(\psi)=C_{twist}\psi^2/2$, where C_{twist} is the twisting constant, which prevents monomers from turning around the protofilament axis. To model the self-avoidance of a polypeptide chain we used the repulsive (~$1/r^6$) Lennard-Jones potential.

To determine the model parameters a, b, c and d, we used Umbrella Sampling simulations [2] in conjunction with the SASA model of implicit solvation and CHARMM19 force field [3]. We used this approach to parametrize two longitudinal interactions (between monomers inside the dimers and between the dimers) and four lateral interactions (between all

possible pairs of tubulin monomers, i.e. α- and β-monomers, α- and α-monomers, β- and α-monomers, and β- and β-monomers. As an example, here we present the potential energy for the lateral interactions between the next-neighbor β-tubulin domains (Figure 1d).

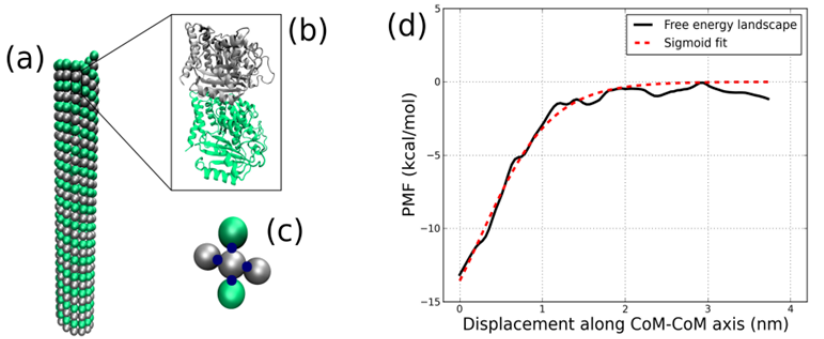

Figure. (a) Microtubule helical cylinder structure: the α- and β- tubulin monomers are represented by the grey and green spheres, respectively. (b) All-atom structure of α- and β-tubulins forming a dimer. (c) Interaction sites for describing domain interactions between the α- and β-tubulin monomers at their interfaces. (blue dots) (d) Potential energy function for the lateral interactions between the two β-tubulin mononers from the Umbrella Sampling simulations (solid black curve) and the numerical fit obtained using the sigmoidal function (red dashed line).

The developed 3D rigid body model of the MT lattice has used to carry out Langevin Dynamics simulations of MT lattice disassembly. To improve the computational performance, the model ported to Graphics Processing Units (GPUs). The obtained values of the rates of disassembly and the duration of pause times observed in the disassembly process compare well with the experimental data and with the results from the previous study [4].

1 Hyman A. A., Chretien D., Arnal I., Wade R. H. *Structural changes accompanying GTP hydrolysis in microtubules: information from a slowly hydrolyzable analogue guanylyl-(alpha,beta) methylenediphosphonate* // J. Cell Biol., **1995**, 128, 117–125.
2 Kästner J. *Umbrella sampling* // WIRE: Comput. Mol. Sci., **2011**, 1, 932–942.
3 Ferrara P., Apostolakis J., Caflisch A. *Evaluation of a fast implicit solvent model for molecular dynamics simulations* // Proteins, **2002**, 46, 24–33.
4 Molodtsov M. I., Ermakova E. A, Shnol E. E., Grishchuk E. L., McIntosh J. R., Ataullakhanov F. I. *A molecular-mechanical model of the microtubule* // Biophys. J., **2005**, 88, 3167–3179.

Approaches to the modeling of NMDA receptor subunit expression and trafficking after exposure to ionizing radiation

Sokol O.[1,2], *Aksenova S.*[1], *Belov O.*[1]

[1] Laboratory of Radiation Biology, Joint Institute for Nuclear Research, Dubna, Russia
E-mail: olga.e.sokol@gmail.com
[2] Faculty of Physics, M.V. Lomonosov Moscow State University

Studying the effects of heavy charged particles on the structures and functions of the central nervous system is one of the fundamental problems of space radiobiology. In particular, last decade's research revealed a serious hazard of the heavy nuclei of the galactic cosmic rays (GCR) for human health. Experiments at heavy ion accelerators have shown that ^{56}Fe ions with energies corresponding to the GCR spectrum at relatively low doses (20–70 cGy) can cause significant behavior and memory disorders in laboratory animals – in particular, rats. In the related physiological processes, the key role belongs to the ionotropic glutamate receptor NMDA, the activation of which is based on Ca^{2+} ions passing through the cell. The observed disorders are associated with decrease in the content of its subunits in the hippocampus of the brain [1].

In this work, we propose a mathematical description of the possible mechanisms that lead to changes in the NMDA subunit levels. A dynamic model of the synthesis of receptor subunits is built based on general concepts of gene expression in mammalian cells; and the effect of the radiation factor is introduced. The process is represented as a series of biochemical reactions, comprising the steps of transcription to produce mRNA, migration of mRNA from the nucleus to the cytoplasm, and translation step resulting in the NMDA subunits formation. At the latter step, we suggest that heavy ions can change the repressor concentrations, thus regulating the speed of gene expression and final protein production. Additionally, the model takes into account the experimentally proved influence of reactive oxygen species on the produced subunits. The mathematical description of the molecular mechanisms is based on kinetic equations for the respective biochemical reactions. The proposed modeling approach shows possible ways to address the effect of radiation on the level of NMDA subunits.

1 Machida M., Lonart G., Britten R.A. *Low (60 cGy) doses of ^{56}Fe HZE-particle radiation lead to a persistent reduction in the glutamatergic readily releasable pool in rat hippocampal synaptosomes* // Radiat Res. **2010**. V. 174. P. 618-623.

Lipid binding through membranes using molecular dynamics

Stanley N.

Universitat Pompeu Fabra, Barcelona, Spain. E-mail: nathaniel.stanley@gmail.com

All-atom molecular dynamics simulations offer the potential to investigate complex molecular interactions in high-definition. This extends to realms where other techniques struggle to offer such capabilities. In our previous work, we have shown that highly-parallel MD simulations can elucidate the binding path and kinetics of a small ligand binding to a globular protein [1]. We have also shown that MD can be used to investigate rare but crucial conformations of proteins [2]. The dynamics of membrane proteins and their interacting ligands is another place where MD can offer unique insights. Here we discuss the results of similar analyses of the binding of highly flexible ligands to two different membrane proteins, Fatty acid amide hydrolase (FAAH) and the S1P receptor.

1 Buch, Ignasi, Toni Giorgino, and Gianni De Fabritiis *Complete Reconstruction of an Enzyme-inhibitor Binding Process by Molecular Dynamics Simulations* // Proceedings of the National Academy of Sciences, (June 6, **2011**). doi:10.1073/pnas.1103547108.

2 Sadiq, S. Kashif, Frank Noé, and Gianni De Fabritiis *Kinetic Characterization of the Critical Step in HIV-1 Protease Maturation* // Proceedings of the National Academy of Sciences 109, no. 50 (December 11, **2012**): 20449–20454. doi:10.1073/pnas.1210983109.

Role of sequence and membrane composition in structure of transmembrane domain of Amyloid Precursor Protein

Straub J.E.

Boston University, USA

Aggregation of proteins of known sequence is linked to a variety of neurodegenerative disorders. The amyloid β (Aβ) protein associated with Alzheimer's Disease (AD) is derived from cleavage of the 99 amino acid C-terminal fragment of Amyloid Precursor Protein (APP-C99) by g-secretase. Certain familial mutations of APP-C99 have been shown to lead to altered production of Aβ protein and the early onset of AD. We describe simulation studies exploring the structure of APP-C99 in micelle and membrane environments. Our studies explore how changes in sequence and membrane composition influence (1) the structure of monomeric APP-C99 and (2) APP-

C99 homodimer structure and stability. Comparison of simulation results with recent NMR studies of APP-C99 monomers and dimers in micelle and bicelle environments provide insight into how critical aspects of APP-C99 structure and dimerization correlate with secretase processing, an essential component of the Aβ protein aggregation pathway and AD.

Lysozyme interaction with neutral and positively charged 5-methylresorsinol clusters

Tereshkina K.B., Krupyanskii Y.F.

N. N. Semenov Institute of Chemical Physics, Russian Academy of Sciences, Russia, 119991, Moscow, Kosygina str. 4,tel. +7(495)939-75-39. E-mail: ksenia.tereshkina@gmail.com

In this work lysozyme interaction with low-molecular ligand 5-methylresorcinol and its clusters was studied. Molecular dynamics and quantum chemistry methods were used. Study of interaction of enzyme proteins with chemical compounds of hydroxyalkylbenzene type or other low-molecular ligands is very important because these molecules influence functional activity, structure and dynamics properties of proteins [1, 2]. Now new experimental methods of investigation of nanocrystal and noncrystalline biomolecular objects are being actively improved by use of X-ray Free Electron Lasers [3, 4]. Preparation of crystals with dimensions suitable for the SAR is often a difficult problem, especially when during crystallization of membrane proteins and larger macromolecular complexes. Usage of powerful X-ray sources during diffraction experiments can lead to significant changes in the electronic and molecular structure of studied objects. It is important to take these changes into account when solving direct problem of X-ray scattering, that is, calculation of the diffraction pattern on the basis of the available atomic model of the object. Molecular dynamics methods can be used to reveal structure of molecular systems after exposure to high-energy X-rays. Classical molecular dynamics methods should be improved for specific tasks. That is, new force fields and potentials should be used. For the development of methods of molecular dynamics, allowing study of the structure of molecules during and after the action of a powerful X-ray pulse, it is necessary to study the structural changes taking place in molecules after losing of one or more electrons and excitation of molecules.

Studies were carried out using molecular dynamics software package GROMACS [5] with trajectories of up to 1000 ns. Systems with periodic boundary conditions, containing one of the ligands in different concentrations were studied. Necessary parameters for adding 5-methylresorcinol and clusters of these compounds to the standard force field OPLS-AA were obtained using

quantum-chemical calculations in the program package FIREFLY [6] with Hartree-Fock method with 6-311++G(d,p), 6-311G(d,p) and 6-31G(d) basis sets. Quantum-chemical calculations of the vibrational frequencies of the monomer and molecular clusters of 5-methylresorcinol (up to $n = 6$) were carried out. Structural characteristics of 5-methylresorcinol clusters and associates with water have been found. It was shown that uncharged 5-methylresorcinol molecules preferably adsorbed on the surface of lysozyme. The radius of gyration of the protein depended on concentration of the ligand. The radial distribution function, showing the spatial distribution of the ligand relative to the protein, and dynamic changes in lysozyme under the influence of ligands were revealed. To improve molecular dynamics force fields for description of high-energy X-rays, excitation and loss of electron by 5-methylresorcinol and its complexes were studied. Methods of time-dependent DFT with aug-cc-pVDZ basis set were used, Møller Plesset perturbation theory of second order was involved. To assess the possible contribution of Interatomic Coulombic decay [7] in the electron density redistribution, electron density maps for different charge states and the degree of excitation were identified. It was shown that geometric structure of the molecules is highly dependent on the degree of excitation and the charge state. There is a dissociation of clusters of 5-methylresorcinol. It was found that behavior of small ligands significantly affects structural changes in the associated protein.

The work was supported by Russian Foundation for Basic Research (project No 12-04-31915) and the Ministry of Education and Science of Russia.

1 Krupyanskii Yu. F., Abdulnasyrov E. G., Loiko N. G., Stepanov A. S., Tereshkina K. B., El'-Registan G. I. *Possible Mechanisms of the Influence of Hexylresorcinol on the Structure-Dynamic and Functional Properties of Lysozyme Protein* // Russian Journal of Physical Chemistry B, **2012**, Vol. 6, No. 2, pp. 301–314

2 Tereshkina K. B., Krupyanskii Yu. F. *Study of the interaction of small molecule ligands and their complexes with lysozyme by molecular dynamics methods* // Mathematics. Computing. Education, Dubna, **2013**, p. 37

3 Krupyanskii Yu.F, Balabaev N.K., Grum-Grzhimailo A.N., Lunin V.Yu., Petrova T.E., Sinitsyn D.O., Gryzlova E.V., Tereshkina K.B., Abdulnasyrov E.G., Stepanov A.S. *Femtosecond X-Ray Free-Electron Lasers: New Tool for Study of Nanocrystals and Single Molecules* // Russian Journal of Physical Chemistry B, **2013**

4 Lunin V.Y., Grum-Grzhimailo A.N., Gryzlova E.V., Sinitsyn D.O., Balabaev N.K., Lunina N.L., Petrova T.E., Tereshkina K.B., Abdulnasyrov E.G., Stepanov A.S., Krupyanskii Y.F. *Computer Simulation of Diffraction of X-ray Pulses by Nanocrystals of Biological Macromolecules Using Unitary Approximation of Nonstationary Atomic Scattering Factors* // Math. Biol. Bioinf. **2013**. 8, 93-118 (rus). http://www.matbio.org/2013/Lunin_8_93.pdf

5 van der Spoel D., Lindahl E., Hess B., Groenhof G., Mark A.E. and Berendsen H.J.C. *GROMACS: Fast, Flexible and Free* // J. Comp. Chem., 26, **2005**. P. 1701-1719

6 Granovsky A.A. *Firefly version 7.1.G.* http://classic.chem.msu.su/gran/firefly/index.html
7 Cederbaum L.S., Zobeley J., Tarantelli F. *Giant Intermolecular Decay and Fragmentation of Clusters* // Phys. Rev. Lett. 1997, 79 (24): 4778–4781.

Implementation of Meso-GSHMC algorithm in GROMACS molecular simulation package

Terterov I.[1], *Escribano B.*[2], *Dubina M.*[1], *Akhmatskaya M.*[2]

[1] St. Petersburg Academic University Nanotechnology Research and Education Center RAS, 8/3 Khlopina str., St. Petersburg 194021, Russia
[2] Basque Center for Applied Mathematics, Alameda de Mazarredo 14, E-48009, Bilbao, Spain

Molecular dynamics is one of the most popular techniques for simulating molecular systems in biology and nanoscience. Standard molecular dynamics (MD) method is naturally performed under conditions of constant energy E, volume V and number of particles N. These conditions are often referred as *micro-canonical ensemble* (*NVE*), but most experimental data corresponds to ensembles with constant temperature (*NVT* or *NPT*, where P is pressure). Constant average temperature in MD simulation may be achieved by introduction of a specific thermostat [1]. Moreover in order to get proper sampling from target *NVT* (*NPT*) ensemble the thermostat should conserve canonical distribution. In contrast to usual global thermostats, stochastic thermostats (e.g. Langevin Dynamics (LD) and Dissipative Particle Dynamics (DPD)) satisfy the latter requirement. Furthermore, in the context of coarse-grained models fluctuation-dissipation impact of stochastic thermostats may also simulate the influence of non-resolvable finer details of the investigated systems. It should be mentioned that inter alia DPD conserves total momentum of the system, and preserves hydrodynamic behavior of the system in macroscopic limit, so it seems to be more accurate for coarse-grained models.

Meso-GSHMC[3] algorithm provides an approach to introduce stochastic thermostats (in general with arbitrary position dependent fluctuation-dissipation terms) in the framework of Hybrid Monte-Carlo methodology [2]. Meso-GSHMC relies on the splitting of equations of motion into conservative and fluctuation-dissipation parts [1]. Conservative part is approximated over L steps with Stormer-Verlet method. This is followed by Metropolis test providing more regular and efficient sampling from target *NVT* ensemble. To increase accepted rate of Metropolis criterion Shadow energies are used as Stormer-Verlet method conserves them more accurately than usual energies

[3] Meso – Generalized Shadow Hybrid Monte-Carlo

[3]. Thereafter fluctuation-dissipation part is numerically approximated over one time step with fixed particle positions. In this way we obtain new velocities from the application of a stochastic thermostat. If we are using Shadow energies new velocities are accepted with Metropolis criterion. To increase the acceptance rate such a velocity refreshment step may be repeated several times. Note that if we use Shadow energies then we sample from ensemble with Shadow Hamiltonians, thus we should perform weighted averaging while computing observables [3].

Previously, related GSHMC method was implemented in GROMACS software package [4] and it was shown to provide more efficient sampling then standard MD for large and complex molecular systems [3, 5]. The GSHMC method differs from Meso-GSHMC in velocity refreshment step that conserves canonical distribution but does not directly relate to known stochastic thermostat equation.

In this work we present an implementation of Meso-GSHMC algorithm in GROMACS software package (v.4.5.4) [4]. The implementation contains velocity updates corresponding to LD and DPD stochastic equations. Solution in both cases conserves the canonical distribution [2]. LD equations are solved explicitly while for DPD solution is found iteratively.

We tested the algorithm on system consisting of 1024 coarse grained water molecules (MARTINI water particle with mass 72u [6]) in the $(5\ \mathrm{nm})^3$ box. We found that radial distribution function does not depend on input parameters (stochastic friction γ, length of constant energy MD between velocity refreshments L, time step of simulation Δt), which indicates that the method does not corrupt physical behavior of the system. Also it was found that the method efficiently works as a thermostat with a various range of input parameters.

We found that one choice of input parameters provides a possibility to use Meso-GSHMC as a pure thermostat, which maintains constant temperature in average and guarantees canonical distribution even with reasonably large L, but does not sufficiently affect low range dynamics. On the other hand it is possible to obtain diffusion coefficients close to those in standard LD without refreshment of velocity at every step.

1 Allen M., Tildesley D. *Computer Simulation of Liquids*. Clarendon Press, Oxford, **1987**.

2 Akhmatskaya E., Reich S. *Meso-GSHMC: A stochastic algorithm for meso- scale constant temperature simulations* // Procedia Computer Science, **2011**, 4, 1353-1362.

3 Akhmatskaya E., Reich S. *GSHMC: An efficient method for molecular simulations* // J. Comput. Phys., **2008**, 227, 4934-4954.

4 Hess B., Kutzner C., van der Spoel D., Lindahl E. *GROMACS 4: Algorithms for highly efficient, load-balanced, and scalable molecular simulation* // J. Chem. Theory Comput., **2008**, 4, 435-447

5 Wee C.L., Sansom M.S., Reich S., Akhmatskaya E. *Improved sampling for simulations of interfacial membrane proteins: application of generalized shadow hybrid Monte Carlo to a peptide toxin/bilayer system* // J Phys Chem B., **2008**, 112(18), 5710-7

6 Marrink S.J., Risselada H.J., Yefimov S., Tieleman D. P., de Vries A. H. *The MARTINI Force Field: Coarse Grained Model for Biomolecular Simulations* // J. Phys. Chem. B, **2007**, 111 (27), 7812-7824

Simulation of conductivity of ionic channel purinergic P2X2 receptor using combined Brownian and molecular dynamic approach

Turchenkov D.A., Turchenkov M.A.

«BioSim» Research Group, Moscow, 115211, Russia. E-mail: biosim.rg@gmail.com

This paper investigates the possibility of using combined approach of molecular and Brownian dynamic methods for modeling of the process of ionic conductivity of purinergic ionc channel P2X2. Electrostatic parameters of particles in simulation were obtained using modern DFT methods of quantum chemistry. The calculations were carried out with PCS (Patch Clamp Simulation) program package, designed for simulation of neurotransmission processes, using Brownian and molecular dynamic methods with GPU acceleration support based on NVIDIA CUDA.

Model of an ionic pore in a membrane suggests three compartments: ionic pore itself in the bilayer, and intra- and extracellular areas.

Langevin equation describes ionic motion in outer membrane region:

$$m\frac{dV}{dt} = -m\gamma V + F_e(t) + F_s(t)$$

where $\gamma = \zeta/m$ – specific friction coefficient, $F_s(t)$ - stochastic force. The intermolecular potential energy between atomic sites can be calculated as a sum of the Coulomb electrostatic interaction and the Lennard–Jones potential. Implementation of difference equations includes correlation of stochastic increments of coordinate X_i and velocity V_i at each integration step [1].

The friction coefficient is divided into viscous and dielectric friction parts:

$$\zeta = 4\pi\eta R + \frac{1}{4\pi\varepsilon_0}\frac{3q^2(\varepsilon - \varepsilon_\infty)\tau_D}{4\varepsilon^2 R^3}$$

Given low ion concentration in the near-membrane region (< 0.8 M), the dependences of the viscosity η and the dielectric constant ε on the concentration of dissolved electrolyte are described by the Eyring [2] and Jones-Dole equations respectively. The movement of ions in the channel part is described using simplified MD methods, ion channel is approximated by solid body, geometric parameters were determined from electron microscopy data [3]. Charges of amino acid residues, which are presumably responsible for a selective filter, were refined by modern methods of quantum chemistry (DFT).

Membrane lipids were simulated explicitly. Absolute surface charge density did not exceed 50 mC/m^2.

At first we calculated ionic conductivity using following parameters: compartment size 100 Å, T =298° K, BD step 0.1 ns, MD step 1 ps, $[NaCl]_{out}/[NaF]_{in}$ = 145/145 (mM), holding membrane potential −100 mV.

Current value $I = -3.0 \pm 0.2$ pA for conductivity $G = 30 \pm 2$ pS is in good agreement with the experimental patch-clamp results (32 pS [4]).

Parameters of the ion currents can be estimated through the current-voltage characteristics. For this purpose, we conducted a series of similar simulations using membrane potential $-20 \div -100$ mV. The comparison between model results and experimental data is presented below (see Figure).

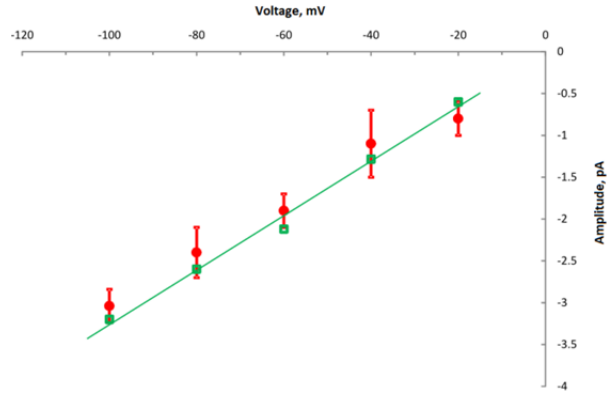

Figure. Current-voltage characteristic of P2X2 ion channel. Experimental data (□) [4, 5], calculation data (•).

At last the selectivity of P2X2 receptor was investigated. For that purpose, LiCl, KCl, NaCl, RbCl and CsCl solutions were simulated with extracellular concentration 145 mM and membrane potential −120 mV. Results are presented in the Table below.

Table

Ion	Li^+	Na^+	K^+	Rb^+	Cs^+
I, pA	−3.52	−3.92	−4.52	−4.36	−4.38
G, pS	29	33	38	36	37

It is seen that the channel permeability for monovalent cations varies in the following order: $K^+ \approx Cs^+ \approx Rb^+ > Na^+ > Li^+$, which corresponds to the experimental data [4]. Note that a similar order is preserved for the diffusion of ions in the water.

1 Turchenkov D. A., Turchenkov M. A., Computer Research and Modeling. **2012**, Vol. 4, 2.
2 Goldsack D. E. Franchetto R., Canadian Journal of Chemistry. **1977**, Vol. 55, 1062.
3 Mio K., Ogura T. Structure, 2009. Vol. 17, no. 2
4 Ding S., Sachs F. The Journal of general physiology. **1999**. Vol. 113, no. 5
5 Wong A. Y., Burnstock G., Gibb A. J, The Journal of Physiology. **2000**. Vol. 527, no. 3

GPU-accelerated Brownian dynamics simulation of protein interactions

Ustinin D.M., Khrushchev S.S., Kovalenko I.B.

Faculty of Biology, Lomonosov Moscow State University

Brownian dynamics simulation is a powerful tool which allows building detailed models of complex subcellular systems such as photosynthetic membrane [1]. Main advantage of Brownian dynamics simulation in comparison to molecular dynamics is that with Brownian dynamics we can simulate systems of hundreds and thousands of interacting proteins and use realistic compartment geometry [2]. Numerical methods which are used in Brownian dynamics simulation can be implemented using parallel algorithms. That is a great advantage because computer hardware now evolves to massive parallel calculation systems. For example, modern graphical processing units (GPU) include hundreds of processor cores in one device and can be utilized for general purpose calculations using specialized APIs, such as NVIDIA CUDA. Our work was dedicated to development of parallel algorithms and software which use GPU for Brownian dynamics simulation of photosynthetic membrane, which includes hundreds of interacting proteins.

Proteins are simulated as solid bodies in 3-dimensional compartments, representing different parts of photosynthetic membrane. We take into account electrostatic interactions of proteins with each other and electric field of the

membrane. Electric charge distribution on proteins is constructed using PDB data. Langevin equation is solved to simulate movement of proteins which happens due to random force and electrostatic forces. Electrostatic field of proteins is calculated by solving Poisson-Boltzmann equation which allows us to consider different dielectric permittivity of protein and water.

Brownian dynamics simulation includes some algorithms which should be adapted to massive parallel calculations:

1) Random number generation. We used two parallel random number generators for GPU: Mersenne-Twister and hybrid Hausworthe generator [3]. The first has better statistical properties but the second one is about ten times faster. Comparison of the simulation results showed that quality of hybrid Hausworthe generator is good enough for our purposes.

2) Electrostatic force calculation can be done simultaneously for each charge of specified protein, so that part is naturally parallel. Each GPU thread calculates interaction of one charge with electrostatic field. 3-dimensional mesh which stores spatial field distribution for proteins is stored in GPU global memory.

3) The most sophisticated part is parallel calculation of collisions between proteins. We use several methods for collision detection – approximation of protein surface with spheres, calculation of distance between charged atoms or between each atom-atom pair. We need special data preparation before calculation of distance between pairs. All interacting pairs (sphere-sphere or atom-atom) are ordered into linear array in GPU memory. After that, each GPU thread calculates distance between pairs in parallel. If at least one of the pairs is closer than minimal accepted distance, collision occurs.

When we implemented all these algorithms as parallel software for GPU using NVIDIA CUDA API, we reached performance gain of about 8 times compared to CPU version.

The work was funded by Russian Foundation of Basic Research grants 12-07-33036, 12-07-00783 and 12-04-31839.

1 Khruschev S.S., et.al. *Multi-particle Brownian Dynamics software ProKSim for protein-protein interactions modeling* // Computer Research and Modeling, **2013**, vol. 5, no. 1, pp. 47-64

2 Ustinin D.M., Kovalenko I.B., Riznichenko G.Yu., Rubin A.B. *Combination of different simulation techniques in the complex model of photosynthetic membrane* // Computer Research and Modeling, **2013**, vol. 5, no. 1, pp. 65-81

3 Howes L., Thompson R. *Efficient Random Number Generation and Application Using CUDA* / In GPU Gems 3, Addison Wesley Professional, **2008**.

Computer simulations of transmembrane helical dimers: From structure to functioning

Volynsky P.E., Polyansky A.A., Efremov R.G.

M.M. Shemyakin and Yu.A. Ovchinnikov Institute of Bioorganic Chemistry Russian Academy of Sciences, ul. Miklukho-Maklaya 16/10, GSP Moscow, 117997 Russia.

Single-span or bitopic membrane proteins (BMP) play a very important role in cell life. They are involved in such processes as cell differentiation, proliferation, communication and so on. Often association of BMP is a necessary step in its functioning. For example, activation of receptor tyrosine kinases occurs as an answer to ligand-induced dimerization. Association of BMP is a very sensitive process, regulated by a lot of factors: interactions with ligands, membrane composition, pH of local environment and so on. According to current knowledge, transmembrane segments (TMS) play an important role in work of such proteins [1]. Transitions between different dimeric states of TMS are an important factor in a proper functioning of the protein system, and shift in equilibrium caused, for instance, by mutations in TMS, lead to development of different diseases. Therefore, investigation of molecular mechanisms of such processes is very important for understanding of BMP functioning in norm and pathology and can help in designing of new drugs, targeting such systems.

Nowadays methods of the computer simulations are quite up to performing of such tasks [2]. Methods of structure prediction permit to obtain a limited set of dimeric conformations, consistent with the experimental studies. Progress in computational equipment makes possible an assessment of dimerization energy, which demands a lot of computations for collection of a large statistics. Combination of different computational approaches permits to analyze dimerization in full – from amino acid sequence to proposal of a model of functional rearrangements.

We illustrate application of computational approaches to study of TMS dimerization on fibroblast growth factor receptor 3 (fgfr3). This protein plays an important role in organism development, acting as a negative regulator of bone growth [3]. Mutations in the transmembrane domain of fgfr3 cause different developmental disorders. This dimer and its mutant homologs are well studied experimentally and thus they are suitable objects to illustrate capabilities of computational approaches.

Principal scheme of dimerization analysis is presented in Figure. The first step is assessment of possible dimeric conformations of a dimer. It is performed using Monte Carlo conformational search in implicit membrane followed by optimization of the best structures via molecular dynamics in explicit bilayers [4]. Then final models are ranged according to dimerization

free energy, calculated by a series of constrained MD runs. Such scheme was applied to study of dimers of fgfr3 and two of its pathogenic mutants (G380R, A391E). Results can be summarized as follows: (1) Structural analysis of fgfr3 TMS dimer permitted to obtain several possible dimer geometries: two symmetric forms and several asymmetric. These conformations were significantly different in packing geometry and stabilizing forces. (2) Assessment of dimerization energy showed that one symmetric conformation of a dimer (major conformation, s1) was much favorable than the others. This model was in a good agreement with the model, proposed previously [5]. (3) Structural analysis of mutants revealed that their behavior in membrane differed from the wild type models. G380R dimer shifted along the membrane normal in the direction of N-termini to expose charged residue R380 into polar phase of the system. In case of A391E changes were not so prominent and consistent in formation of new intermonomer contacts or water penetration depending on the model. (4) Mutation did not significantly affect dimerization energy of the major conformation. On the other hand they facilitated dimerization for the second symmetric model (s2) and one of the asymmetric models (a3). (5) Analysis of all simulations data allows to offer a model of rearrangements of TMS domains during activation. In the absence of ligand, fgfr3 exist in inactive form with TMS packed as in model s1 (Fig e). Binding of one ligand molecule leads to repacking of TMS domain into some asymmetric structure and binding of second ligand molecule transits it to the s2-like structure (fig 1e). This activation model agrees well with the experimental data and explains effects of substitutions (over-activation).

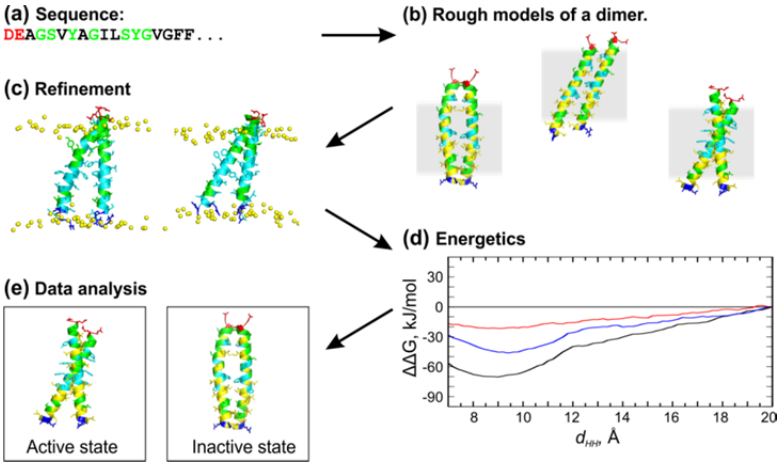

Figure. Exploring dimerization of helical TMS using computational approaches.

1 Li E., Hristova K. *Role of receptor tyrosine kinase transmembrane domains in cell signaling and human pathologies* // Biochemistry. **2006**. 45(20):6241-51
2 Polyansky A.A., Volynsky P.E., Efremov R.G. *Structural, dynamic, and functional aspects of helix association in membranes: a computational view* // Adv Protein Chem Struct Biol. **2011**; 83:129-61
3 Deng C., Wynshaw-Boris A., Zhou F., Kuo A., Leder P. *Fibroblast growth factor receptor 3 is a negative regulator of bone growth* // Cell. **1996**. 84(6):911-21.
4 Volynsky P.E., Mineeva E.A., Goncharuk M.V., Ermolyuk Y.S., Arseniev A.S., Efremov R.G. *Computer simulations and modeling-assisted ToxR screening in deciphering 3D structures of transmembrane alpha-helical dimers: ephrin receptor A1* // Phys Biol. **2010**. 7:16014.
5 Li E., You M., Hristova K. *FGFR3 dimer stabilization due to a single amino acid pathogenic mutation* // J Mol Biol. **2006**. 356(3):600-12.

Constructing the model of redox-cofactor as a center of electron localization with a potential well from *ab initio* calculations

Yaroshevitch I.A.[1], *Nesterenko A.M.*[1,2], *Krasilnikov P.M.*[1]

[1] Lomonosov Moscow State University, Faculty of Biology, Department of Biophysics
[2] A.N. Belozersky Institute of Physico-Chemical Biology MSU

The efficiency of electron transfer in a model of pair-wise interacting redox centers depends on the overlap of initial and final state wave functions. For the purpose of overlap calculation, donor center and acceptor sites of electron localization can be interpreted as three dimensional potential wells (PWs). An overlap of corresponding wave functions drastically depends on wave function spatial decay rate, which in turn depends on the structure of donor's and acceptor's PW. Wave functions can be determined from PW analytically which allows us to directly define the electronic matrix element which governs the rate of electron transfer between electron donor and acceptor molecules.

The aim of this work was to develop a quantum model of electron donor and acceptor molecules as a donor and acceptor PWs. PW of the donor was defined as an electrostatic potential of all nuclei and all electrons except the electron on the highest occupied molecular orbital (HOMO). PW of the acceptor was defined as an electrostatic potential of all nuclei and of all electrons. The main task of the work was to calculate electrostatic potential of several biologically important agents such as chlorophyll, pheophytin and quinone in oxidized and reduced states.

Two forms of each molecule were studied: acceptor (neutral) and donor (anion). Geometries of all molecules were optimized using ROFH-DFT

(B3LYP5) method with mini-aug-cc-pvDZ basis set. Wave functions corresponding to optimal structure were further improved using ROHF-MP2 method and were used for PW calculations. To verify the method, electron affinity and ionization energy for parabenzoquinone were estimated. The values of 2 eV and 11.5 eV were obtained. The values are in a good agreement with the experimental data (1.92 eV and 10 eV according to [Sasaki, et. al., 1990]). PW of the acceptor was calculated as electrostatic potential of the neutral molecule. PW of the donor was obtained by calculating electrostatic potential of a neutral molecule, with electronic structure described by wave function obtained for the anion form. Figure depicts a parabenzoquinone PW cross section along orthogonal axes passing through the center of the molecule. Both states are presented in the figure. Horizontal lines mark energy of two highest occupied molecular orbitals of the anion radical. In both cases PWs can be fitted with a hyperbole. Note that PW's cross section along the axis, which passes through both oxygen atoms, has a region of negative electrostatic potential, that was called "locking EP". Electron potential estimated for the acceptor form differs quantitatively but not qualitatively (see Figure).

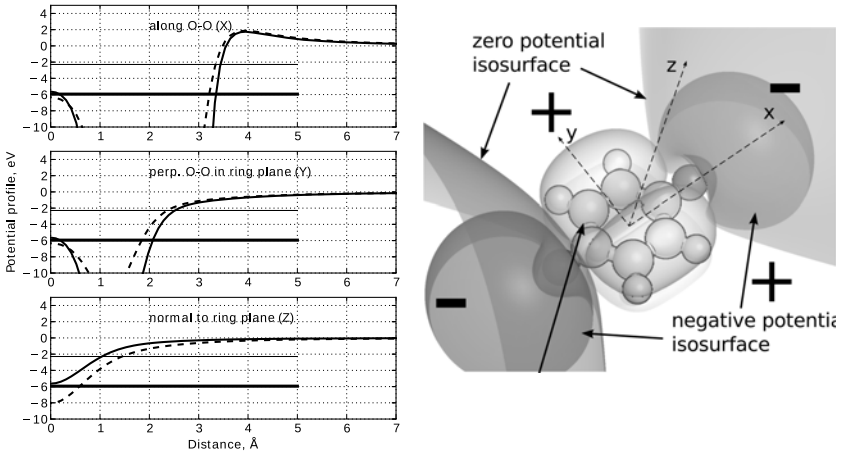

Figure. Shape of potential well for p-benzoquinone along 3 directions is depicted in the right. Straight line corresponds to anion state, dashed line – to neutral state.

Same way we obtained PWs for octamethyl porpherine (as a model of pheophytine), octamethyl magnesium porphyrin (as a model of chlorophyll) and 2,3-dimethoxy-5-(3-methylbut-2-enyl)-6-metyl-paraquinone (as a model of Q10). Existence of locking EP was typical for all studied molecules. Absolute

value of locking EP varies from 0.5 to 3 eV and its value and direction are strongly dependent on substituents.

On the basis of performed calculations one can conclude that the shape of potential is different for different directions and in some directions there are areas of negative EP. The effectiveness of electron tunneling in those directions is decreased. So relevant biomolecules have preferred directions for electron transfer and their orientation should affect kinetics of the redox reaction. Presented calculations allow development of a 4-dimensional model of a PW of a low-molecular cofactor. If the shape of potential barrier is calculated precisely then it is possible to estimate amplitude of wave functions outside the nuclear skeleton of molecule. Obtained results will be used to calculate a wave functions' overlap integral for interacting redox centers.

The work is supported by the RFBR (project no. 13-04-00403). *Ab initio* calculations were performed using supercomputer complex SKIF MSU [2].

1 Sasaki K., Kashimura T., Masahiro O., Yasushi O., Nobuaki, O. Journal of The Electrochemical Society, **1990**, 137(8), 2437–2443. doi:10.1149/1.2086957

2 Voevodin V.V., Zhumatiy S.A., Sobolev S.I., Antonov A.S., Bryzgalov P.A., Nikitenko D.A., Stefanov K.S., Voevodin V.V. Open Systems J. (Russian). **2012**. № 7. [http://www.osp.ru/os/2012/07/13017641]

Microscopic mechanism of transition from"catch" bonds to "slip" bonds in cell adhesion

Zhukov P.I.[1], *Zhmurov A.A.*[1,2,*], *Hyeon C.*[3], *Barsegov V.A.*[2,1]

[1] Division of Computational Mathematics, Moscow Institute of Physics and Technology, Moscow region, Russia, 141700
[2] Department of Chemistry, University of Massachusetts, Lowell, MA 01854, USA
[3] School of Computational Sciences, Korea Institute for Advanced Study, Seoul 130-722, South Korea
[*] +7-495-408-73-81; zhmurov@gmail.com

P-selectins, members of the selectin family of adhesion proteins, are known to facilitate leukocyte rolling during inflammatory response. It was shown experimentally that under application of an external force the bond between P-selectins and their complementary ligand, P-selectin glycoprotein-1 (PSGL-1), exhibit non-standard behavior. When the external force increases, the P-selectin–PSGL-1 bond's lifetime initially increases, and only after that it decreases [1, 2]. This phenomenon was called the "catch"-"slip" bond and was later found in several other receptor-ligand pairs [3]. The existence of the initial increase of the receptor-ligand bond strength can be explained by two-state unbinding kinetics [4, 5]. In this model there exists a second state with much

larger dissociation barrier. Upon force application, the system can undergo a transition to the second state, and the dissociation force is larger compared to one step kinetics (i.e. when dissociation occurs for the native state). Although the second state can explain the emergence of the "catch"-"slip" duality of a non-covalent bond, the molecular basis of this state is unknown. Computer simulations continue to play an increasingly more important role in providing detailed information about the unfolding and unbinding transitions in biomolecules. Molecular simulations can be used to resolve structural basis of the second bound state. However, given the long timescales underlying the dissociation kinetics for this process (10^{-2}–10^{1} seconds) and low dissociation forces for the "catch" bond (10–50 pN), the use of the traditional molecular dynamics approach is problematic. This technique has already been used to explore the "catch"-"slip" transition in the P-selectin–PSGL-1 bond [6]. However, due to short timescales of simulations (~5 ns), only small deviations of the molecular complex from the native state has been probed.

In this work, we have utilized computational acceleration with Graphics Processing Units (GPU) in conjunction with implicit solvent models to resolve the structural details of the second bound state in the P-selectin–PSGL-1 bond dissociation profile. Combination of the implicit solvent approach and GPU acceleration allowed us to follow the dynamics of the system in 1-2 μs timescale. Using the force-ramp pulling protocol, we compared the results obtained with three different pulling speeds ($v_f = 10^4$, 10^5 and 10^6 μs). We showed that with $v_f = 10^6$ μm/s the unbinding occurs in one step with no detectable alternative bound state in all the trajectories. Interestingly, when we decreased the pulling speed to $v_f = 10^4$ μm/s, ~30% of the trajectories followed a different binding pattern characterized by a larger unbinding force (Figure 1b). In these trajectories, the number of contacts between P-selectin and PSGL-1 initially increased with the increasing force (Figure 1a), which was shown to be due to the structural transition at the microscopic level. Specifically, the loop containing amino acids Asn57-Glu74 in lectin domain dissociates from the EGF-domain and associates with the PSGL-1 ligand (Figure 1c).

It was suggested that formation of the "catch" bond is mediated by the flexibility of the hinge region between the EGF domain and the lectin domain of the P-selectin receptor [7, 8]. The Asn57-Glu74 loop is bound to this hinge region of the P-selectin receptor in its native state. The observed bending motion can be shown to be directly related to the fluctuating strength of interactions that hold the Asn57-Glu74 loop bound to the EGF domain in the native state. Hence, when the receptor is stretched, these interactions become stronger constraining the position of the loop. As a result, the strength of the bond does not change ("slip" bond). When the external force is low, the loop is relatively free to move and can switch its binding contacts from the EGF

domain to the PSGL-1 ligand, thus mediating formation of the "catch" bond. This dynamic behavior dominates the dissociation kinetics until the mechanical force reaches some characteristic force at which all the cryptic contacts buried in the receptor-ligand interface in the unstretched state are fully engaged. Above the characteristic force, these newly emerging interactions become weaker and the dissociation kinetics enters the "slip" regime of bond rupture.

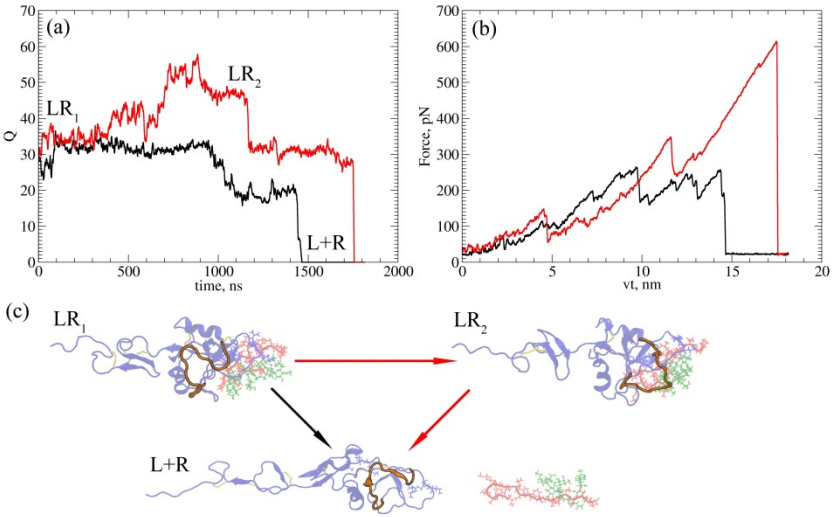

Figure. P-selectin–PSGL-1 forced dissociation dynamics observed at a pulling speed $u_f = 10^4$ μm/s. (a): The dependence of the number of contacts Q on time during forced dissociation. (b): Force-extension profiles observed in a course of forced dissociation. (c): Structural snapshots which represent the two-state kinetics of unbinding underlying the forced dissociation of the P-selectin–PSGL-1 bond [4, 5]. P-selectin receptor is shown in blue. The protein and polysaccharide parts of the PSGL-1 are shown in red and green, respectively. Disulfide bonds are shown in yellow. The movable loop (residues Asn57-Glu74) is highlighted in orange. The trajectory of unbinding that occurs in one step ($LR_1 \rightarrow L + R$) is shown in black color, whereas the trajectory of unbinding that occurs through the formation of the second bound state ($LR_1 \rightarrow LR_2 \rightarrow L + R$) is shown in red.

The reported study was partially supported by RFBR (research project No. 12-04-31861 mol_a) and Russian Ministry of Education and Science (grant 14.A18.21.1520).

1 Marshall B. T., Long M., Piper J. W., Yago T., McEver R. P., Zhu C. *Direct observation of catch bonds involving cell-adhesion molecules* // Nature, **2003**, vol. 423, no. 6936, pp. 190–193.
2 Evans E., Leung A., Heinrich V., Zhu C. *Mechanical switching and coupling between two dissociation pathways in a P-selectin adhesion bond* // Proc. Nat. Acad. Sci. USA, **2004**, vol. 101, no. 31, pp. 11281–11286.
3 Hertig S., Vogel V. *Catch bonds* // Curr. Biol., **2012**, vol. 22, no. 19, p. R823.
4 Barsegov V., Thirumalai D. *Dynamics of unbinding of cell adhesion molecules: transition from catch to slip bonds* // Proc. Nat. Acad. Sci. USA, **2005**, vol. 102, no. 6, pp. 1835–1839.
5 Barsegov V., Thirumalai D. *Dynamic competition between catch and slip bonds in selectins bound to ligands* // J. Phys. Chem. B., **2006**, vol. 110, no. 51, pp. 26403–26412.
6 Lu S., Long M. Forced dissociation of selectin-ligand complexes using steered molecular dynamics simulation // Mol. Cell. Biomech., **2005**, vol. 2, no. 4, pp. 161–167.
7 Beste M. T., Hammer D. A. Selectin catch–slip kinetics encode shear threshold adhesive behavior of rolling leukocytes // Proc. Nat. Acad. Sci. USA, **2008**, vol. 105, no. 52, pp. 20716–20721.
8 Springer T. A. Structural basis for selectin mechanochemistry // Proc. Nat. Acad. Sci. USA, **2009**, vol. 106, no. 1, pp. 91–96.

Preparation of ferredoxin and FNR molecular models

Zlenko D.V., Diakonova A.N.

Lomonosov Moscow State University, biophysical division of biological department.
119992, Leninskiye grory 1/12, Moscow, Russia. E-mail: dvzlenko@gmail.com

The main goal of this work was to create accurate molecular mechanic models of ferredoxin and ferredoxin:$NADP^+$-reductase (FNR) molecules in aqueous solution. Both ferredoxin and FNR are members of photosynthetic electron-transport chain in thylakoid membrane of chloroplasts. These molecular models will be used as initial conditions for detailed molecular simulation of ferredoxin-FNR complex formation and transition between preliminary and final complexes of these proteins. Transition between preliminary and final complexes is essential for electron transfer and thus for overall redox chain functioning.

Equilibration of protein molecules' models in aqueous salt solution is also necessary for rigid body modeling of protein molecules. Rigid body molecules are used in Brownian dynamics simulation of thylakoid membrane functional activity [1]. Integration of classical all-atom molecular mechanics approach with coarse-grain Brownian dynamics simulation of multi protein scene of

thylakoid membrane and its surrounding medium allows us to predict kinetic constants of reactions in photosynthetic electron transport chain.

Atomic coordinates for ferredoxin and FNR protein molecules were taken from 1EWY PDB data file. GROMACS [2] software package was used for all molecular dynamics simulations. Force parameters for core proteins were set according to standard CHARMM [3] set. Force parameters, partial charges and VdW parameters for [2Fe2S]-cluster of ferredoxin were set as in [4]. Force parameters for FAD molecule were combined from FMN [5], pyrophosphate ion [6] and common riboadenosin CHARM parameters.

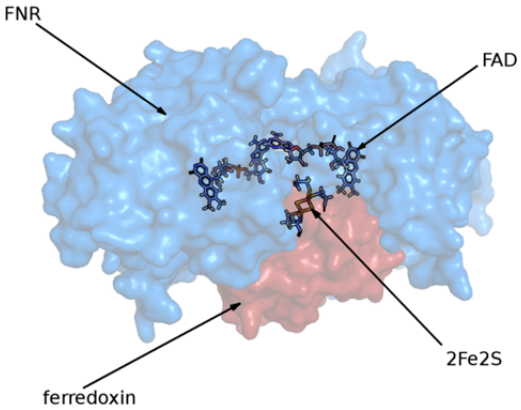

Figure. Crystal structure of ferredoxin/FNR complex from 1EWY PDB entry.

First we create valid CHARMM topologies of FNR and ferredoxin. Than we place proteins and their complex into a cubic box with the edge length of 9 nm. Such a big cube is necessary due to significant interaction of protein molecules with their periodic images through periodic boundary conditions in smaller boxes. Protein molecules were solved in a preliminary equilibrated NaCl solution with concentration 150 mM in TIP4P water [7]. After the geometry optimization step we accomplished relaxation simulations of 100 ns length in periodic boundary conditions. Integration step was set to 1 fs, for electrostatic energy calculation PME [8]. Langevin equations were used for motion simulation.

The work is supported by the RFBR (project no. 12-04-31839 and 12-07-33036).All MD simulations were accomplished with a LOMONOSOV supercomputer in MSU Research Computing Center [9].

1 Kovalenko I.B., Diakonova A.N., Abaturova A.M., Riznichenko G.Yu., Rubin A.B. *Direct computer simulation of ferredoxin and FNR complex formation in solution* // Phys. Biol. **2010**. 7(3): 026001.
2 Pronk S., Páll S., Schulz R., Larsson P., Bjelkmar P., Apostolov R., Shirts M.R., Smith J.C., Kasson P.M., van der Spoel1 D., Hess B., Lindahl E. *GROMACS 4.5: a high-throughput and highly parallel open source molecular simulation toolkit*. Bioinformatics // **2013**. 29 (7): 845-854.
3 Jorgensen W.L. Maxwell D.S., Tirado-Rives J. *Development and Testing of the OPLS All-Atom Force Field on Conformational Energetics and Properties of Organic Liquids* // J. Amer. Chem. Soc. **1996.** 118:11225-11236.
4 Chang C.H., Kim K. *Density functional theory calculation of bonding and charge parameters for molecular dynamics studies of [FeFe]-hedrogenases* // J. Chem. Theory Comput. **2009**. 5: 1135-1145
5 Freddolino P.L., Dittrich M., Schulten K. *Dynamic switching mechanisms in LOV1 and LOV2 domains of plant phototropins* // Biophys. J. **2006**. 91: 3630-3639.
6 Pavelites J.J., Gao J., Bash P.A., Mackerell A.D. Jr. *A molecular mechanics force field for NAD+, NADH, and the pyrophosphate groups of nucleotides* // J. Comp. Chem. 1997. 18: 221-239.
7 Lawrence C.P., Skinner J.L. *Flexible TIP4P model for molecular dynamics simulation of liquid water* // Chem. Phys. Lett. **2003**. 372: 842–847.
8 Essmann U., Perera L., Berkowitz M.L., Darden T., Lee H., Pedersen L.G. *A smooth particle mesh Ewald method* // J. Chem. Phys. **1995**. 103: 8577–8593.
9 Voevodin V.V., Zhumatiy S.A., Sobolev S.I., Antonov A.S., Bryzgalov P.A., Nikitenko D.A., Stefanov K.S., Voevodin V.V. *Practice of "Lomonosov" Supercomputer* // Open Systems J. (Russian). **2012**. № 7. [http://www.osp.ru/os/2012/07/13017641]

Mapping the intramolecular signal transductions of biomolecules

Hyeon C.

Korea Institute for Advanced Study

Dynamics of biomolecules is regulated by a multitude of signals transmitted inside the molecular structure. To gain better insights into the signaling mechanism at residue level, an allosteric wiring diagram of intramolecular signal transductions would be of great help.

Here, by analyzing the graph representation of protein structure, we calculated the maps of information flow in GPCRs, and identify key residues for signal transductions and their pathways. In strong correlation with biochemical data from mutation studies and X-ray structures at distinct states, our simple approach outperforms the preexisting bioinformatics approach in identifying the rotameric microswitches, which are deemed critical for mediating orthosteric signal transductions in GPCRs. For A2AAR, the intramolecular cross-correlation map calculated using equilibrium structural ensemble from molecular dynamics simulations of the apo and agonist-bound states, reveals that strong signals of long-range transmembrane communications exist in the agonist-bound state. A seemingly subtle variation in structure, found in different GPCR subtypes or imparted by agonist bindings or a point mutation at an allosteric site, can lead to a drastic difference in the map of signaling pathways and protein activity. The map of intramolecular signal transduction elucidated for a given biomolecular structure provides valuable insights into allosteric modulations as well as reliable identifications of intramolecular signaling pathways. If time is allowed, I will further discuss the allosteric signaling from a perspective of random walk on complex networks by considering the trans-ring signaling of GroEL.

Mechanical properties of microtubules from nanoindentation experiments *in silico*

Kononova O.[1,2]*, Barsegov V.*[1,2]

[1]Department of Chemistry, University of Massachusetts, Lowell, MA 01854
[2]Division of Computational Mathematics, Moscow Institute of Physics and Technology, Moscow region, Russia, 141700

Mechanical properties of microtubules (MTs) play an essential role in eukaryotic cellular processes, such as cytoskeletal support, cell motility, and mitosis. The MT structure is long, hollow cylindrical polymer with outer diameter of ~25nm consisting of 13 parallel protofilaments (PFs), each formed by the head-to-tail assembly of αβ-tubulin dimers (Figure). MTs can switch stochastically between growing and shrinking phases, a phenomenon called "dynamic instability" controlled by the GTP hydrolysis [1]. A number of experiments [2, 3] and theoretical studies [1,4] show that the mechanism of MT's polymerization and depolymerization is not yet fully understood. Due to the high complexity of MT structure, the existing theoretical models [1, 3, 4] use a number of approximations that are difficult to justify.

We utilized Self-Organized Polymer (SOP) model [5] and high-performance computing on graphics processing units (GPUs) to model the mechanical nanoindentation experiments on MT *in silico*. This allowed us to perform meaningful simulations utilizing experimental force loads [2], i.e. using force loading rate υ_f = 1.0 μm/s, cantilever spring constant κ = 0.05 N/m and tip radius R_{tip} = 15 nm. To explore the mechanism(s) of MT response to the applied compressive force, we used the simulation output (trajectories of forced indentation) to calculate the surface map of Cauchy stress tensor for the entire MT surface. Nine components of Cauchy stress tensor were calculated numerically for each *i*-th amino acid residue according to the formula: $\sigma_i^{\alpha\beta} = -1/(2\Omega_i)\sum dU_{ij}(r_{ij})/dr_{ij} \cdot r_{ij}^{\alpha} r_{ij}^{\beta} / r_{ij}$ [6], where r_{ij} is the distance between the *i*-th and *j*-th residue, dU_{ij}/dr_{ij} is the force of interactions between them (U_{ij} is the SOP potential energy function [5]), and Ω_i is the molecular volume occupied by the *i*-th residue, $\Omega_i = 4\pi/3a_i^3$, where $a_i = \sum r_{ij}^{-1} / \sum r_{ij}^{-2}$ is "effective size" of a residue. Also, indexes α and β = 1, 2, 3 run over all vector components in 3D space. In order to work with the scalar quantities of the stress tensor, we calculated a normal component of the Cauchy stress tensor obtained by using a projection of the tensor on a normalized vector (***n***), collinear with the MT cylinder axis, $\sigma_i^n = \sum \sigma_i^{\alpha\beta} n^{\alpha} n^{\beta}$.

The results obtained from the SOP model based simulations of the mechanical indenation, accelerated on GPUs several hundred fold, showed that

the theoretical force (F)-indentation (Z) curves are in almost quantitative agreement with the experimental FZ curves [2, 3] (see Figure). The results obtained revealed, quite unexpectedly, unique physic-chemical properties of MT, which cannot be fully understood using experimental data alone. Based on the results of the surface distribution of Cauchy stress tensor, we have purposed a new tensor model describing the mechanical properties of MT lattice.

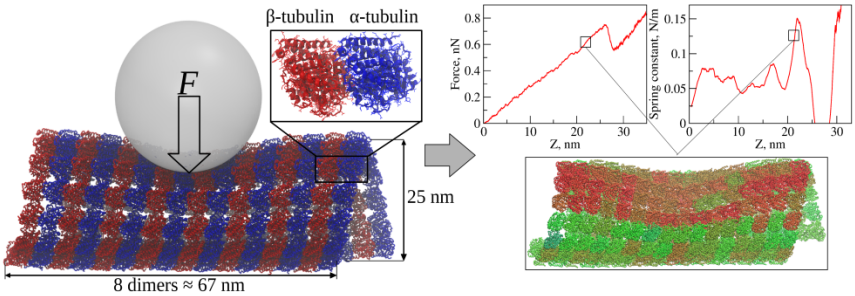

Figure: Left panel: Structure of microtubule, MT, used in force indentation *in silico*: 13 protofilaments (PFs), each PF is 8 dimers long, form a cylindrical structure. The total size of the MT lattice used in simulations is ~67nm in length and ~25nm in diameter. Each dimer consists of α-tubulin (blue) and β- tubulin (red). Right panel: theoretical results of forced indentation *in silico* (R_{tip} = 15 nm, υ_f = 1.0 μm/s): shown are a typical *FZ* curve and "the spring constant' k_{MT} versus *Z*, which quantify the mechanical response of MT. Magnified below is the distribution of Cauchy stress tensor on the MT surface for a particular moment of time. Color denotation: the green (red) color corresponds to less stressed (more stressed) regions in MT lattice.

1 Wu, Z., E. Nogales, and J. Xing. (2012). Comparative studies of microtubule mechanics with two competing models suggest functional roles of alternative tubulin lateral interactions. *Biophys. J.* **102**, 2687-2696.

2 de Pablo, P. J., I. A. T. Schaap, F. C. MacKintosh, and C. F. Schmidt. (2003). Deformation and collapse of microtubules on the nanometer scale. *Phys. Rev. Lett.* **91**, 098101-098104.

3 Shaap, I. A. T., C. Carrasco, P. J. de Pablo, F. C. MacKintosh, and C. F. Schmidt. (2006). Elastic response, buckling, and instability of microtubules under radial indentation. *Biophys. J.* **91**, 1521-1531.

4 Molodtsov, M. I., E. A. Ermakova, E. E. Shnol, E. L. Grishchuk, J. R. McIntosh, and F. I. Ataullakhanov. (2005). A molecular-mechanical model of the microtubule. *Biophys. J.* **88**, 3167-3179.

5 Hyeon, C., R. I. Dima, and D. Thirumalai. (2006). Pathways and kinetic barriers in mechanical unfolding and refolding of RNA and proteins. *Structure* **14**, 1633-1639.

6 Ishikura, T., T. Hatano, and T. Yamato. (2012). Atomic stress tensor analysis of proteins. *Chem. Phys. Lett.* **539,** 144-150.

Monte-Carlo simulations of heavy ions track structures and applications

Plante I.[1]*, Cucinotta F.A.*[2]

[1]Division of Space Life Sciences, Universities Space Research Association, Houston, TX, USA
[2]NASA Johnson Space Center, Houston, TX, USA

In space, astronauts are exposed to protons, high-energy heavy (HZE) ions that have a high charge (Z) and energy (E), and secondary radiation, including neutrons and recoil nuclei produced by nuclear reactions in spacecraft walls or in tissue [1]. The astronauts can only be partly shielded from these particles. Therefore, on travelling to Mars, it is estimated that every cell nucleus in an astronaut's body would be hit by a proton or secondary electron (e.g., electrons of the target atoms ionized by the HZE ion) every few days and by an HZE ion about once a month. The risks related to these heavy ions are not well known and of concern for long duration space exploration missions. Medical ion therapy is another situation where human beings can be irradiated by heavy ions, usually to treat cancer. Heavy ions have a peculiar track structure characterized by high levels of energy-deposition clustering, especially in near the track ends in the so-called 'Bragg peak' region. In radiotherapy, these features of heavy ions can provide an improved dose conformation with respect to photons, also considering that the relative biological effectiveness (RBE) of therapeutic ions in the plateau region before the peak is sufficiently low [2]. Therefore, several proton and carbon ion therapy facilities are under construction at this moment.

The biological effects of radiation are numerous and complex; however, they are initiated by physical, physicochemical and chemical interactions of the radiation with the medium. The DNA damage is considered to be particularly important for the radiobiological effects. Since radiation interactions are stochastic, Monte-Carlo simulations techniques are very convenient not only to help our understanding of the mechanisms of interaction of ionizing radiation with matter, but they are also used in practical applications such as in microdosimetry, accelerator design and radiotherapy treatment planning. The first Monte-Carlo code of track structure simulations was developed in the 1980's [3]. Since then, many other simulation codes have been developed, with different purposes (reviewed in [4]).

The software RITRACKS (Relativistic Ion Tracks) is a Monte-Carlo code developed at the NASA Johnson Space Center to simulate radiation tracks for heavy ions and electrons [5-7]. The main components of RITRACKS are 1) The differential and integrated interaction cross sections of ions and electrons with water; 2) Cross sections sampling algorithms and routines; 3) Particles transport routines; 4) Data collection and management (notably calculation of

dose); 5) Input/output routines; 6) A graphic user interface (GUI); 7) A 3D interface for the visualization of the track structure; 8) Cross section visualization windows; 9) A help file; 10) Redistributable libraries. The calculation part is an independent program which is compiled separately from the GUI, and which can be executed on Linux systems as well. This part of the software calculates the energy deposition events, ionization and excitation of water molecules by the heavy ion and the energy, the position and direction of the secondary electrons, as well as the tracks of the secondary electrons and the positions of all radiolytic species. The ion and electron cross sections, transport methods and simulation results were given in our previous publications [5] and references therein.

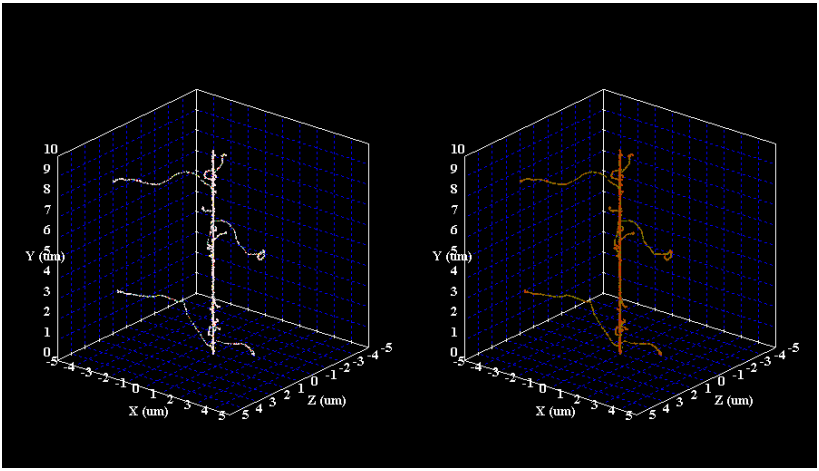

Figure 1. Visualization of the radiolytic species (left) and voxel dose (right) of the track structure of a $^{12}C^{6+}$ ion, 25 MeV/u, as simulated by RITRACKS (linear energy transfer ~78 keV/μm).

In principle any ion track can be simulated if the energy is within the range of which the cross sections for interactions of primary particles and secondary electrons with target molecules are known. The dose deposited by the radiation can be calculated in microvolumes [6] and in nanovolumes (voxels). An example of a track structure calculated by RITRACKS is shown in Figure 1. More recently, RITRACKS was used with nuclei models to calculate the radiation-induced double-strand breaks [7].

In future work, we would like to use RITRACKS to provide a better understanding of DNA damage by ionizing radiations at the molecular scale, since detailed information on the radiolytic species forming the track structure and energy deposition events is provided by RITRACKS. A chromatin fiber

model has been developed. To simulate the direct effect (direct ionization of DNA), the transport algorithms of RITRACKS will be modified to include the ionization cross sections of the bases, sugar and phosphates [8]. To simulate the indirect effect (attack by the ·OH radical), a new approach based on the Green's functions of the diffusion equation will be used [9].

1 Cucinotta F.A., Durante M. Lancet Oncol., **2006**, 7, 431-435.
2 Ballarini F., Alloni D., Facoetti A., Ottolenghi A. New J. Phys., **2008**, 10 075008.
3 Turner J.E., Hamm R.N., Wright L.A., Ritchie R.H., Magee J.L., Chatterjee A., Bolch W.E. Radiat. Phys. Chem., **1988**, 32, 503-510.
4 Nikjoo H., Uehara S., Emfietzoglou D., Cucinotta F.A. Radiat. Meas., **2006**, 41, 1052–1074.
5 Plante I., Cucinotta F.A. *Monte-Carlo simulation of ionizing radiation tracks* / In Mode, C.B. (ed), "Applications of Monte Carlo Methods in Biology, Medicine and Other Fields of Science". Rijeka, Croatia, **2011**.
6 Plante I., Cucinotta F.A. Radiat. Env. Biophys., **2010**, 49, 5-13.
7 Plante I., Ponomarev A.L., Cucinotta F.A. Submitted to Phys. Med. Biol.
8 Edel S. PhD Thesis, University of Toulouse, **2006**.
9 Plante I., Devroye L., Cucinotta F.A. J. Comp. Phys., **2013**, 242, 531-543.

What governs the hole transport in DNA?

Shirmovsky S.Eh.

Theoretical and experimental physics cathedra, Far Eastern Federal University,
8 Sukhanov St., Vladivostok, 690950, Russia

The idea of DNA having charge conducting properties has already been discussed for quite a while and proved in many experimental works [1], [2]. The different approaches modeling a charge transfer dynamics through DNA were suggested [3–5]. However, the problem of modeling a charge transfer through DNA still remains to be solved. It is first of all connected with the complexity of constructing a realistic DNA-charge mathematical model due to a large number of factors responsible for the charge transfer being involved. As a rule, two set of parameters are used to describe the process of a charge migrating through a DNA chain. The first one is that of ionization potentials ε_n which determine the energy profile of DNA. The second important energy parameter is the coupling matrix elements $\nu_{n,m}$ between n, m bases which determine the rate of charge transport between the bases. Generally speaking, both ionization potentials and coupling matrix elements are dynamic values. They are gated by the structure and dynamics of DNA as well as by the DNA interaction with the environment [6, 7]. Thus, Kubar and the co-authors determine several factors responsible for the charge transfer in DNA: 1) the

environment factors, i. e., the electrostatic interaction of the charge with the remainder of DNA and solvent; the fluctuation of counterions; the DNA bases fluctuation leading to the oscillations of ionization potentials which has a crucial impact on the energy of the hole transfer through a DNA strand; 2) correlations between the onsite energies of neighboring bases which lead to the conformational gating type charge transport mechanism; 3) coupling matrix elements depend on DNA conformation and mutual base arrangement – twist, rise, stretch, etc. – and they are not affected by the solvent. Furthermore it has been found experimentally that the charge migration through the DNA chain can present two opposite processes: charge transport is reversible as in the experiments of Lewis et al. [2]. On the other hand, charge transport could be irreversible process as in the experiments of Giese et al. [1]. Today, there is no standard method to include irreversible dynamics in the theory. It is a complex theoretic problem in itself. In the work, we are trying to answer whether and in what manner the solvent factors and DNA dynamics affect the nature of the hole migration through DNA molecule. In other words, does hole transport result from the DNA interaction with the environment, DNA dynamics rather than from its intrinsic properties as a charge conducting medium?

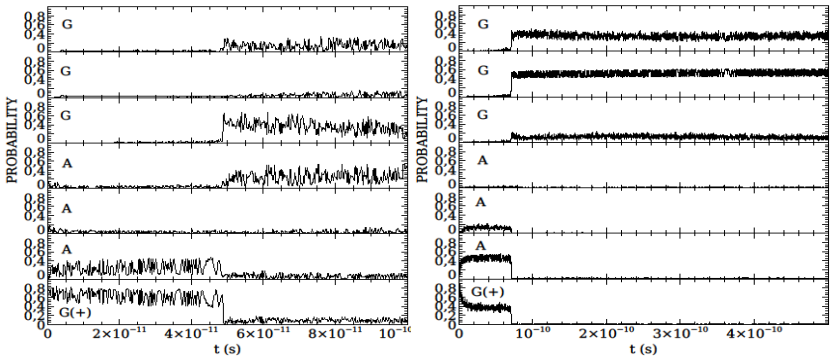

Figure

Figure shows the probable hole location on the bases of the sequence G(+)AAAGGG for the two different cases. At the initial moment the hole is located on the adenine G(+) base of the sequence with a probability of 1 (100%). The case **a** corresponds to the case when: ε_n does not dependent on DNA denamics, $\nu_{n,m}$ – dynamic values. The case **b** corresponds to the case: ε_n – dynamic, $\nu_{n,m}$ – dynamic values. It is seen the behavior of hole acting on the DNA chain, is governed by dynamics of DNA and environment factors.

1 Meggers E., Michel-Beyerle M. E., Giese B. *Sequence dependent long range hole transport in DNA* // J. Am. Chem. Soc. **1998**. 120. 12950-12955.
2 Lewis F. D., Zuo X., Liu J., Hayes R. T., Wasielewski M. R. *Dynamics of inter~- and intrastrand hole transport in DNA hairpins* // J. Am. Chem. Soc. **2002**. 124. 4568-4569.
3 Conwell E. M., Rakhmanova S. V. *Polarons in DNA* //Proc. Natl. Acad. Sci. U.S.A. **2000**. 97. 4556-4560.
4 Lakhno V. D. *Soliton-like solutions and electron transfer in DNA* // J. of Biol. Phys. **2000**. 26. 133-147.
5 Fialko N. S., Lakhno V. D. *Nonlinear dynamics of excitations in DNA* Phys. Lett. A **2000**. 278. 108-112.
6 Kubar T., Woiczikowski P. B., Cuniberti G., Elstner M. *Efficient calculation of charge-transfer matrix elements for hole transfer in DNA* // J. Phys. Chem. B **2008**. 112. 7937-7947.
7 Voityuk A. A. *Electronic couplings and on-site energies for hole transfer in DNA: Systematic quantum mechanical/molecular dynamic study* J. Chem. Phys. **2008**. 128. 115101-115106.

COMPUTER RESEARCH & MODELING

http://crm.ics.org.ru

“Computer Research and Modeling” is a multidisciplinary scientific journal. It is distributed in electronic (online free of charge) and printed versions. We publish both research articles and reviews on theory and application of mathematical modeling in natural and social sciences and techniques. All articles are reviewed. The journal is approved by Higher Attestation Commission (VAK) and is listed in Russian Science Citation Index and eLibrary. Articles are published in Russian or English language. Publication fee is not charged.

ISSN: 2076-7633 (Print), 2077-6853 (Online).



International Workshop

Analysis of Complex Biological Systems: Models and Experiment

This Workshop is a satellite event of "Mathematics. Computing. Education" Interdisciplinary Conference. The Conference is held at the end of January in scientific centers nearby Moscow, Russia – at Joint Institute for Nuclear Research, Dubna (even year event) and at Biology Research Center of Puschino (odd year event). Working languages of the Workshop are English and Russian.

With advance in experimental sciences it becomes obvious that for deep understanding of biological phenomena at different spatial and time scales new comprehensive approaches are required. The need for integration between different branches of knowledge led to emergence of such disciplines as bioinformatics and systems biology. The Workshop is aimed at facilitating dialogue between experimental, computational, and theoretical aspects of life sciences and will address interdisciplinary practices across the natural sciences.

Organized by:

- Lomonosov Moscow State University,
- Joint Institute for Nuclear Research (Dubna),
- Puschino Scientific Center (Puschino, Russian Academy of Science)

in cooperation with

- Interregional Public Organization "Women in Science and Education"

For further information please visit **http://www.mce.su/** website

Education Computing Mathematics

Organizing Committee address:
Biophysics Dept., Faculty of Biology,
Lomonosov Moscow State University,
Leninskiye Gory, Moscow 119991
Phone: +7 (495) 939-02-89,
Fax: +7 (495) 939-11-15
E-mail: **mce@mce.su**